Gravitational waves from black holes and neutron star mergers

Helmholtz International Summer School "COSMOLOGY, STRINGS, NEW PHYSICS"

JINR August 9, 2019

Konstantin Postnov
SAI MSU

Very short history

- 1916, A. Einstein
- 1920s (Einstein, Eddington, …)
- 1962, M.E. Gertsenstein & V.I. Pustovoit – laser interferometers as GW detectors
- 1970s, R&D (R. Weiss, R. Drever, K. Thorne, V. Braginskii …)
- End of the 1980s: start of LIGO project
- 2002-2010, initial LIGO operation
- 2010-2015, LIGO modernization
- September 14, 2015, first detection of binary BH coalescence (GW 150914)
- August 17, 2017, first detection of binary NS coalescence (GW 170817), start of multichannel astronomy

Main results 2015-2019

- 10 reliably detected BH+BH with M=10-50 $M_\odot$ from distances 500-1000 Mpc
- Merging rate ~12-213 Gpc^{-3} yr^{-1}
- Measured properties consistent with GR up to a few %
- 1 most likely NS+NS merging (GW170817) and observations of gamma-ray to radio afterglow from relativistic jet and kilonova

Nobel Prize in physics 2017

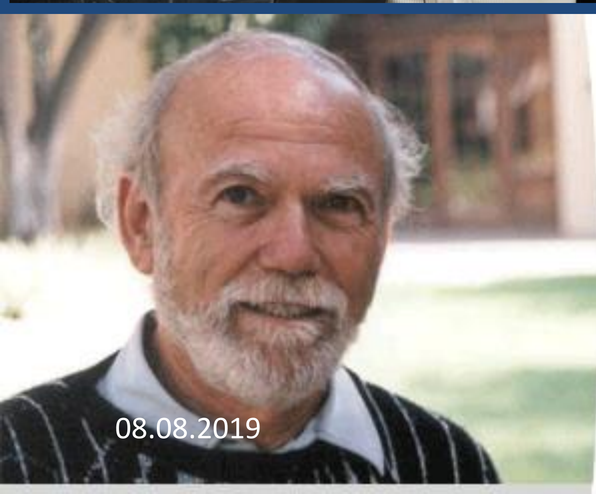

General Relativity

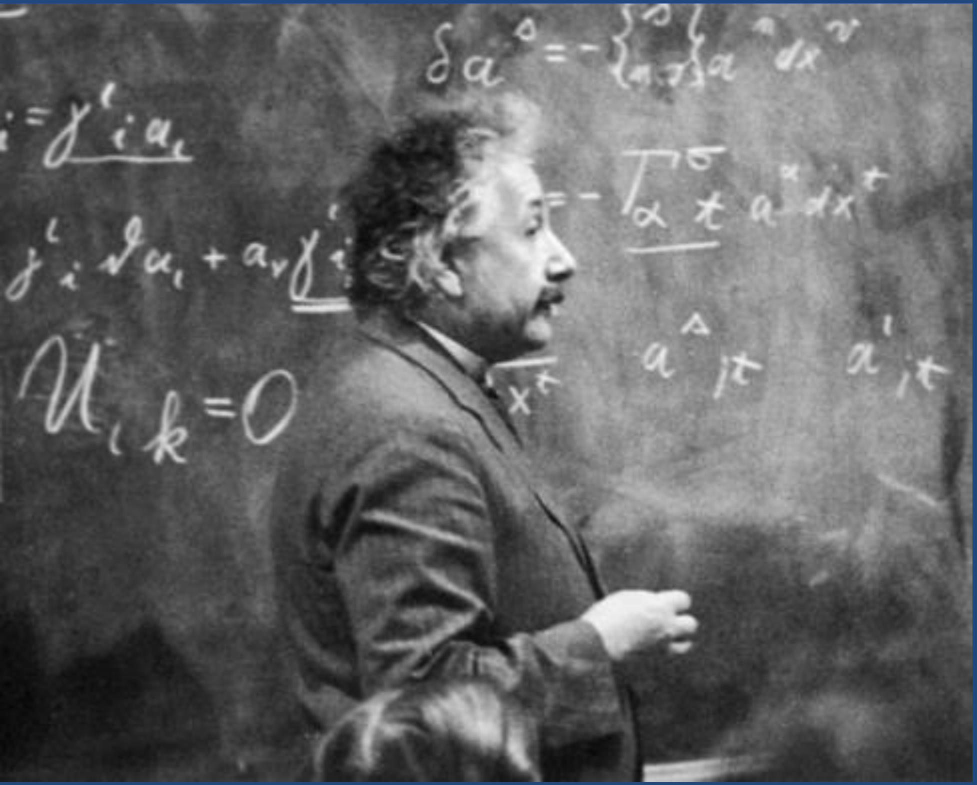

- **A. Einstein, 1915**
- **Gravitation = curvature of space-time**

$$R_{\mu\nu} - \frac{1}{2} R g_{\mu\nu} = \frac{8\pi G}{c^4} T_{\mu\nu}, \qquad ds^2 = g_{\mu\nu} dx^{\mu} dx^{\nu}$$

GW as a «ripple» of space-time

$$g_{\alpha\beta} = g^{\mathrm{B}}_{\alpha\beta} + h_{\alpha\beta} \,, \qquad R_{\alpha\beta\gamma\delta} = R^{\mathrm{B}}_{\alpha\beta\gamma\delta}$$

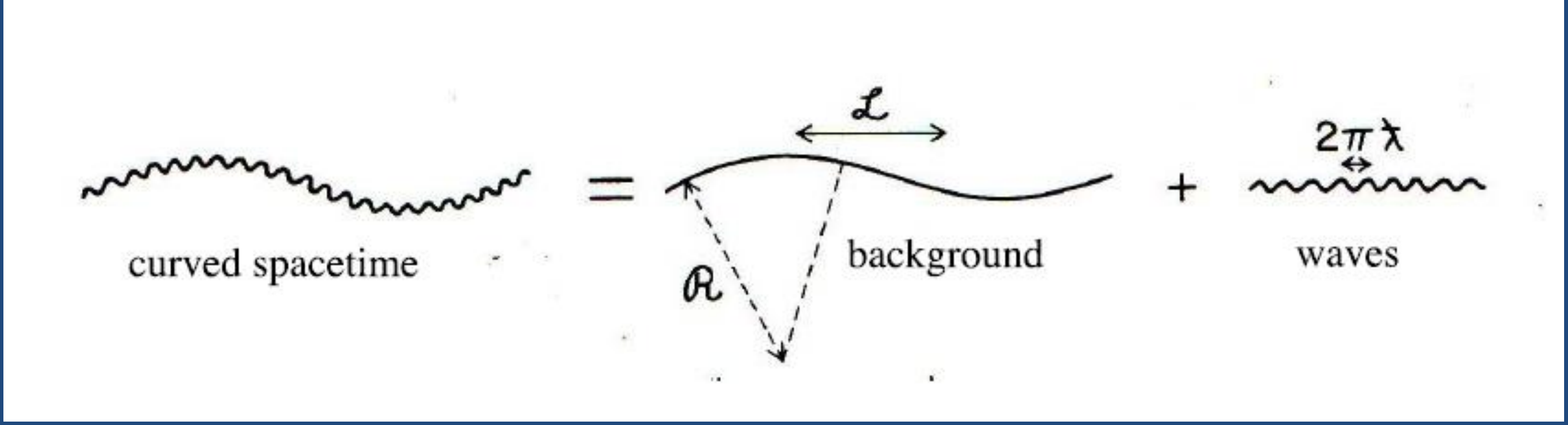

Linearized gravity

$$g_{\mu\nu} = \eta_{\mu\nu} + h_{\mu\nu}, \qquad |h_{\mu\nu}| \ll 1.$$

$$x^\mu \longrightarrow x'^\mu = x^\mu + \xi^\mu(x)$$

$$h_{\mu\nu}(x) \longrightarrow h'_{\mu\nu}(x') = h_{\mu\nu}(x) - (\partial_\mu \xi_\nu + \partial_\nu \xi_\mu)$$

$$R_{\mu\nu\rho\sigma} = \frac{1}{2}(\partial_\nu\partial_\rho h_{\mu\sigma} + \partial_\mu\partial_\sigma h_{\nu\rho} - \partial_\mu\partial_\rho h_{\nu\sigma} - \partial_\nu\partial_\sigma h_{\mu\rho})$$

Gauge-invariant!!!

$$\bar{h}_{\mu\nu} = h_{\mu\nu} - \frac{1}{2}\eta_{\mu\nu} h,$$

$$\bar{h}_{\mu\nu} \longrightarrow \bar{h}'_{\mu\nu} = \bar{h}_{\mu\nu} - (\partial_\mu \xi_\nu + \partial_\nu \xi_\mu - \eta_{\mu\nu}\partial_\rho \xi^\rho)$$

$$\Box \bar{h}_{\mu\nu} = -\frac{16\pi G}{c^4} T_{\mu\nu} \qquad \partial^\nu \bar{h}_{\mu\nu} = 0.$$

$$\partial^\nu T_{\mu\nu} = 0$$

Gravitational waves

$$c^2 \bar{h}^{00} = -4\phi \quad c^2 h_{00} = -2\phi \quad \Delta\phi = 4\pi G\rho$$

- Convenient gauge

$$\Box \xi_\mu = 0.$$

$$\xi_{\mu\nu} = \partial_\mu \xi_\nu + \partial_\nu \xi_\mu - \eta_{\mu\nu} \partial_\rho \xi^\rho \qquad \Box \xi_{\mu\nu} = 0$$

- Does not change linearized equations and harmonic (Lorentz) gauge $\partial^\nu \bar{h}_{\mu\nu} = 0.$
- **4 arbitrary functions ξ can be used to vanish 4 components to leave only 2 independent components (polarizations)**

TT-gauge (transverse-traceless)

$$1)\, Vanish\ trace: \xi_0(x): \bar{h} = 0 \Rightarrow \bar{h}_{\mu\nu} = h_{\mu\nu}$$

$$2)\, Make\ transverse: \xi_i(x): h_{0\mu} = 0: \quad \partial^i h_{ij} = 0$$

$$h_{0\mu} = 0, \quad h^i{}_i = 0, \quad \partial^j h_{ij} = 0$$

$$h_{ij}^{\mathrm{TT}} = e_{ij}(\mathbf{k}) \cos(k_\mu x^\mu)$$

$$k_\mu = (\omega/c, \mathbf{k}) \qquad \omega = c|\mathbf{k}|$$

$$\partial^j h_{ij} = 0 \Rightarrow \mathbf{k}^j h_{ij}^{\mathrm{TT}} = 0 \qquad n^j h_{ij}^{\mathrm{TT}} = 0 \qquad \hat{\mathbf{n}} = \mathbf{k}/|\mathbf{k}|$$

$$h_{ij}^{\mathrm{TT}} = \begin{pmatrix} h_+ & h_\times & 0 \\ h_\times & -h_+ & 0 \\ 0 & 0 & 0 \end{pmatrix}_{ij} \cos\left[\omega(t - z/c)\right]$$

Transition to TT-gauge

$$h_{\alpha\beta} = h_{\alpha\beta}(t - \mathbf{n} \cdot \mathbf{x})$$

$$\bar{h}_{\alpha\beta} = \bar{h}_{\alpha\beta}(t - \mathbf{n} \cdot \mathbf{x})$$

$$P^{jk} \equiv \delta^{jk} - n^j n^k$$

$$h_{jk}^{\mathrm{TT}} = (\bar{h}_{jk})^{\mathrm{TT}} = P_j{}^l P_k{}^m \bar{h}_{lm} - \frac{1}{2} P_{jk} P^{lm} \bar{h}_{lm}$$

- For example. For a wave moving along z-axis:

$$h_+ = h_{xx}^{\mathrm{TT}} = \bar{h}_{xx} - \frac{1}{2}(\bar{h}_{xx} + \bar{h}_{yy}) = \frac{1}{2}(h_{xx} - h_{yy}) \;, \quad h_\times = h_{xy}^{\mathrm{TT}} = \bar{h}_{xy}$$

TT-GW acting on two test masses

$$\frac{d^2 x^\mu}{d\tau^2} + \Gamma^\mu_{\nu\rho}(x)\frac{dx^\nu}{d\tau}\frac{dx^\rho}{d\tau} = 0$$

$$\frac{d^2(x^\mu + \zeta^\mu)}{d\tau^2} + \Gamma^\mu_{\nu\rho}(x+\zeta)\frac{d(x^\nu + \zeta^\nu)}{d\tau}\frac{d(x^\rho + \zeta^\rho)}{d\tau} = 0$$

$$\frac{d^2 \zeta^\mu}{d\tau^2} + 2\Gamma^\mu_{\nu\rho}\frac{dx^\nu}{d\tau}\frac{d\zeta^\rho}{d\tau} + \zeta^\sigma \partial_\sigma \Gamma^\mu_{\nu\rho}(x)\frac{dx^\nu}{d\tau}\frac{dx^\rho}{d\tau} = 0.$$

$$\frac{DV^\mu}{D\tau} = \frac{dV^\mu}{d\tau} + \Gamma^\mu_{\nu\rho}V^\nu\frac{dx^\rho}{d\tau}$$

$$\frac{D^2\zeta^\mu}{D\tau^2} = -R^\mu{}_{\nu\rho\sigma}\zeta^\rho\frac{dx^\nu}{d\tau}\frac{dx^\sigma}{d\tau}$$

- In local Lorentz frame :

$$\Gamma^{\mu}_{\nu\rho}(P) = 0.$$

$$\frac{d^2\zeta^i}{d\tau^2} = -R^i{}_{0j0}\zeta^j \left(\frac{dx^0}{d\tau}\right)^2$$

- Non-relativistic motion of masses:

$$dx^0/d\tau \simeq c$$

$$\ddot{\zeta}^i = -c^2 R^i{}_{0j0}\zeta^j$$

$$R^i{}_{0j0} = R_{i0j0} = -\frac{1}{c^2}\ddot{h}^{\mathrm{TT}}_{ij}$$

$$R_{\alpha\beta\gamma\delta} = \frac{1}{2}h^{\mathrm{TT}}_{\{\alpha\beta,\gamma\delta\}} \equiv \frac{1}{2}(h^{\mathrm{TT}}_{\alpha\delta,\beta\gamma} + h^{\mathrm{TT}}_{\beta\gamma,\alpha\delta} - h^{\mathrm{TT}}_{\alpha\gamma,\beta\delta} - h^{\mathrm{TT}}_{\beta\delta,\alpha\gamma})$$

$$\ddot{\zeta}^i = \frac{1}{2}\ddot{h}^{\mathrm{TT}}_{ij}\zeta^j.$$

$$\delta x^j = \frac{1}{2}h^{\mathrm{TT}}_{jk}x^k$$

Simple argument by R.Feynmann (1957, Chapel Hill conference)

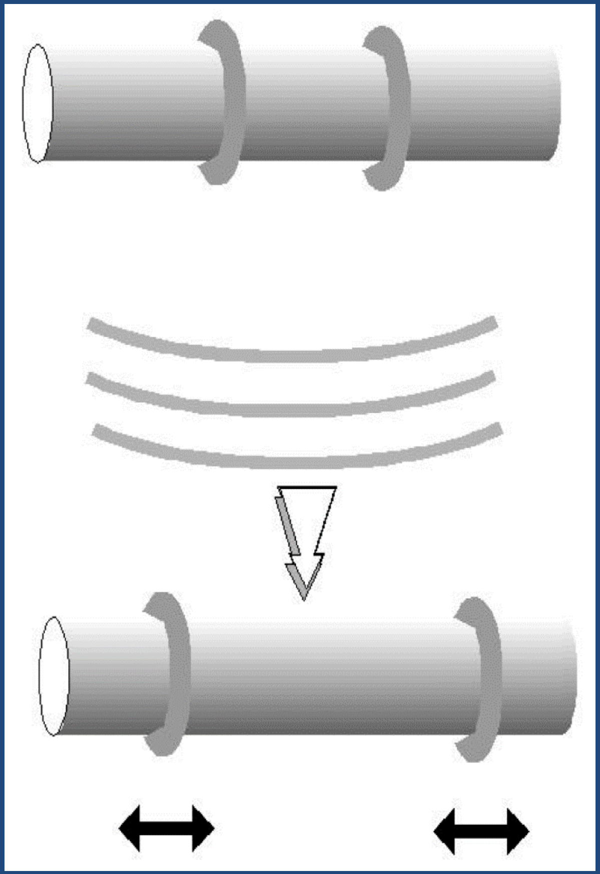

- “I was surprised to find that a whole day of the conference was spent on this issue and that ‘experts’ were confused. That’s what happens when one is considering energy conservation tensors, etc. instead of questioning, can waves do work?”

(after F. Pirani’s talk)

Energy flux in GW

- Energy density

$$t^{00} = \frac{c^2}{16\pi G}\langle \dot{h}_+^2 + \dot{h}_\times^2 \rangle$$

- Energy flux

$$\frac{dE_{\rm GW}}{dt} = \frac{c^3 r^2}{16\pi G}\int d\Omega\, \langle \dot{h}_+^2 + \dot{h}_\times \rangle.$$

- GW carries energy and momentum that can act on test masses

$$T^{\rm GW\,0z} \simeq \frac{\pi}{4}\frac{c^3}{G} f^2 h_{\rm amp}^2 \simeq 300 \frac{\rm ergs}{\rm cm^2\ sec}\left(\frac{f}{1\ \rm kHz}\right)^2 \left(\frac{h_{\rm amp}}{10^{-21}}\right)^2$$

GW sources

$$\bar{h}_{\mu\nu}(t,\mathbf{x}) = -4\frac{G}{c^2}\int_{\mathcal{V}} \frac{T_{\mu\nu}(t-|\mathbf{x}-\mathbf{x}'|/c,\mathbf{x}')}{|\mathbf{x}-\mathbf{x}'|} d^3\mathbf{x}'$$

- Lowes order -- quadrupole. For v/c<<1:

$$h_{jk}^{\mathrm{GW}} = 2G\frac{\ddot{I}_{jk}}{r} \sim G\frac{\omega^2(ML^2)}{r} \sim G\frac{E_{\mathrm{kin}}/c^2}{r}$$

$$h_{jk}^{\mathrm{GW}} \sim h_+ \sim h_\times \sim 10^{-21}\left(\frac{E_{\mathrm{kin}}}{M_\odot c^2}\right)\left(\frac{100\mathrm{Mpc}}{r}\right)$$

GE creates tidal acceleration field in a freely faling (local Lorentz) reference frame

$$\mathcal{E}_{ij} = R_{i0j0} = -\frac{1}{2}\ddot{h}_{ij}^{\mathrm{TT}}$$

$$h_{ij}^{\mathrm{TT}} \equiv -2\int dt \int dt\, \mathcal{E}_{ij}$$

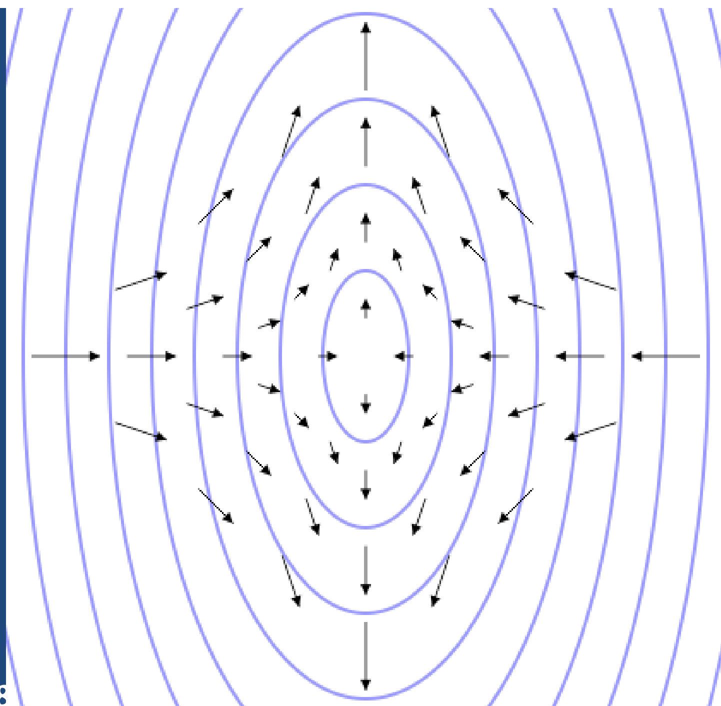

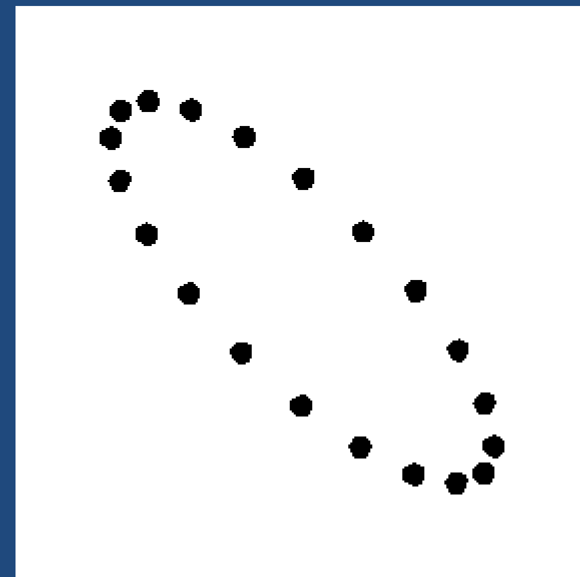

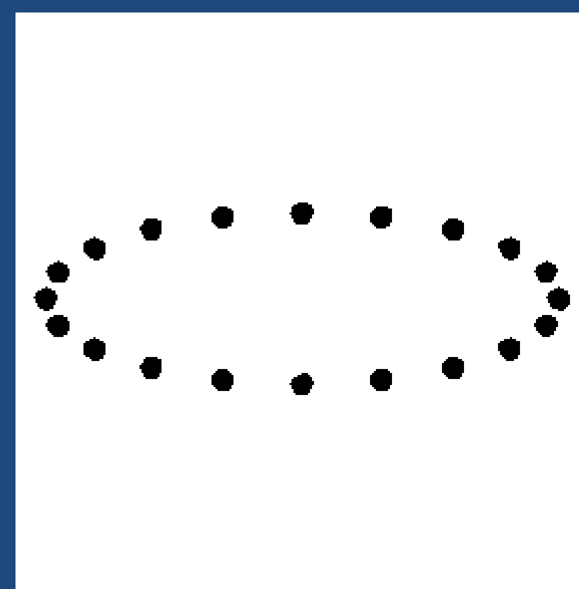

GW amplitude h = relative expansion/compression

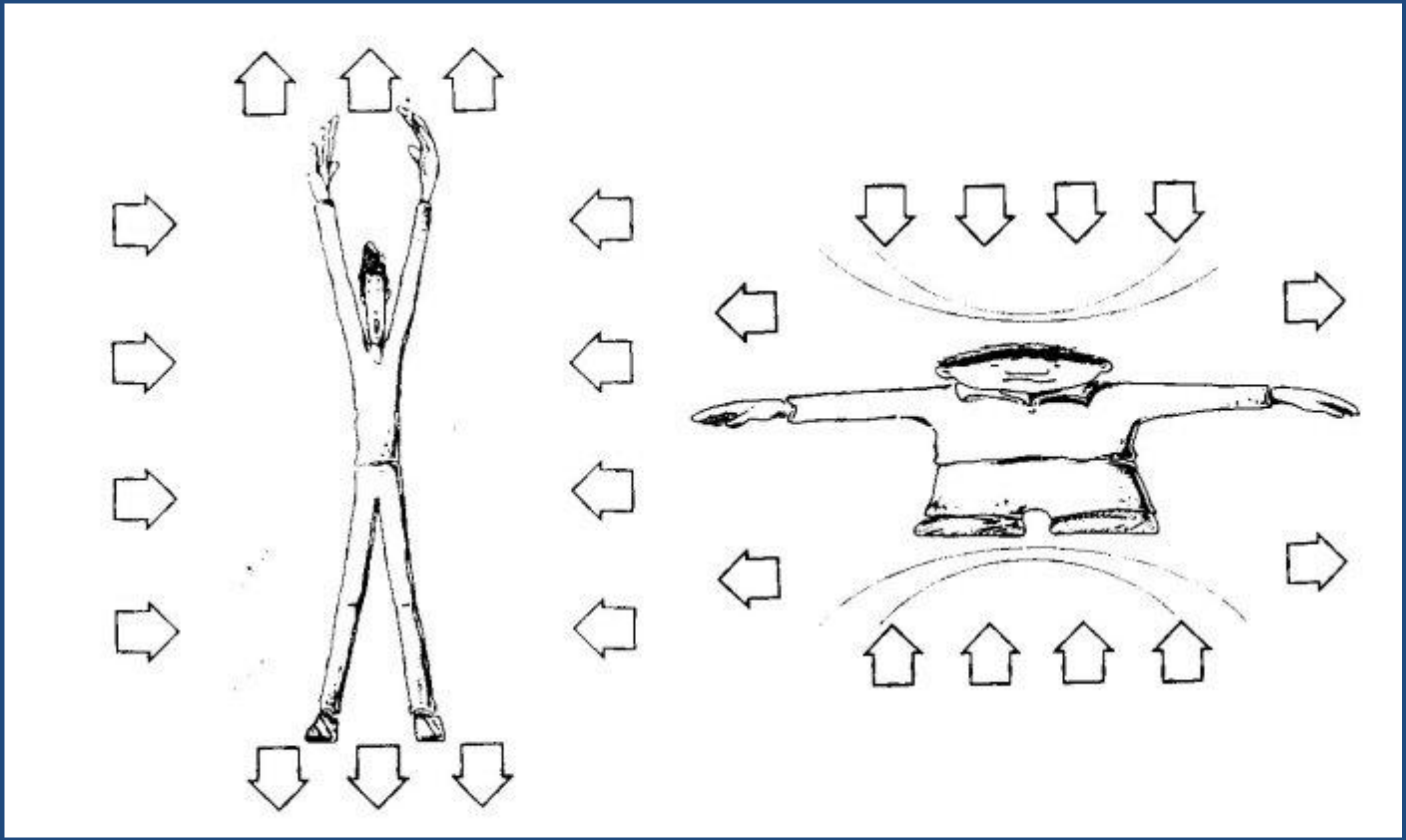

Tidal acceleration field

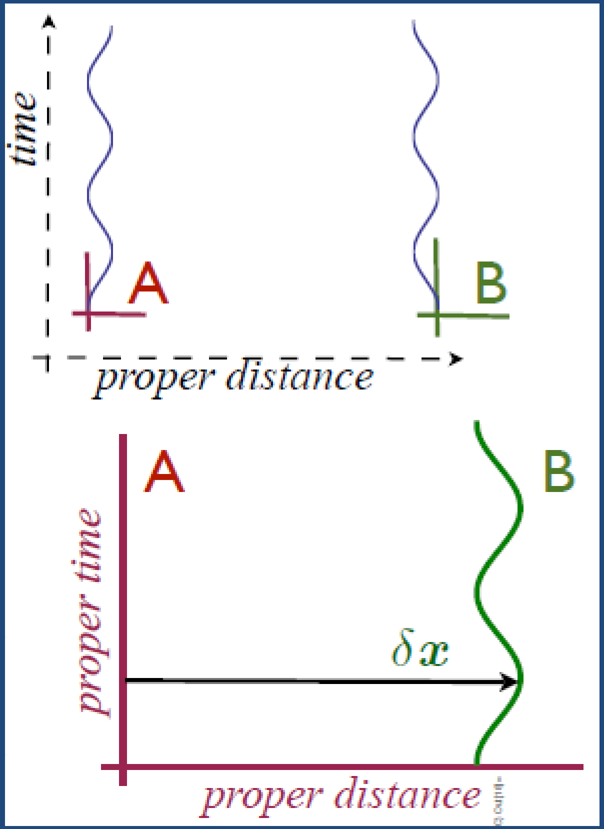

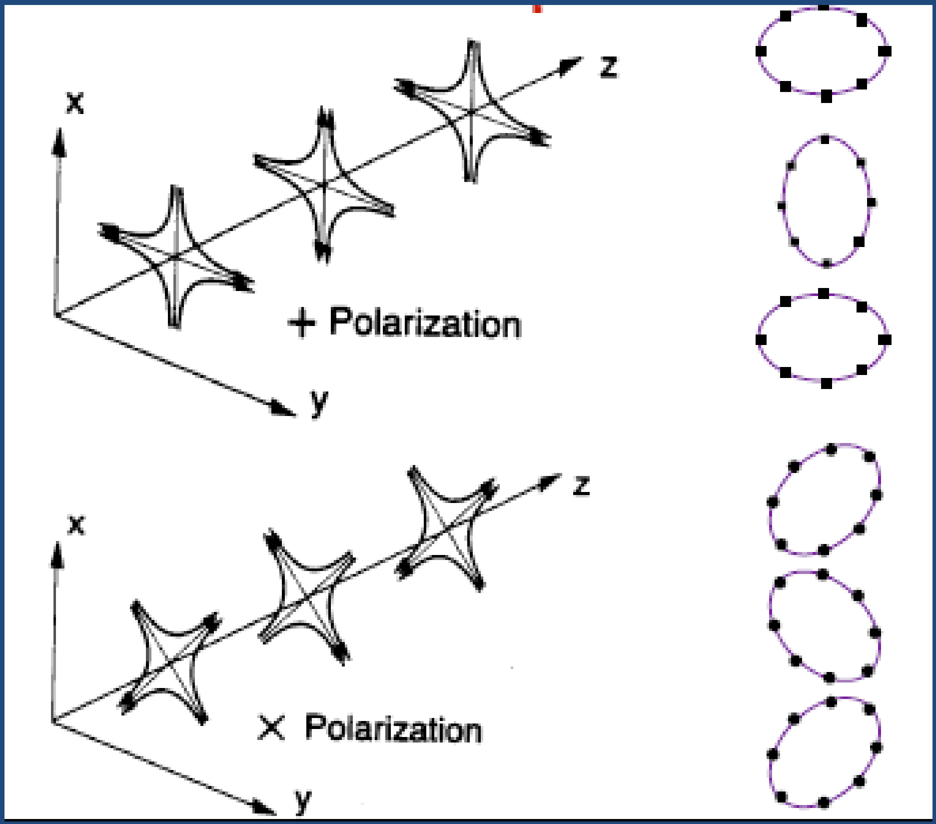

$$\delta x_j = \frac{1}{2} h_{jk}^{\mathrm{GW}} x_k$$

Astrophysical GW sources

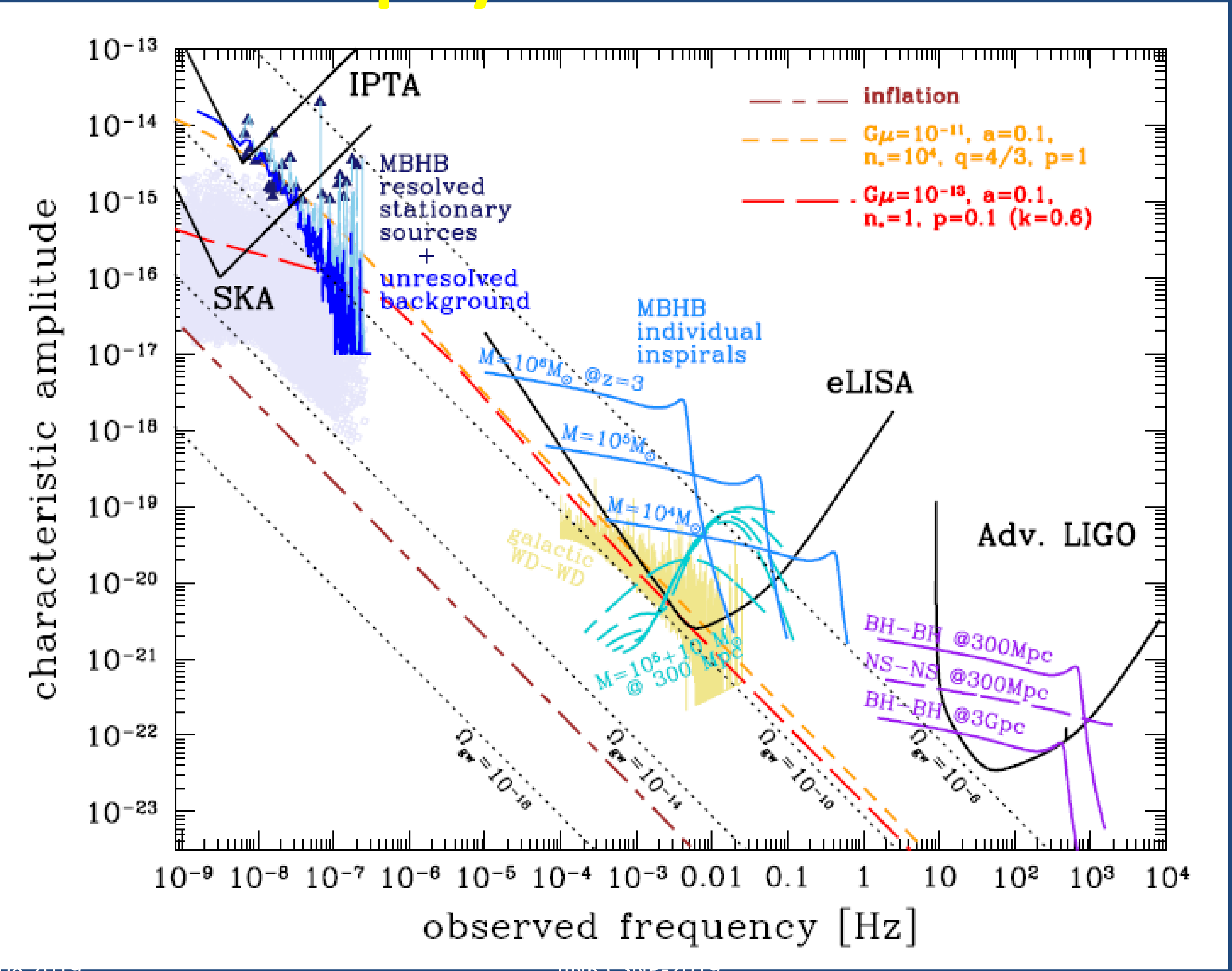

Credit: A. Sesana

Coalescing compact binaries

E pur si existare!

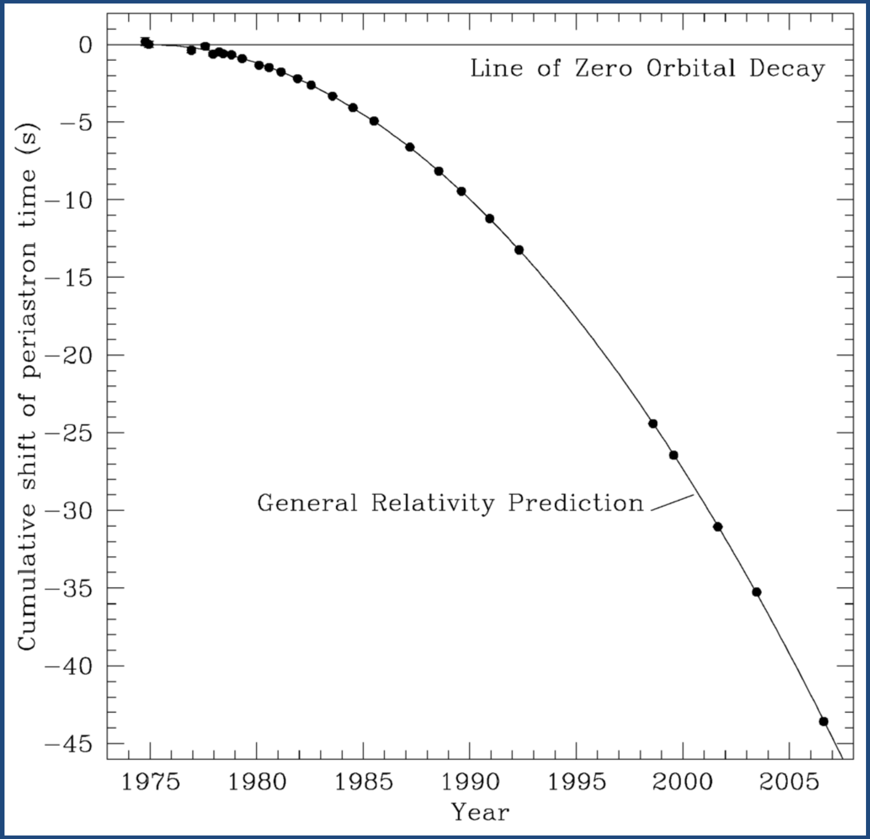

- 1974, binary pulsar PSR 1913+16 (Hulse, Taylor, Nobel Prize 1993)

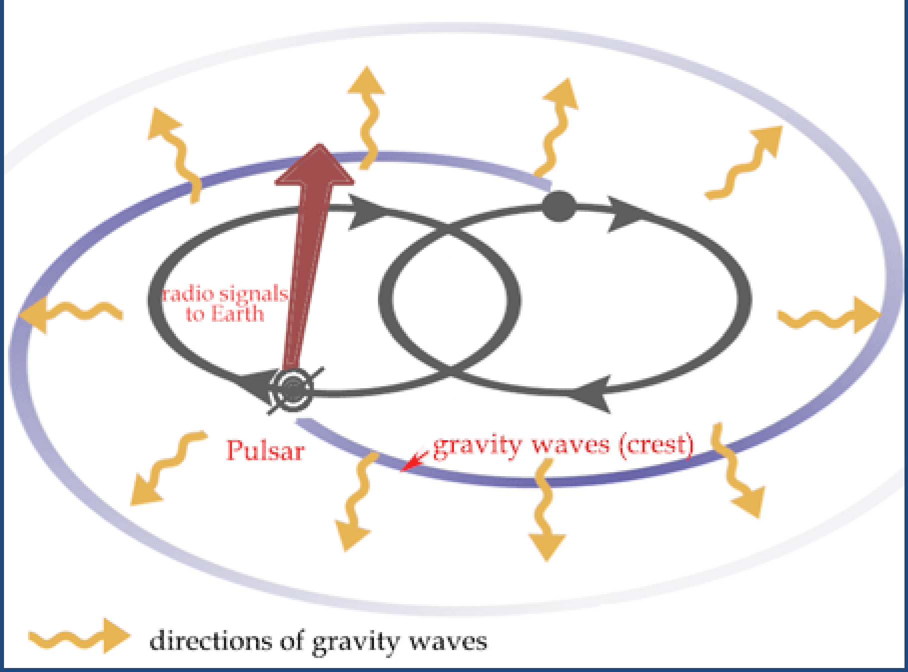

Orbital period decay
in agreement with GR (~0.1%)

EM vs GW

	EM	GW
Charge	q	m
Size	R	$\omega^2 \sim \frac{m}{R^3}[G]$
Dipole radiation	$A \sim \frac{qR\omega}{r}$	no
Quadrupole radiation	Dipole x (v/c)	$h \sim \frac{mR^2\omega^2}{r}\left[\frac{G}{c^4}\right]$
Energy flux	$F_{EM} \sim \omega^2 A^2 \sim \frac{q^2\ddot{R}^2}{r^2}$	$F_{GW} \sim \omega^2 h^2 \sim \frac{m^2R^4\omega^6}{r^2}\left[\frac{G}{c^4}\right]^2$
Power	$\frac{dE}{dt} = -\frac{2}{3}\ddot{d}^2$	$\frac{dE}{dt} = -\frac{128}{5}m^2R^4\omega^6\left[\frac{G}{c^5}\right]$

- Waveform from two coalescing point-like masses is determined by a combination of component masses (the chirp mass)
- ➔ blackboard

$$M_{ch} = (\mu^3 M^2)^{1/5}$$

$$h \sim M_{ch}^{5/3} f^{2/3} / r$$

$$\mathcal{M} = \frac{(m_1 m_2)^{3/5}}{(m_1 + m_2)^{1/5}} = \frac{c^3}{G}\left(\frac{5}{96}\pi^{-8/3} f^{-11/3} \dot{f}\right)^{3/5}$$

Chirp signal from a coalescing binary

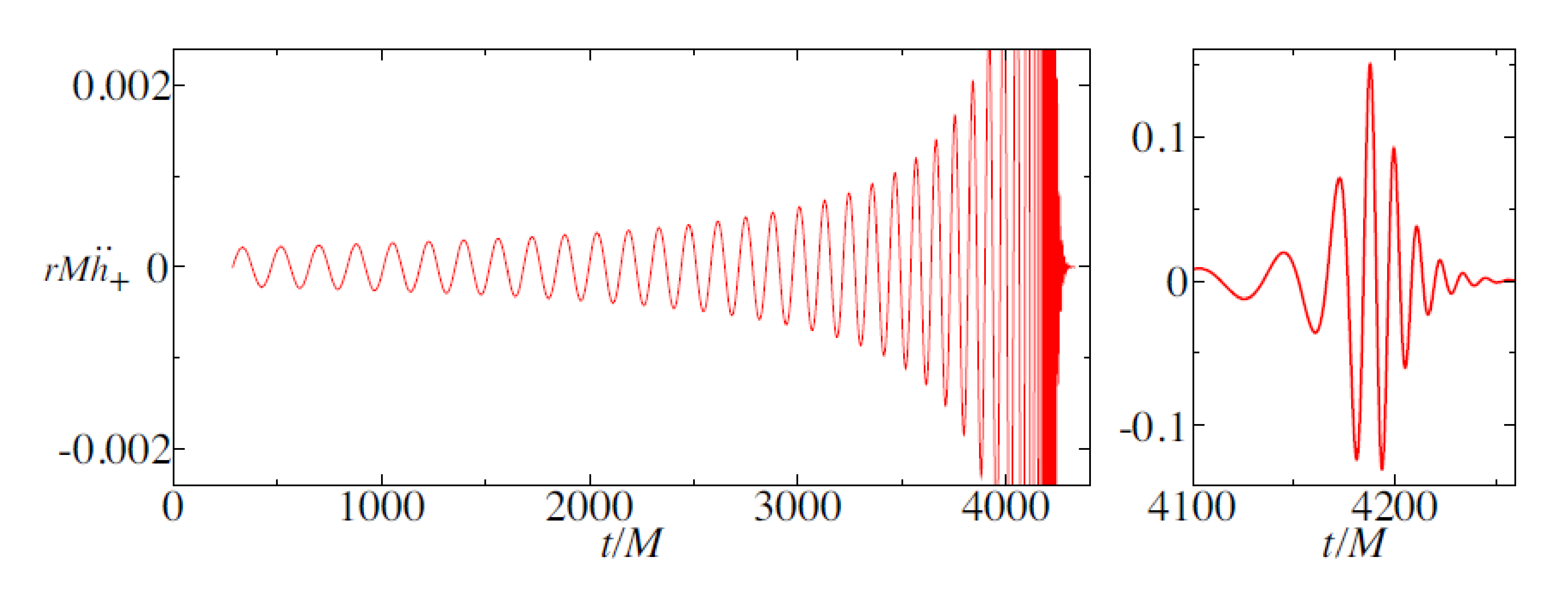

$$h_+ = h^{TT}_{\hat\theta\hat\theta} = \frac{2}{r}[\ddot{I}_{\hat\theta\hat\theta}(t-r)]^{TT} = -2(1+\cos^2\theta)\ \frac{\mu(M\Omega)^{2/3}}{r}\cos[2(\Omega t - \Omega r - \phi)]$$

$$h_\times = h^{TT}_{\hat\theta\hat\phi} = \frac{2}{r}[\ddot{I}_{\hat\theta\hat\phi}(t-r)]^{TT} = -4\cos\theta\ \frac{\mu(M\Omega)^{2/3}}{r}\sin[2(\Omega t - \Omega r - \phi)] \, .$$

Energy release in binary BH mergings

$$E_N = (m_1 + m_2)c^2 - \frac{G m_1 m_2}{2r}$$

$$r_{insp} \approx \frac{5G(m_1 + m_2)}{c^2} \quad \Rightarrow$$

$$\Delta E_{GW,insp} \approx \frac{1}{10} \frac{m_1 m_2}{m_1 + m_2} \approx 5\% mc^2 \sim 2.5\% Mc^2$$

$$\Delta E_{GW,total} = \Delta E_{GW,insp} + \Delta E_{GW,coal} + \Delta E_{GW,ringd} \approx 5\% Mc^2$$

$$\Delta E_{GW,total} = (M_i^{source} - M_f^{source})c^2 = 3^{+0.5}_{-0.5} M_\odot c^2$$

Maximum luminosity

$$\frac{dE}{dtdA} = \frac{c^3}{16\pi G}(\langle \dot{h}_\times \rangle^2 + \langle \dot{h}_\times \rangle^2)$$

$$h_{\max} \sim 10^{-21}, d \sim 400\,Mpc \quad \Rightarrow$$

$$\left(\frac{dE}{dt}\right)_{GW,\max} \sim 10^{56}\,erg/s \sim 200 M_\odot c^2/s$$

$$\left(\frac{dE}{dt}\right)_{GW,\max} \le L_0 = \frac{c^5}{16\pi G} \approx 7\times 10^{57}\,erg/s$$

$$(Cf\ \ the\ brightest\ GRB: 2\times 10^{54}\,erg/s)$$

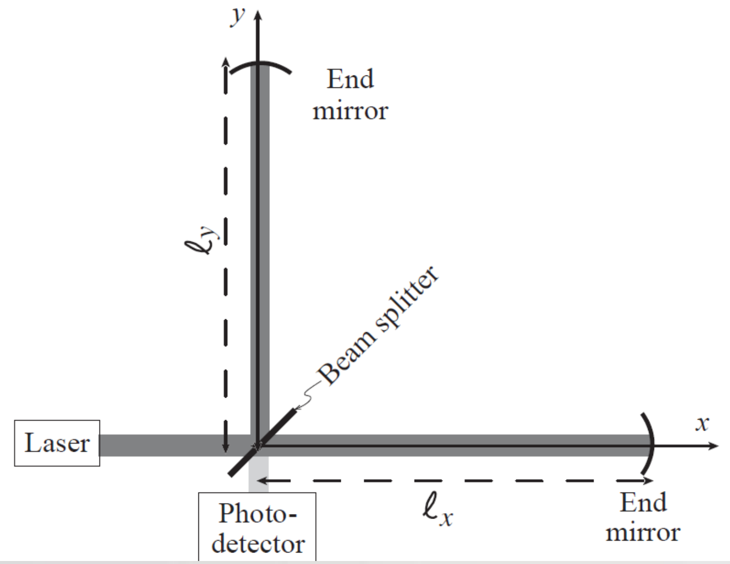

Laser Interferometer

- Gertsenstein, Pustovoit 1962

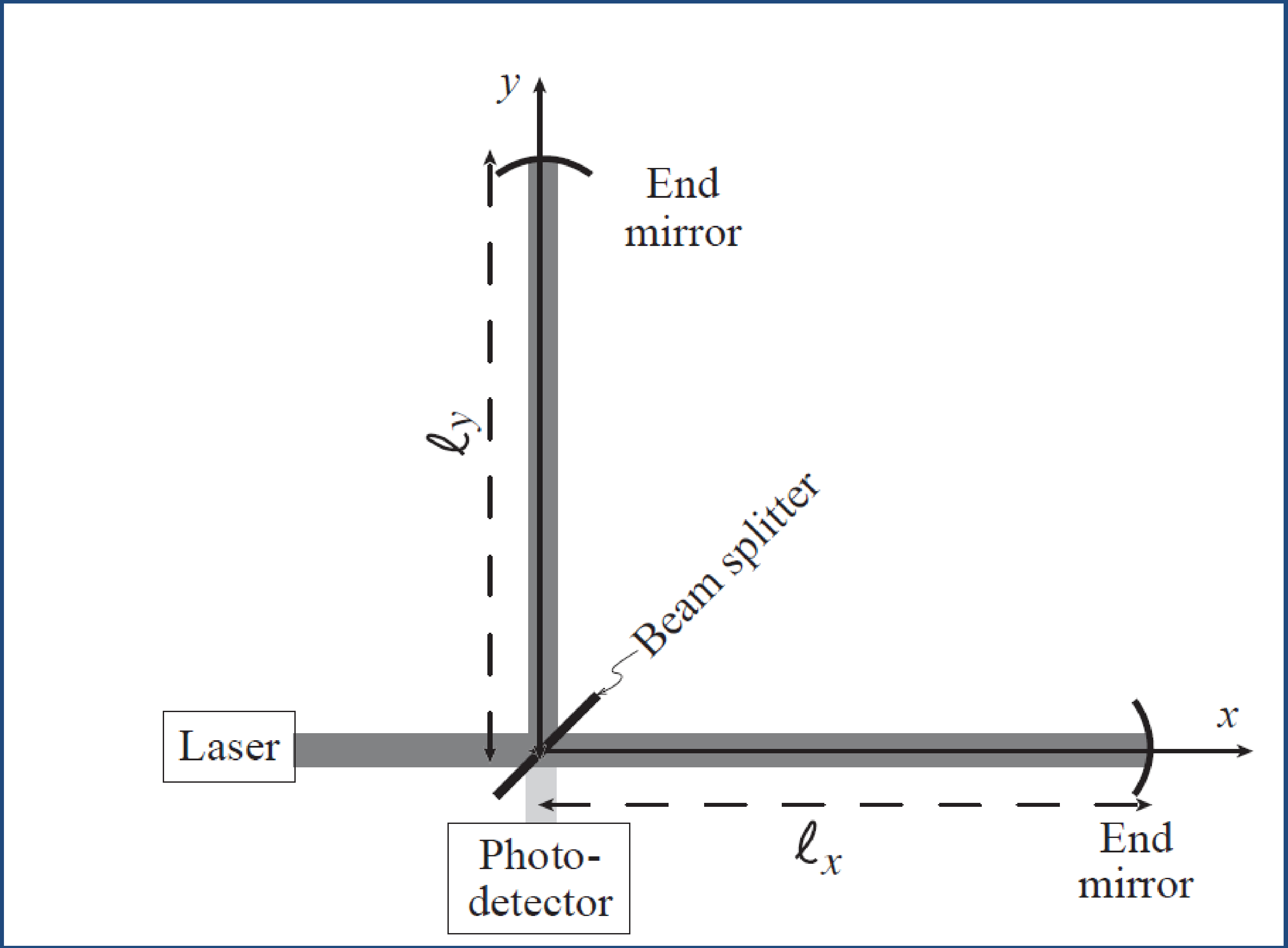

$$ds^2 = -dt^2 + [1 + h_+(t - z)]dx^2 + [1 - h_+(t - z)]dy^2 + dz^2$$

Principle of operation

$$\delta x = \frac{1}{2} h_+ \ell_x \quad \delta y = -\frac{1}{2} h_+ \ell_y$$

Phase difference

$$\Delta\varphi(t) = \omega_o(2\delta y - 2\delta x) = \omega_o(\ell_x + \ell_y) h_+(t)$$

Intensity modulation

$$\boxed{\Delta I_{\mathrm{PD}}(t) \propto \Delta\varphi(t) = 2\omega_o \ell h_+(t)}$$

Achievable sensitivity

$$\Delta\Phi = B\frac{hL}{\lambda}, \quad \frac{BL}{c} \le \frac{1}{2}\left(\frac{1}{f_{GW}}\right) \Rightarrow B_{\max} \approx 400$$

$$Shot\,noise: \; \Delta\Phi_{\min} \sim \frac{1}{\sqrt{N_{ph}}},$$

$$N_{ph} = \frac{P_{laser} \times (\#\; recycling)}{\hbar\omega} \times \Delta t \sim 2\times 10^{20}$$

$$@\, P = 60W, \; \Delta t = 10ms$$

$$h_{\min} \sim \frac{\lambda}{BL}\frac{1}{\sqrt{N_{ph}}} = \frac{0.5\mu}{400\times 4km}\frac{1}{\sqrt{2\times 10^{20}}} \sim 10^{-22}\,!$$

LIGO interferometer

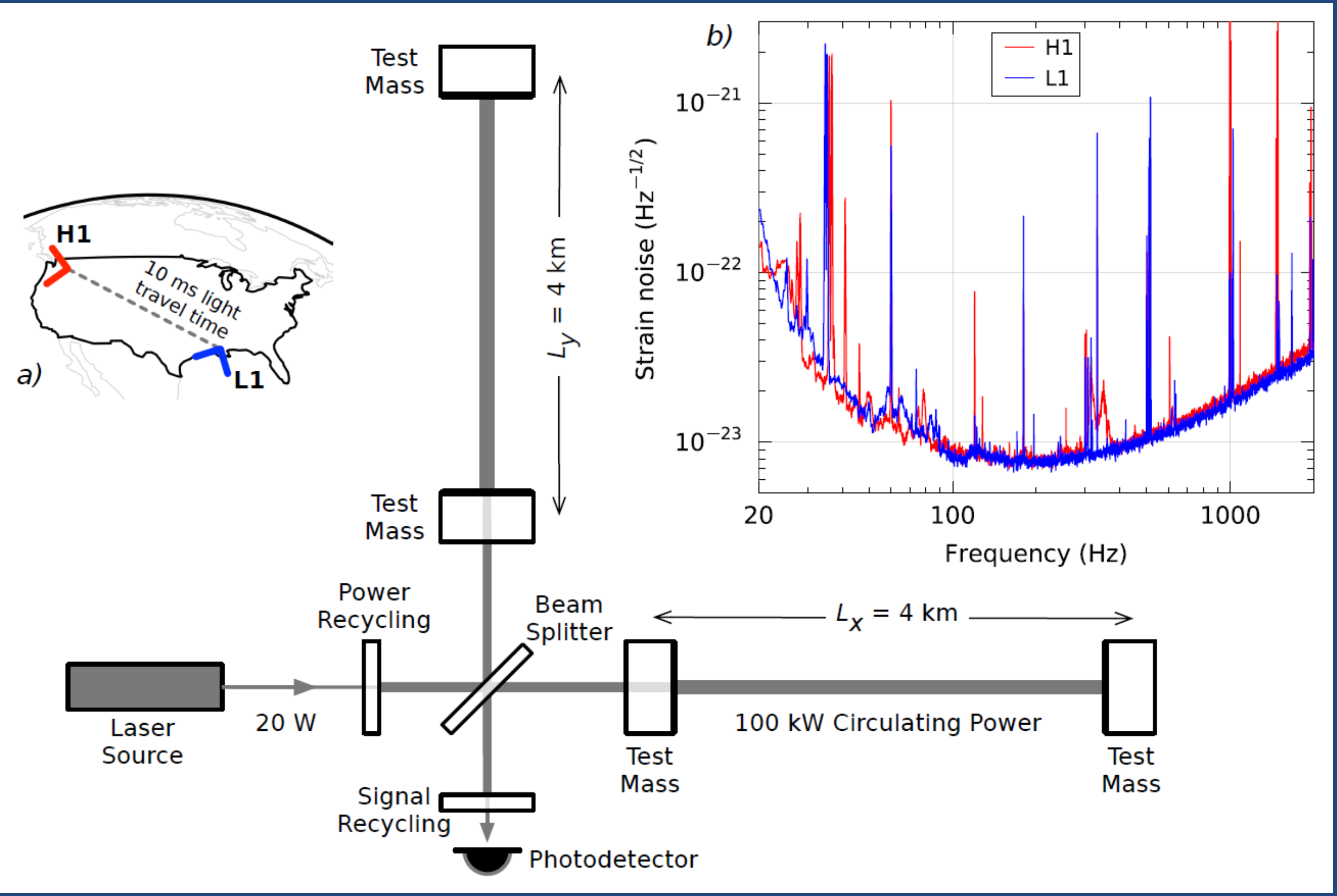

D. Reitze Phys.-Usp. 2017

Noise budget

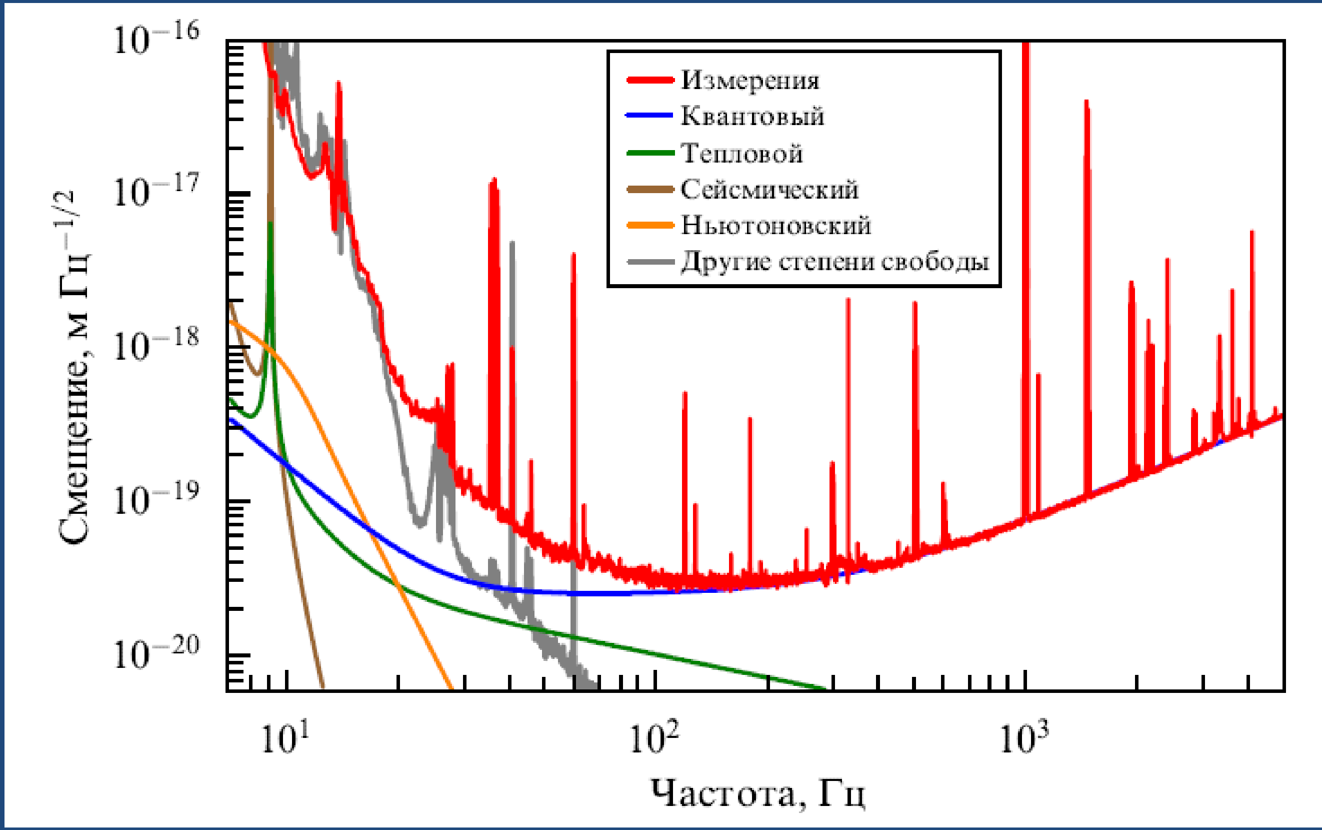

Operating interferometers

- 2 LIGO (USA)
- Virgo (Italy)
- GEO-600 (Germany)


LIGO Hanford


LIGO Livingston


Virgo


GEO-600

LIGO O1

- 18/09/2015-13/01/2016

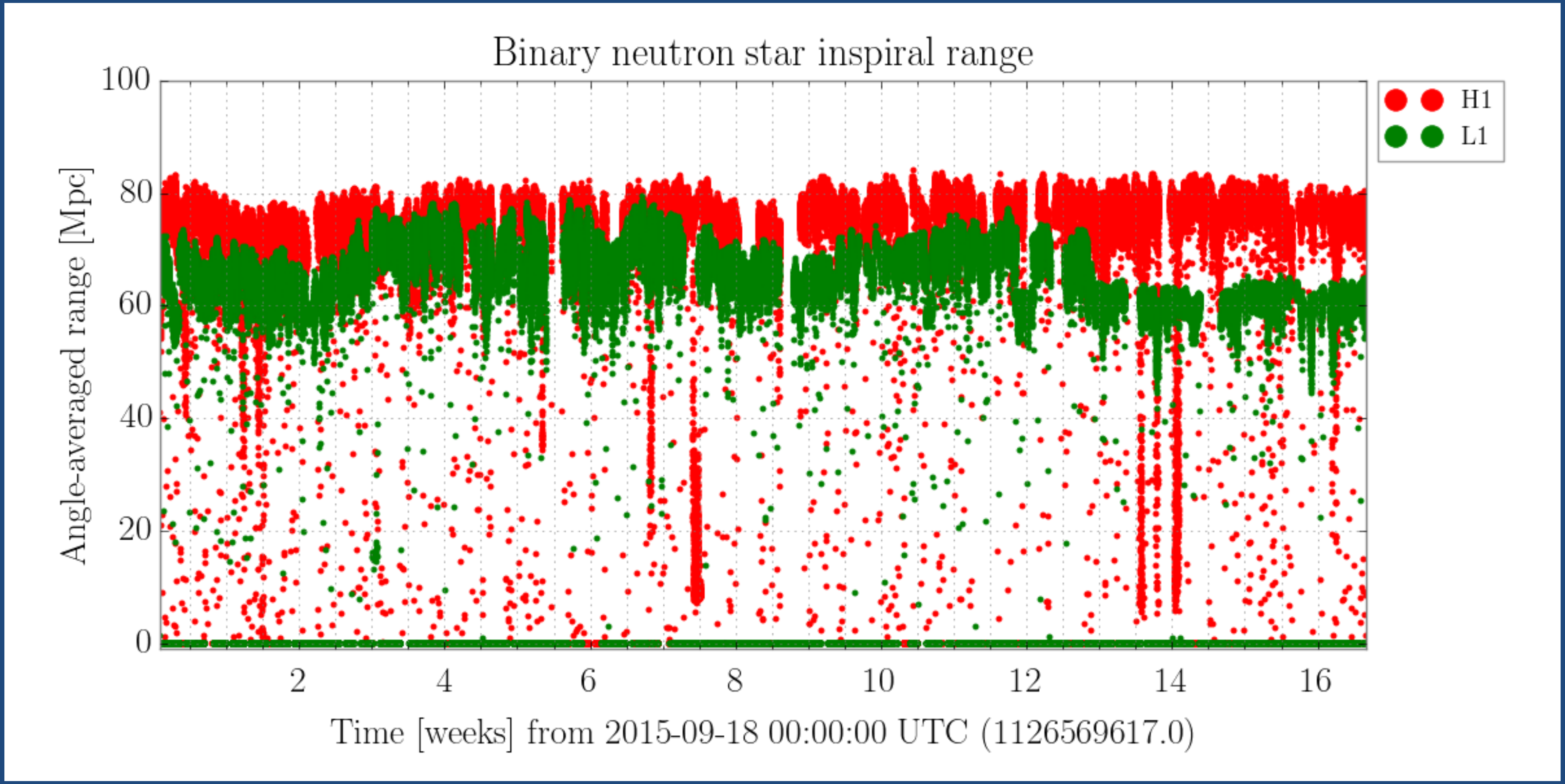

$D_h \sim M_{chirp}^{5/6}$

LIGO O2

- 30/11/2016-25/08/2017

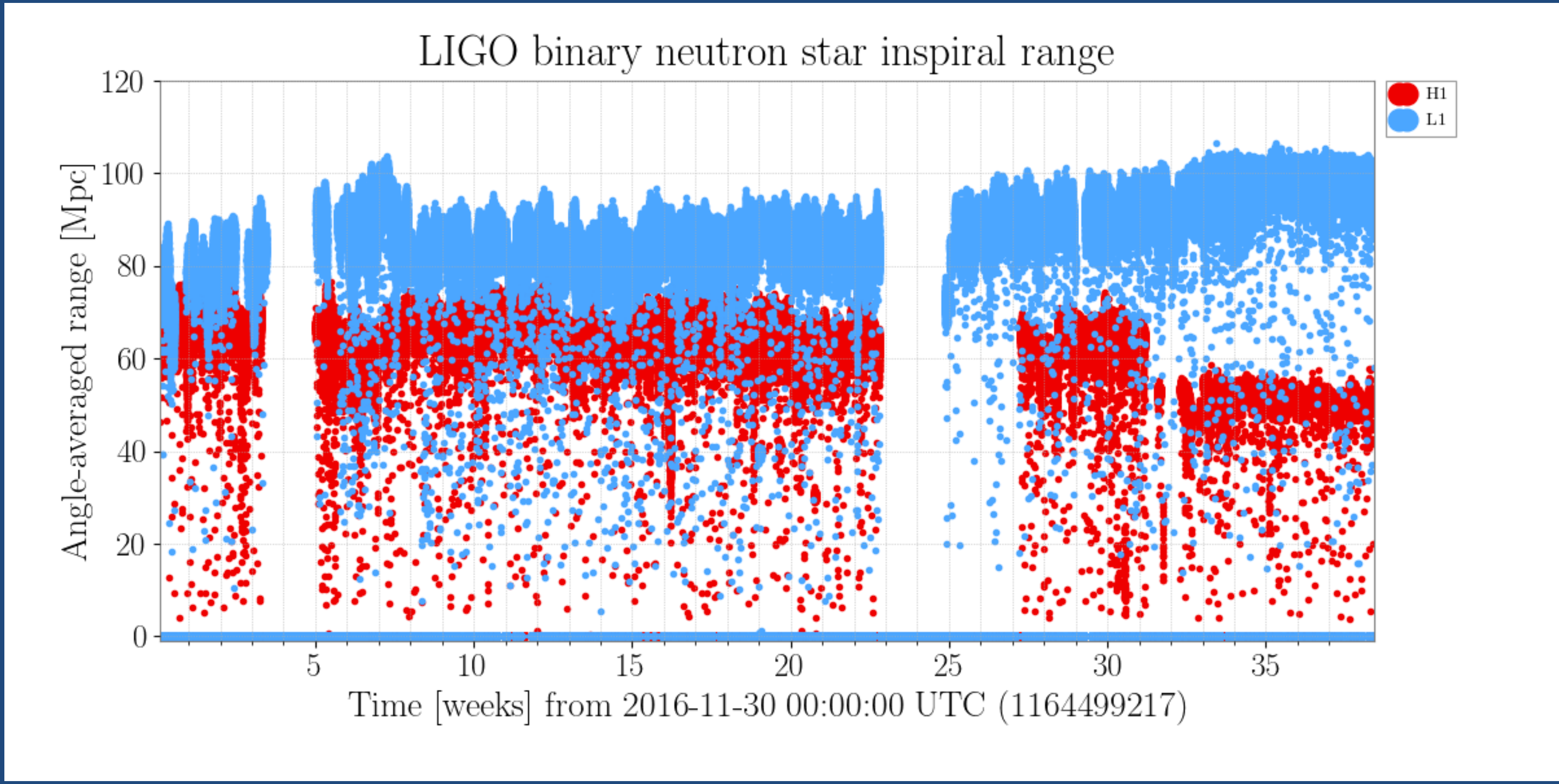

$D_h \sim M_{chirp}^{5/6}$

LIGO/Virgo/GEO-600 O3

- 03/04/2019 --

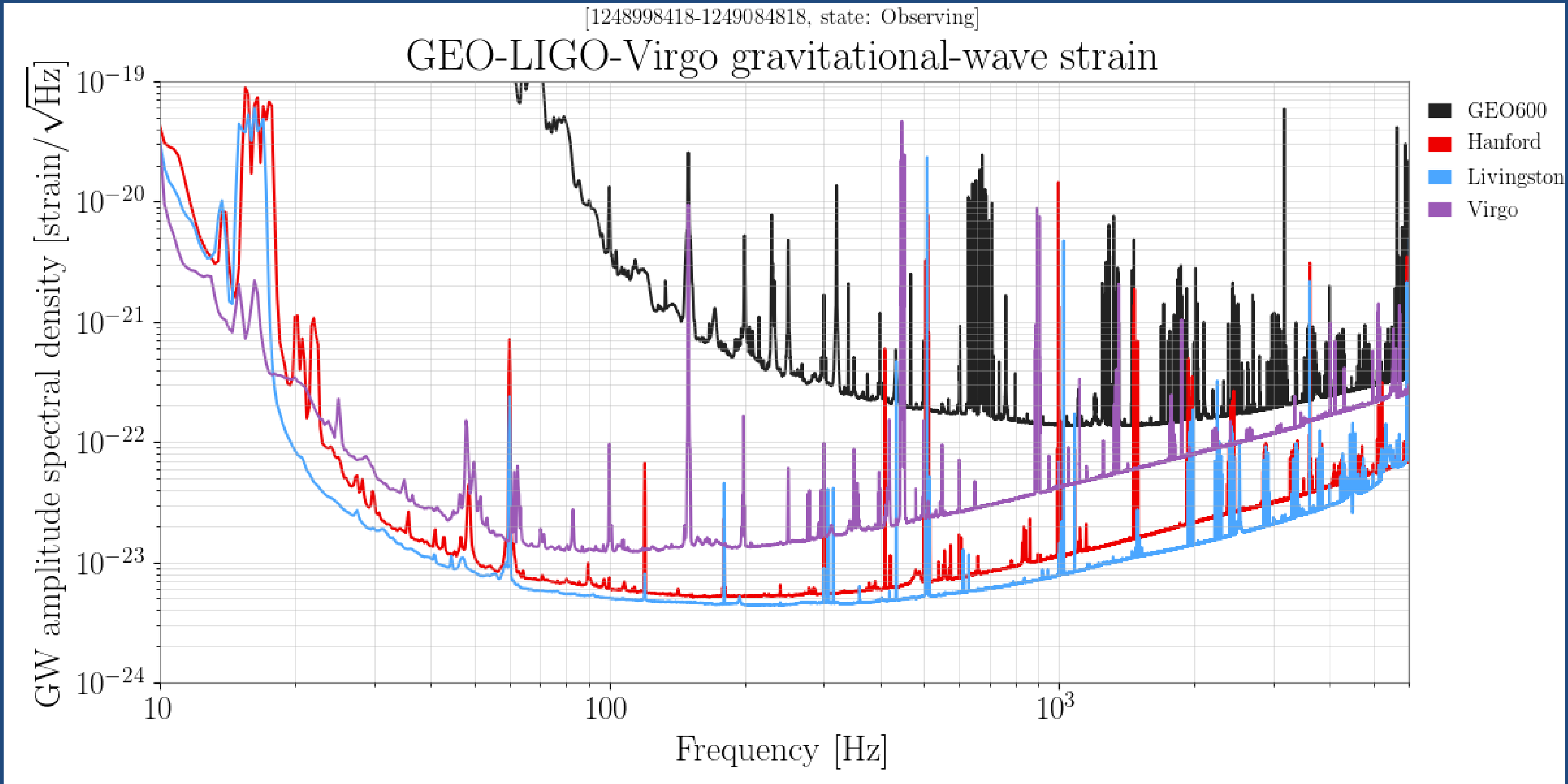

Current Detection horizon

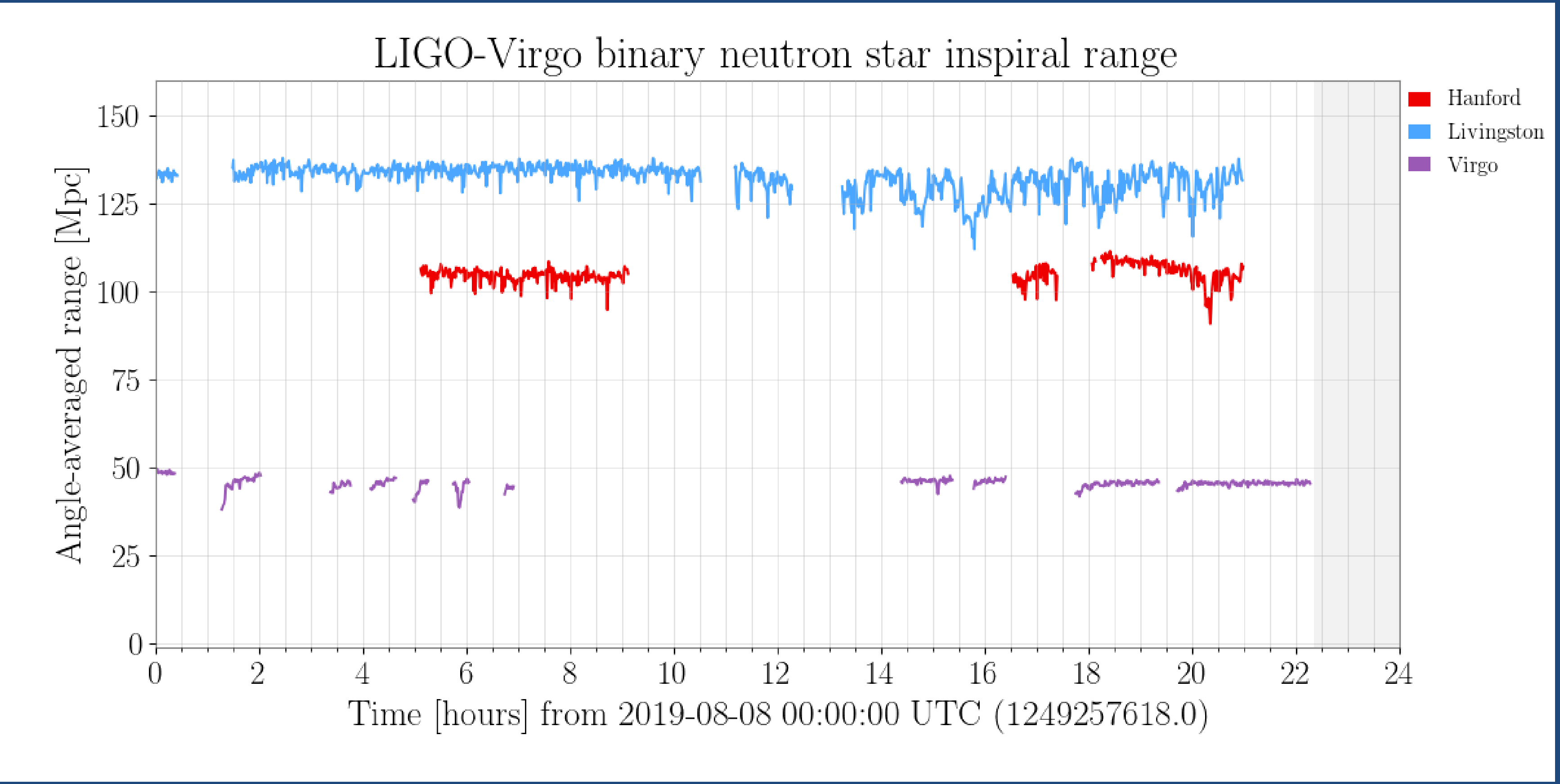

$D_h \sim M_{chirp}^{5/6}$

https://www.gw-openscience.org/

Binary BH mergings

Binary Black Hole Mergers

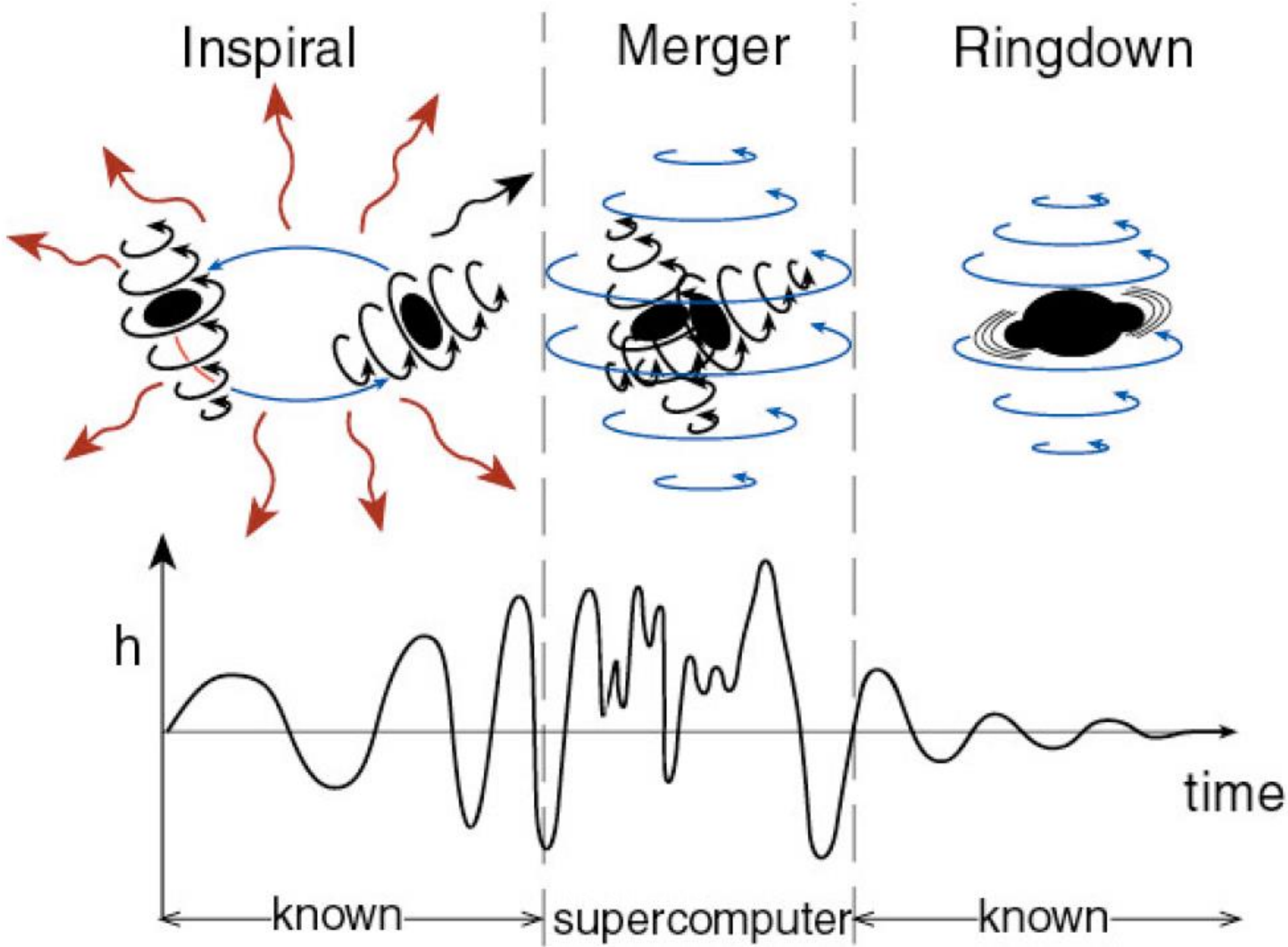

1) Inspiraling phase

$$h_k = F_k^{(+)} h_+ + F_k^{(\times)} h_\times$$

$$h_+(t) = A_{\rm GW}(t)\left(1+\cos^2\iota\right)\cos\phi_{\rm GW}(t)\,,$$
$$h_\times(t) = -2A_{\rm GW}(t)\cos\iota\sin\phi_{\rm GW}(t)\,,$$

- Depends on chirp mass only (in main order in v/c ~ 0.2-0.5 for GW150914)

$$\mathcal{M} = \frac{(m_1 m_2)^{3/5}}{M^{1/5}} \simeq \frac{c^3}{G}\left[\frac{5}{96}\pi^{-8/3} f^{-11/3}\dot{f}\right]^{3/5}$$

⇒ Chirp mass determination (the most accurate parameter)

2) Merging phase

- Frequency at the peak luminosity is determined by total mass f_lim~1/M
- Total mass and chirp mass ➔ mass ratio
- Amplitude is determined by the chirp mass:

$$h(f,\mathcal{M},r) = (\langle h_+^2\rangle + \langle h_\times^2\rangle)^{1/2} = \left(\frac{32}{5}\right)^{1/2} \frac{G^{5/3}}{c^4}\frac{\mathcal{M}^{5/3}}{r}(\pi f)^{2/3}$$

- [Frequency]=[mass]$^{-1}$ ➔ frequency redshift (1+z) ⇔ mass rescaling: $m_{det}=(1+z)m_{source}$ ➔ $h\sim m_s/d_m=m_d/(1+z)d_m=m_d/d_l$ ➔ **Photometric distance from GW observations only!**

132 Hz

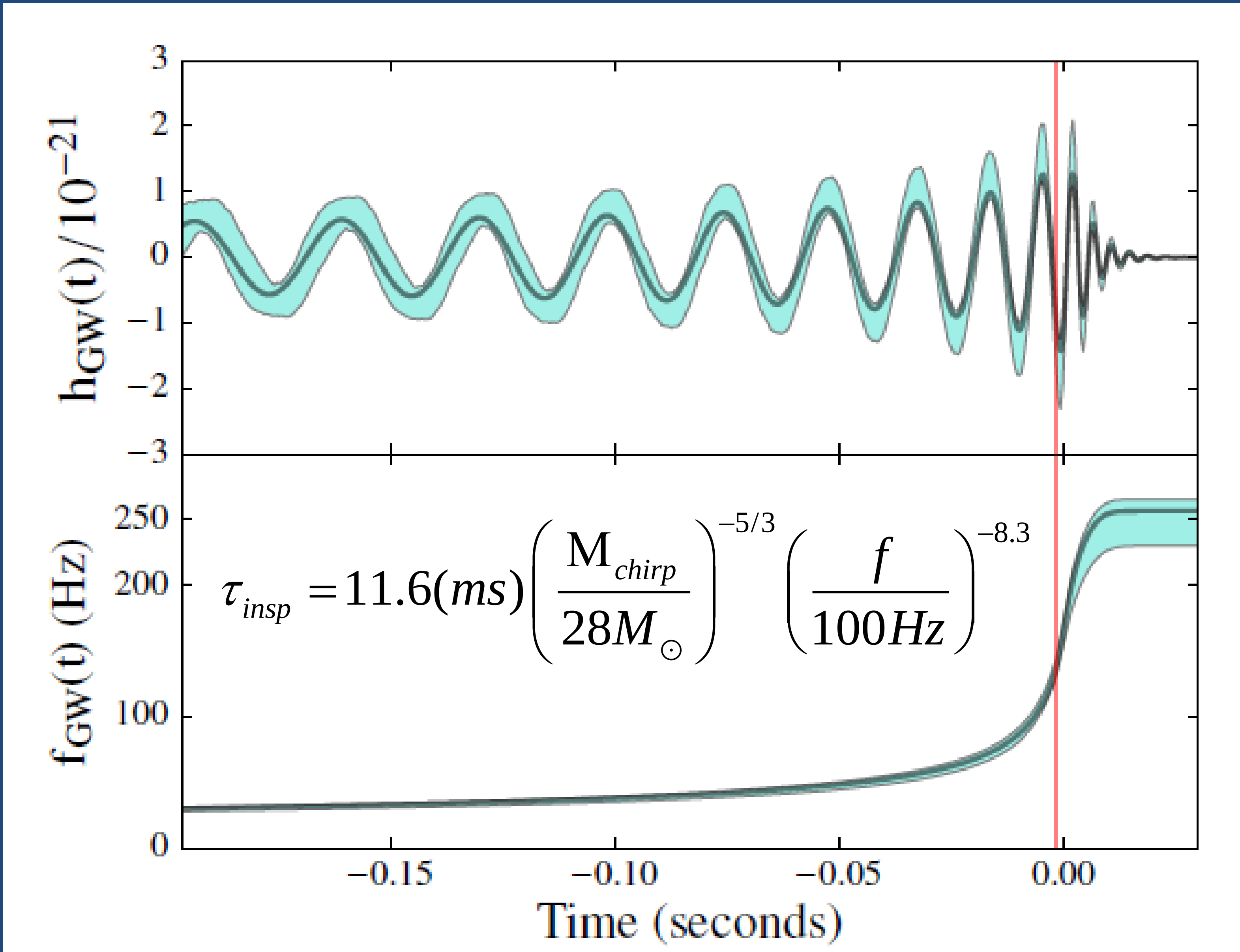

$$\tau_{insp} = 11.6(ms)\left(\frac{M_{chirp}}{28M_{\odot}}\right)^{-5/3}\left(\frac{f}{100Hz}\right)^{-8.3}$$

3) Ring-down phase

- Proper oscillations of BH horizon (Starobinsky, Chandrasekhar) → information on the BH mass → GR tests
- Deviations from GR < a few %

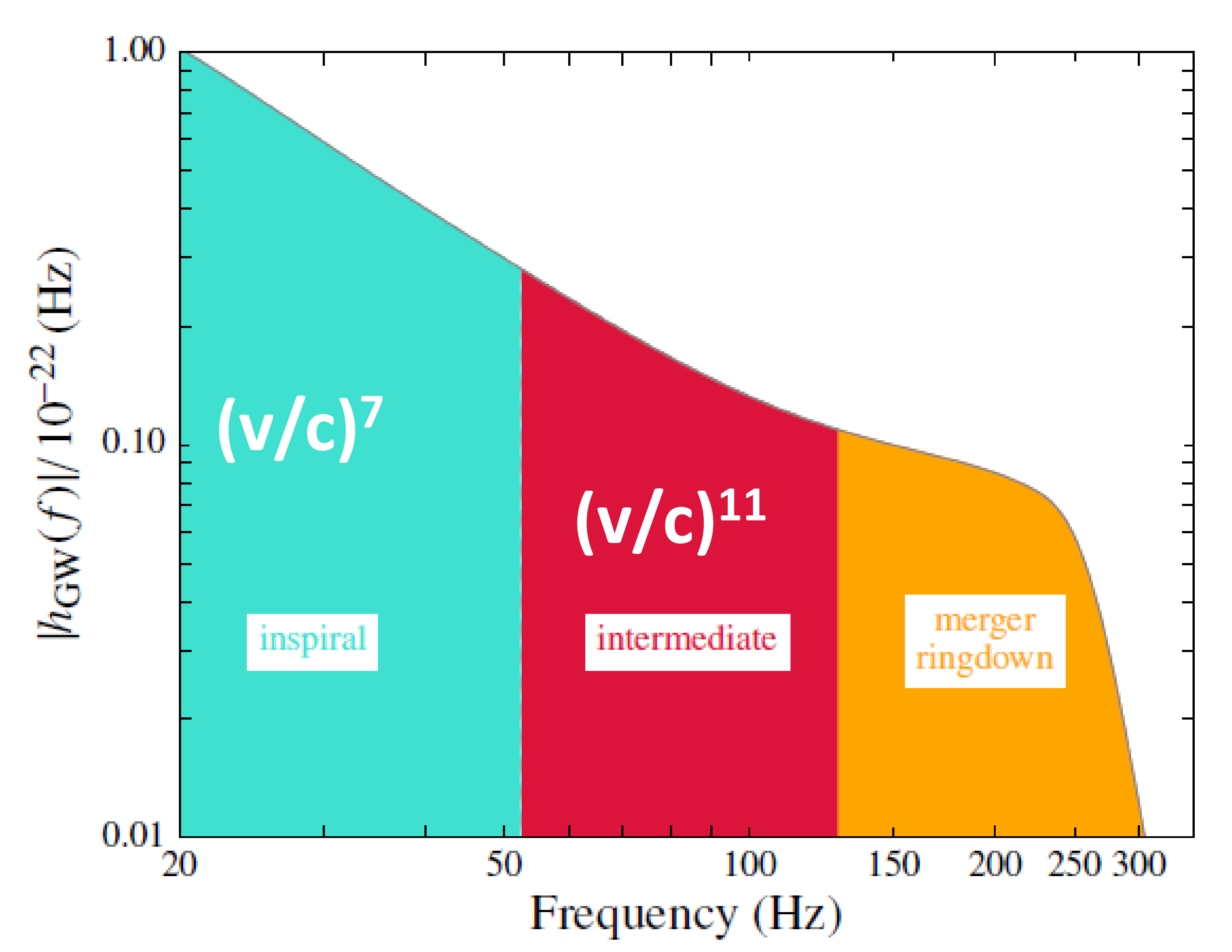
1.00
0.10
0.01
20
50
100
150
200
250
300
Frequency (Hz)
|hGW(f)|/ 10−22 (Hz)
(v/c)7
(v/c)11
inspiral
intermediate
merger
ringdown

h=h(f) f

GW 150914 template vs observations: 94(+2/-3)%

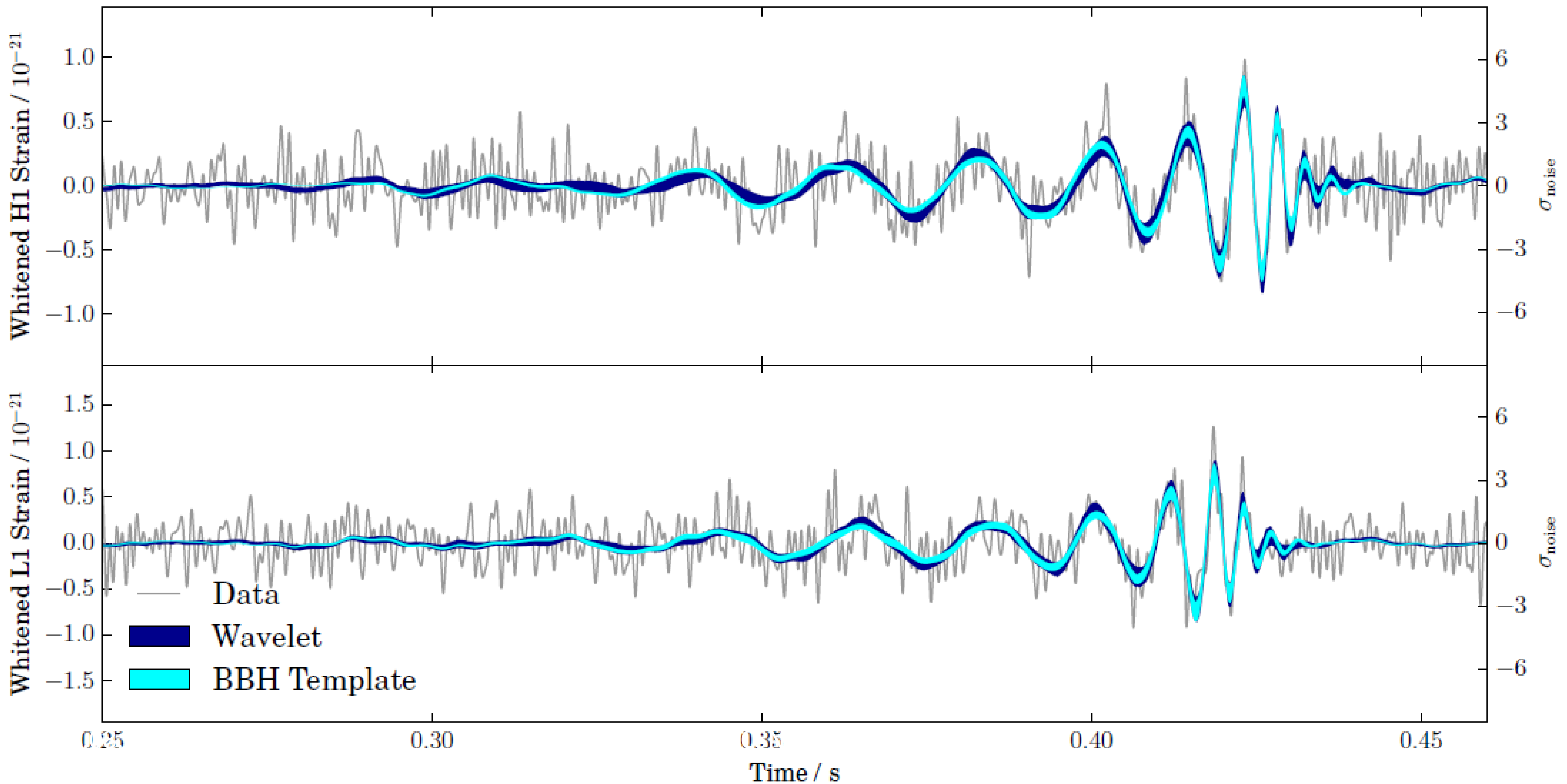

LIGO BHs

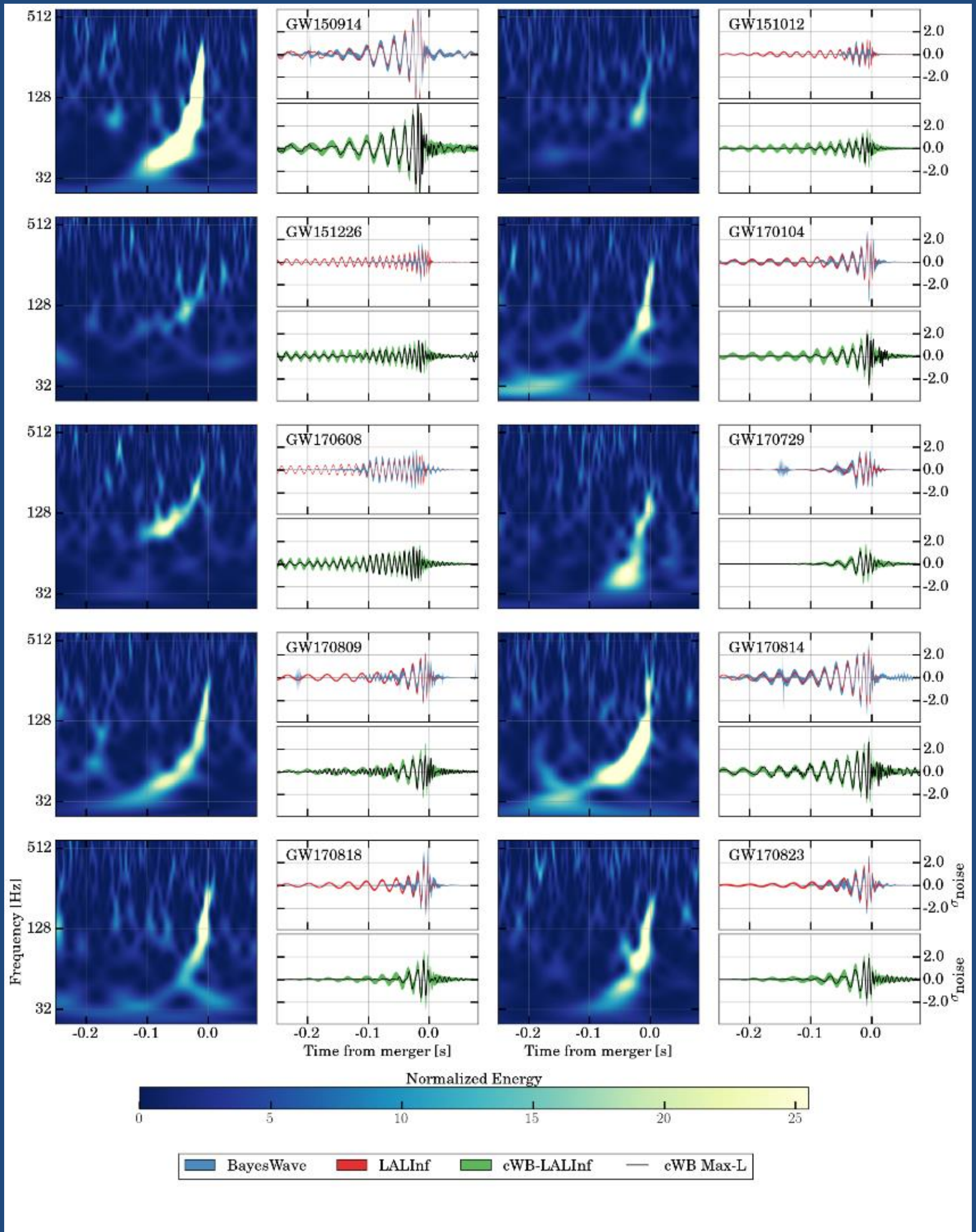

GWTC-1 Catalog arXiv:1811.12907

Parameters from GW observations

$$\mathcal{M} = \frac{(m_1 m_2)^{3/5}}{M^{1/5}}$$

Chirp mass

$$\chi_{\rm eff} = \frac{(m_1 \vec{\chi}_1 + m_2 \vec{\chi}_2) \cdot \hat{L}_N}{M}$$

Effective spin

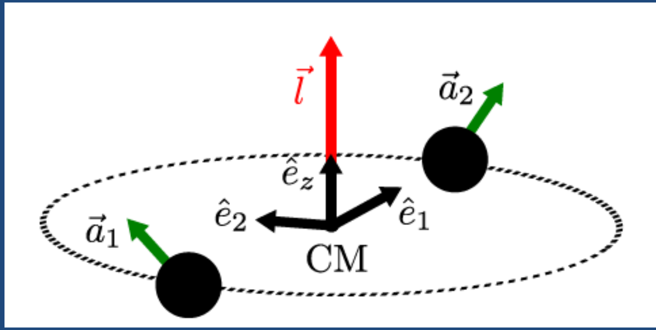

Event	$m_1/\mathrm{M}_\odot$	$m_2/\mathrm{M}_\odot$	$\mathcal{M}/\mathrm{M}_\odot$	$\chi_{\rm eff}$	$M_{\rm f}/\mathrm{M}_\odot$	$a_{\rm f}$	$E_{\rm rad}/(\mathrm{M}_\odot c^2)$	$\ell_{\rm peak}/(\mathrm{erg\,s}^{-1})$	d_L/Mpc	z	$\Delta\Omega/\mathrm{deg}^2$
GW150914	$35.6^{+4.8}_{-3.0}$	$30.6^{+3.0}_{-4.4}$	$28.6^{+1.6}_{-1.5}$	$-0.01^{+0.12}_{-0.13}$	$63.1^{+3.3}_{-3.0}$	$0.69^{+0.05}_{-0.04}$	$3.1^{+0.4}_{-0.4}$	$3.6^{+0.4}_{-0.4} \times 10^{56}$	430^{+150}_{-170}	$0.09^{+0.03}_{-0.03}$	180
GW151012	$23.3^{+14.0}_{-5.5}$	$13.6^{+4.1}_{-4.8}$	$15.2^{+2.0}_{-1.1}$	$0.04^{+0.28}_{-0.19}$	$35.7^{+9.9}_{-3.8}$	$0.67^{+0.13}_{-0.11}$	$1.5^{+0.5}_{-0.5}$	$3.2^{+0.8}_{-1.7} \times 10^{56}$	1060^{+540}_{-480}	$0.21^{+0.09}_{-0.09}$	1555
GW151226	$13.7^{+8.8}_{-3.2}$	$7.7^{+2.2}_{-2.6}$	$8.9^{+0.3}_{-0.3}$	$0.18^{+0.20}_{-0.12}$	$20.5^{+6.4}_{-1.5}$	$0.74^{+0.07}_{-0.05}$	$1.0^{+0.1}_{-0.2}$	$3.4^{+0.7}_{-1.7} \times 10^{56}$	440^{+180}_{-190}	$0.09^{+0.04}_{-0.04}$	1033
GW170104	$31.0^{+7.2}_{-5.6}$	$20.1^{+4.9}_{-4.5}$	$21.5^{+2.1}_{-1.7}$	$-0.04^{+0.17}_{-0.20}$	$49.1^{+5.2}_{-3.9}$	$0.66^{+0.08}_{-0.10}$	$2.2^{+0.5}_{-0.5}$	$3.3^{+0.6}_{-0.9} \times 10^{56}$	960^{+430}_{-410}	$0.19^{+0.07}_{-0.08}$	924
GW170608	$10.9^{+5.3}_{-1.7}$	$7.6^{+1.3}_{-2.1}$	$7.9^{+0.2}_{-0.2}$	$0.03^{+0.19}_{-0.07}$	$17.8^{+3.2}_{-0.7}$	$0.69^{+0.04}_{-0.04}$	$0.9^{+0.05}_{-0.1}$	$3.5^{+0.4}_{-1.3} \times 10^{56}$	320^{+120}_{-110}	$0.07^{+0.02}_{-0.02}$	396
GW170729	$50.6^{+16.6}_{-10.2}$	$34.3^{+9.1}_{-10.1}$	$35.7^{+6.5}_{-4.7}$	$0.36^{+0.21}_{-0.25}$	$80.3^{+14.6}_{-10.2}$	$0.81^{+0.07}_{-0.13}$	$4.8^{+1.7}_{-1.7}$	$4.2^{+0.9}_{-1.5} \times 10^{56}$	2750^{+1350}_{-1320}	$0.48^{+0.19}_{-0.20}$	1033
GW170809	$35.2^{+8.3}_{-6.0}$	$23.8^{+5.2}_{-5.1}$	$25.0^{+2.1}_{-1.6}$	$0.07^{+0.16}_{-0.16}$	$56.4^{+5.2}_{-3.7}$	$0.70^{+0.08}_{-0.09}$	$2.7^{+0.6}_{-0.6}$	$3.5^{+0.6}_{-0.9} \times 10^{56}$	990^{+320}_{-380}	$0.20^{+0.05}_{-0.07}$	340
GW170814	$30.7^{+5.7}_{-3.0}$	$25.3^{+2.9}_{-4.1}$	$24.2^{+1.4}_{-1.1}$	$0.07^{+0.12}_{-0.11}$	$53.4^{+3.2}_{-2.4}$	$0.72^{+0.07}_{-0.05}$	$2.7^{+0.4}_{-0.3}$	$3.7^{+0.4}_{-0.5} \times 10^{56}$	580^{+160}_{-210}	$0.12^{+0.03}_{-0.04}$	87
GW170817	$1.46^{+0.12}_{-0.10}$	$1.27^{+0.09}_{-0.09}$	$1.186^{+0.001}_{-0.001}$	$0.00^{+0.02}_{-0.01}$	≤ 2.8	≤ 0.89	≥ 0.04	$\geq 0.1 \times 10^{56}$	40^{+10}_{-10}	$0.01^{+0.00}_{-0.00}$	16
GW170818	$35.5^{+7.5}_{-4.7}$	$26.8^{+4.3}_{-5.2}$	$26.7^{+2.1}_{-1.7}$	$-0.09^{+0.18}_{-0.21}$	$59.8^{+4.8}_{-3.8}$	$0.67^{+0.07}_{-0.08}$	$2.7^{+0.5}_{-0.5}$	$3.4^{+0.5}_{-0.7} \times 10^{56}$	1020^{+430}_{-360}	$0.20^{+0.07}_{-0.07}$	39
GW170823	$39.6^{+10.0}_{-6.6}$	$29.4^{+6.3}_{-7.1}$	$29.3^{+4.2}_{-3.2}$	$0.08^{+0.20}_{-0.22}$	$65.6^{+9.4}_{-6.6}$	$0.71^{+0.08}_{-0.10}$	$3.3^{+0.9}_{-0.8}$	$3.6^{+0.6}_{-0.9} \times 10^{56}$	1850^{+840}_{-840}	$0.34^{+0.13}_{-0.14}$	1651

LIGO BH: Masses

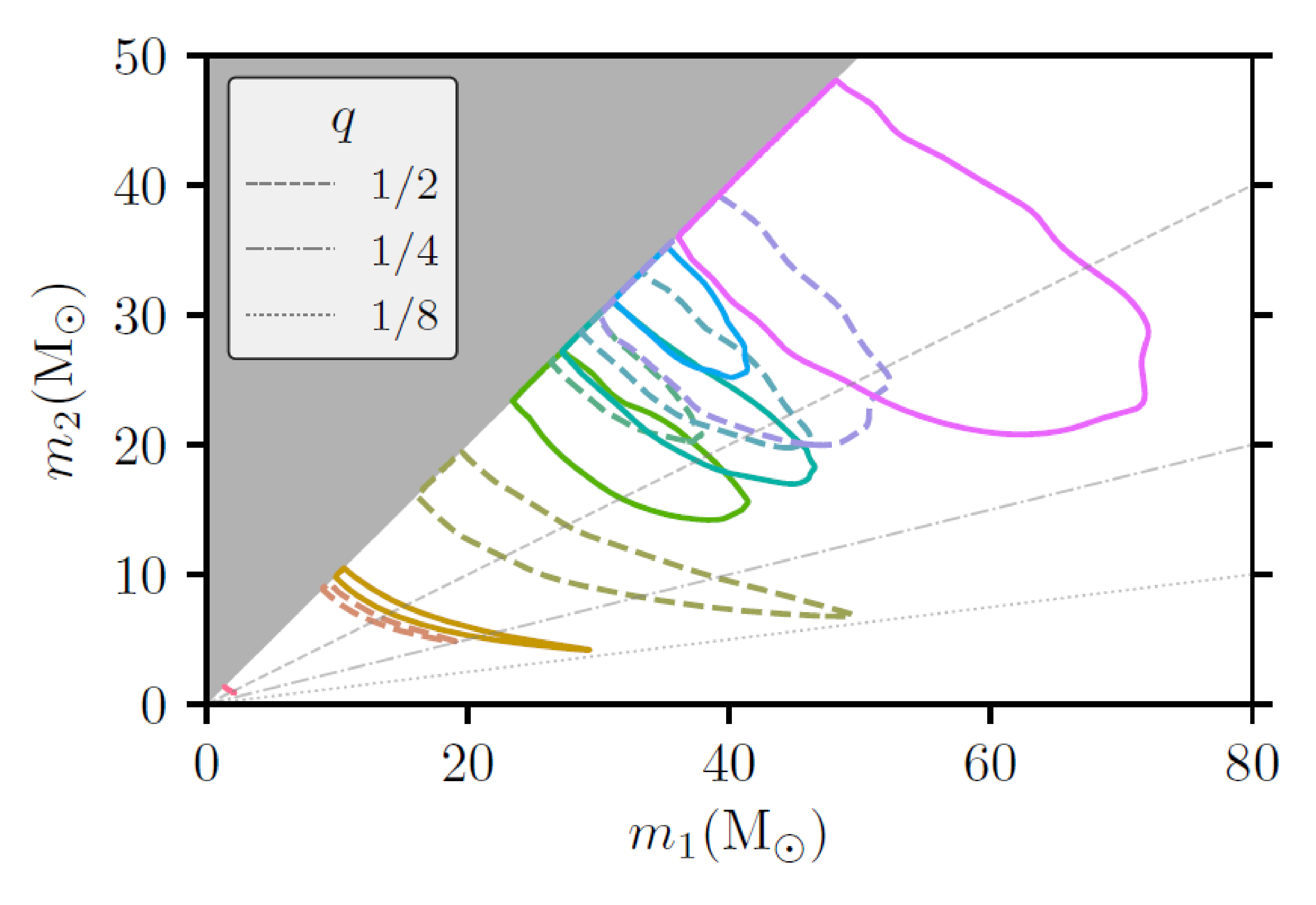

BH and NS masses

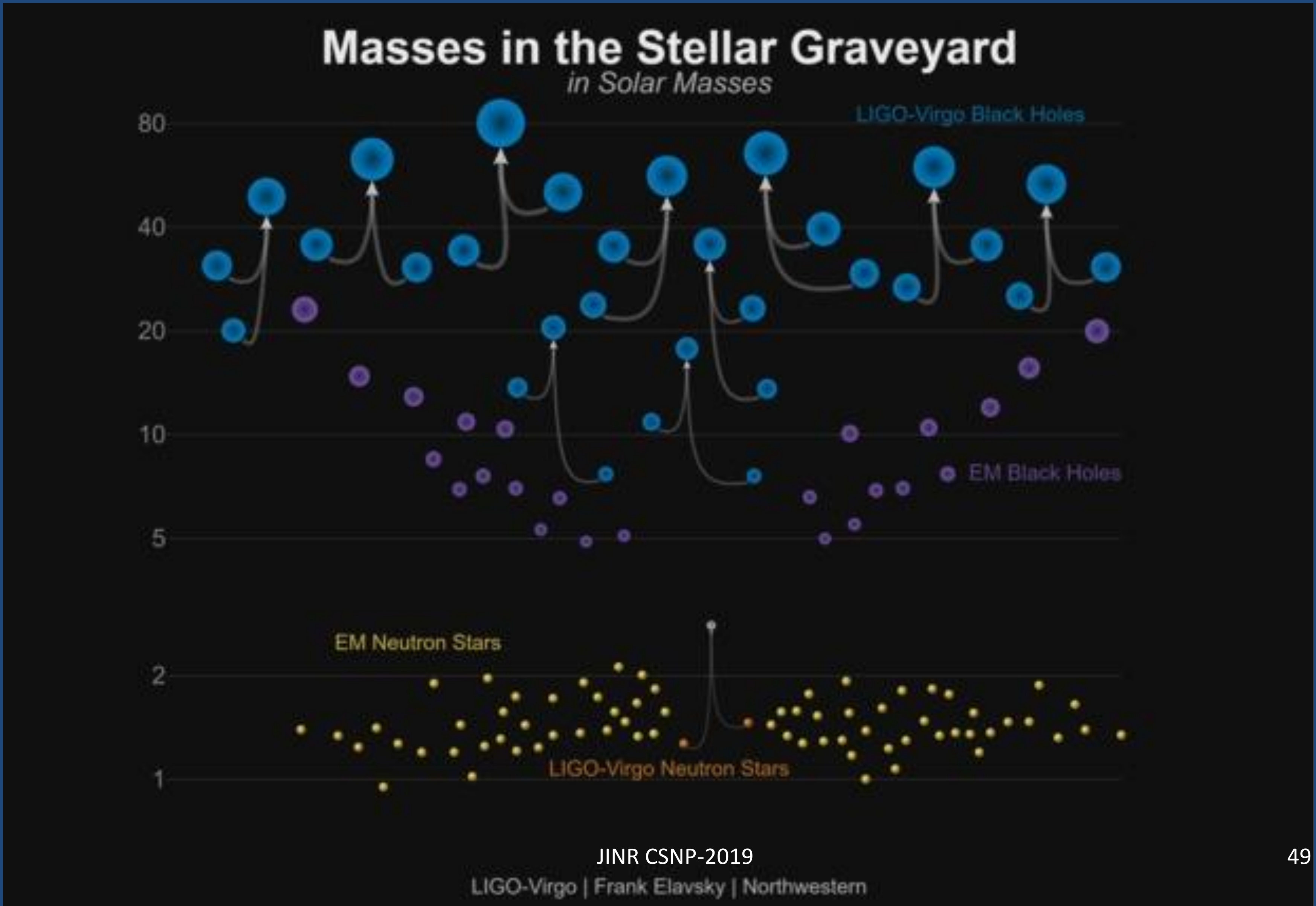

LIGO BH: effective spins

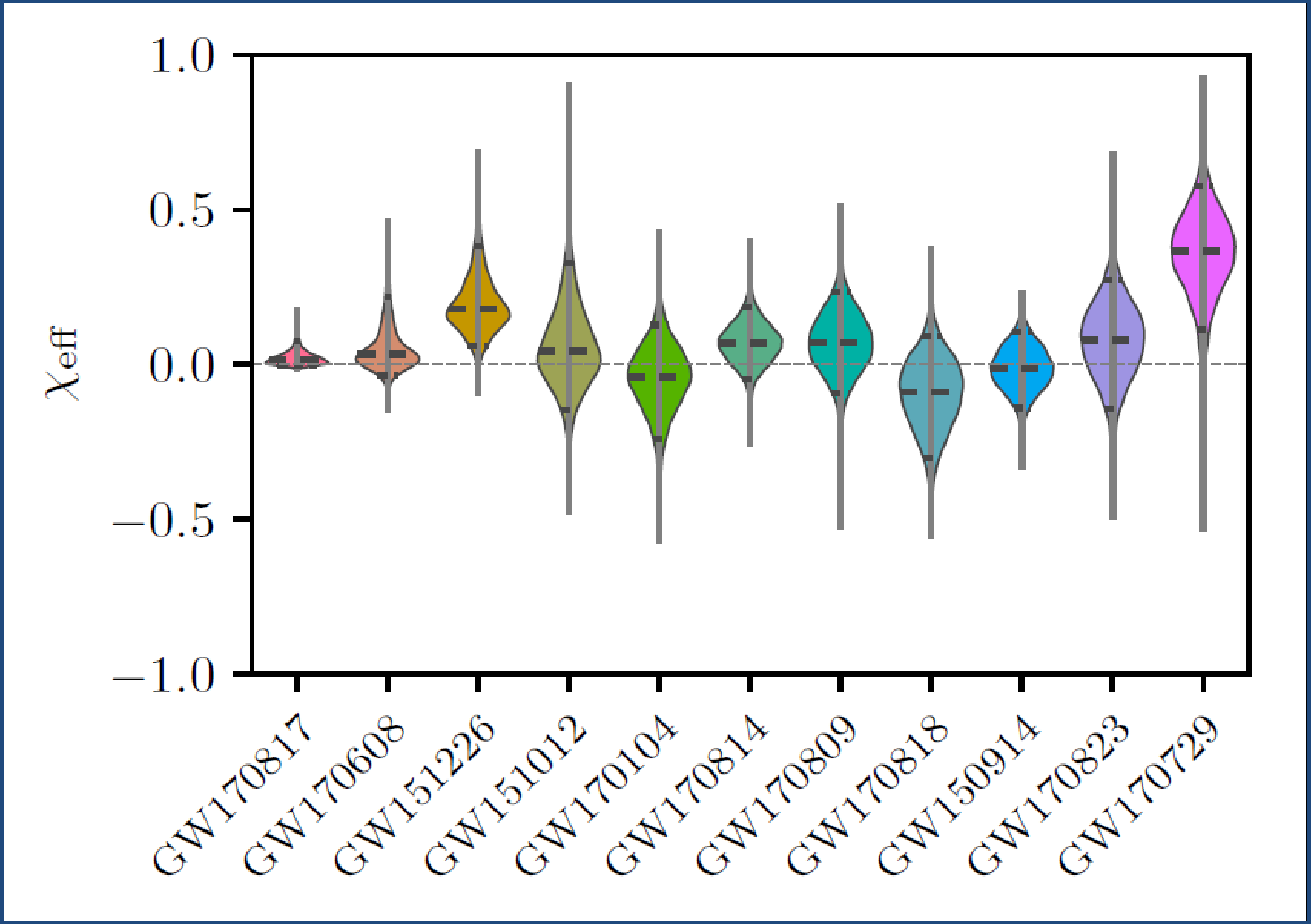

Corollary:

- Larger masses (compared to BHs in XRBs)
- Low effective spins (but GW170729 and possibly GW151226)

Independnent search for BH-Bh events in LIGO O1 (arXiv:1902.10331)

$P_{\rm astro} \sim 0.71$

	Flat $\chi_{\rm eff}$ prior	Isotropic spin prior
Chirp mass $\mathcal{M}^{\rm det}$	$31^{+2}_{-3}\,M_\odot$	$29^{+2}_{-2}\,M_\odot$
Primary mass m_1	$31^{+13}_{-6}\,M_\odot$	$38^{+11}_{-11}\,M_\odot$
Secondary mass m_2	$21^{+5}_{-6}\,M_\odot$	$16^{+6}_{-3}\,M_\odot$
Mass ratio m_2/m_1	$0.7^{+0.3}_{-0.3}$	$0.4^{+0.3}_{-0.1}$
Total mass M	$52^{+9}_{-6}\,M_\odot$	$54^{+10}_{-8}\,M_\odot$
Primary aligned spin χ_{1z}	$0.86^{+0.12}_{-0.27}$	$0.73^{+0.18}_{-0.28}$
Secondary aligned spin χ_{2z}	$0.79^{+0.19}_{-0.65}$	$0.30^{+0.51}_{-0.46}$
Effective aligned spin $\chi_{\rm eff}$	$0.81^{+0.15}_{-0.21}$	$0.60^{+0.16}_{-0.18}$
Cosine of inclination $\lvert\cos\iota\rvert$	$0.81^{+0.18}_{-0.52}$	$0.81^{+0.18}_{-0.51}$
Luminosity distance D_L	$2.4^{+1.2}_{-1.1}$ Gpc	$2.1^{+1.0}_{-0.9}$ Gpc
Source redshift z	$0.43^{+0.17}_{-0.17}$	$0.38^{+0.15}_{-0.15}$

TABLE I. Source properties for GW151216 : we give un-

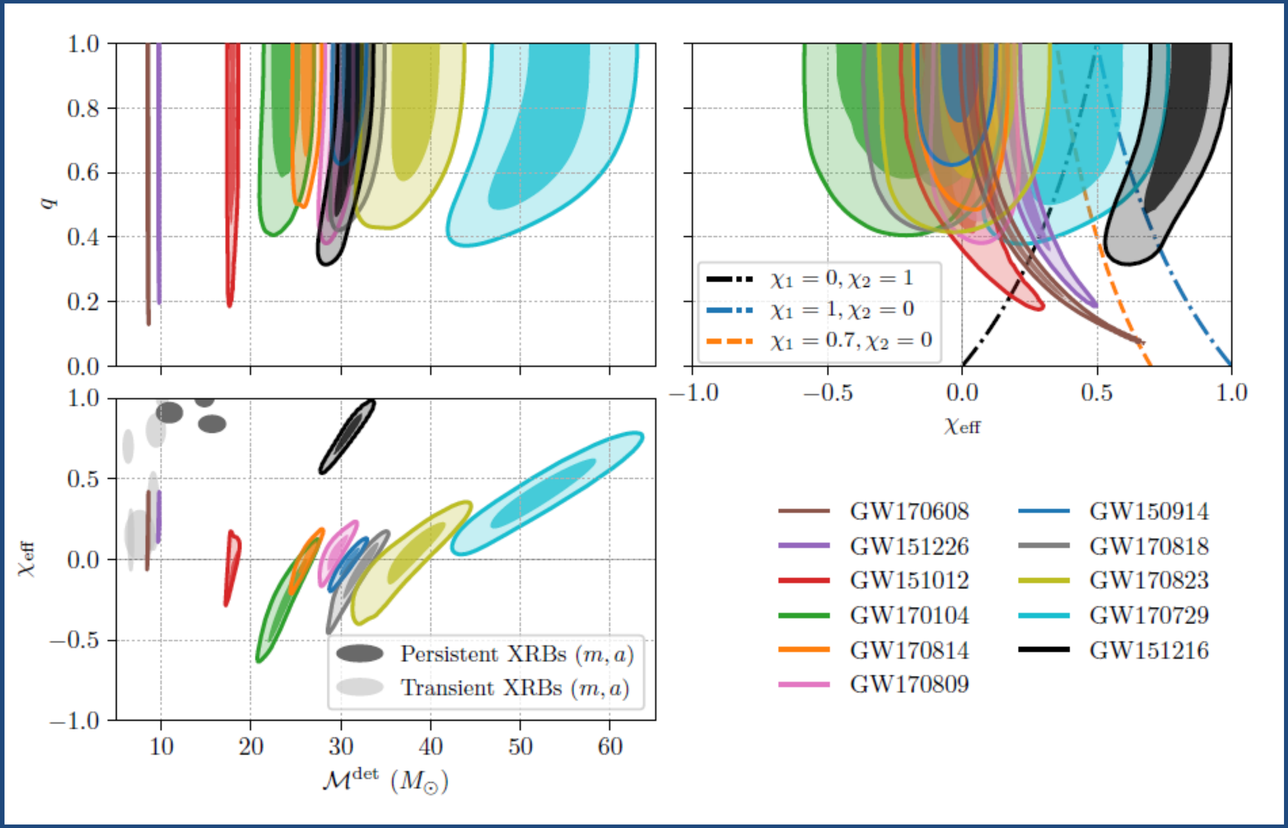

O3 detections

- 23 triggers, about 20 BH+BH, one possible NS+NS
- No electromagnetic counterparts so far

S190728q	BBH (95%), MassGap (5%)
S190727h	BBH (92%), Terrestrial (5%), MassGap (3%)
S190720a	BBH (99%), Terrestrial (1%)
S190718y	Terrestrial (98%), BNS (2%)
S190707q	BBH (>99%)
S190706ai	BBH (99%), Terrestrial (1%)
S190701ah	BBH (93%), Terrestrial (7%)
S190630ag	BBH (94%), MassGap (5%)
S190602aq	BBH (99%)
S190524q	Terrestrial (71%), BNS (29%)
S190521r	BBH (>99%)
S190521g	BBH (97%), Terrestrial (3%)
S190519bj	BBH (96%), Terrestrial (4%)
S190518bb	BNS (75%), Terrestrial (25%)
S190517h	BBH (98%), MassGap (2%)
S190513bm	BBH (94%), MassGap (5%)
S190512at	BBH (99%), Terrestrial (1%)
S190510g	Terrestrial (58%), BNS (42%)
S190503bf	BBH (96%), MassGap (3%)
S190426c	BNS (49%), MassGap (24%), Terrestrial (14%), NSBH (13%)
S190425z	BNS (>99%)
S190421ar	BBH (97%), Terrestrial (3%)
S190412m	BBH (>99%)
S190408an	BBH (>99%)
S190405ar	Terrestrial (>99%)

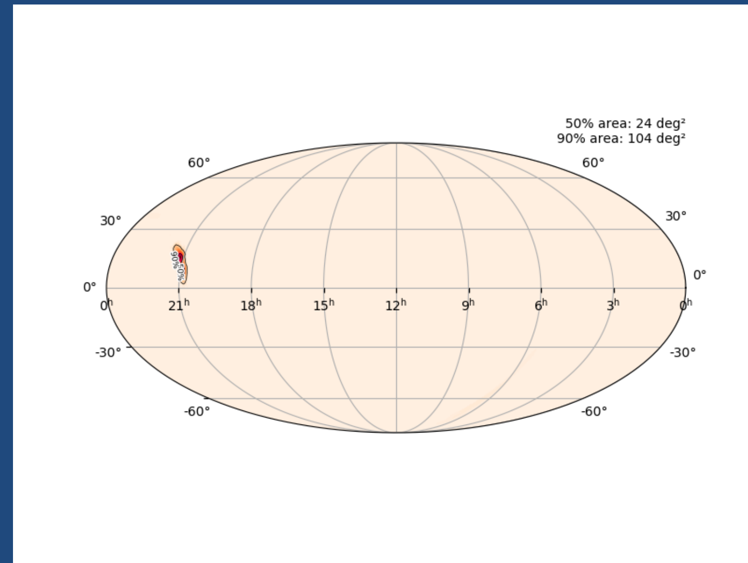

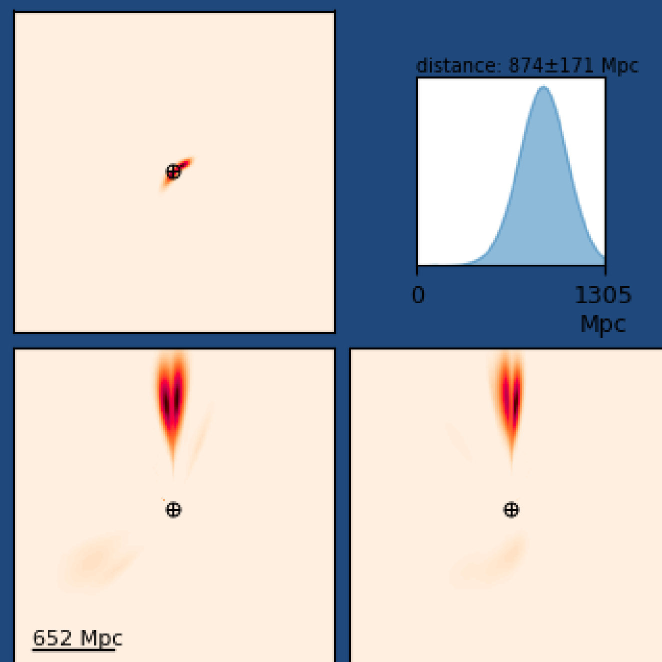

https://gracedb.ligo.org

Astrophysical binary BHs

- BH formation
  - Initial ZAMS mass
  - Initial rotation
  - Possible kick
- BH in binaries
  - From massive binary systems
  - In dense stellar clusters (dynamical)
  - Primordial BHs

BH formation from stars (solar metallicity)

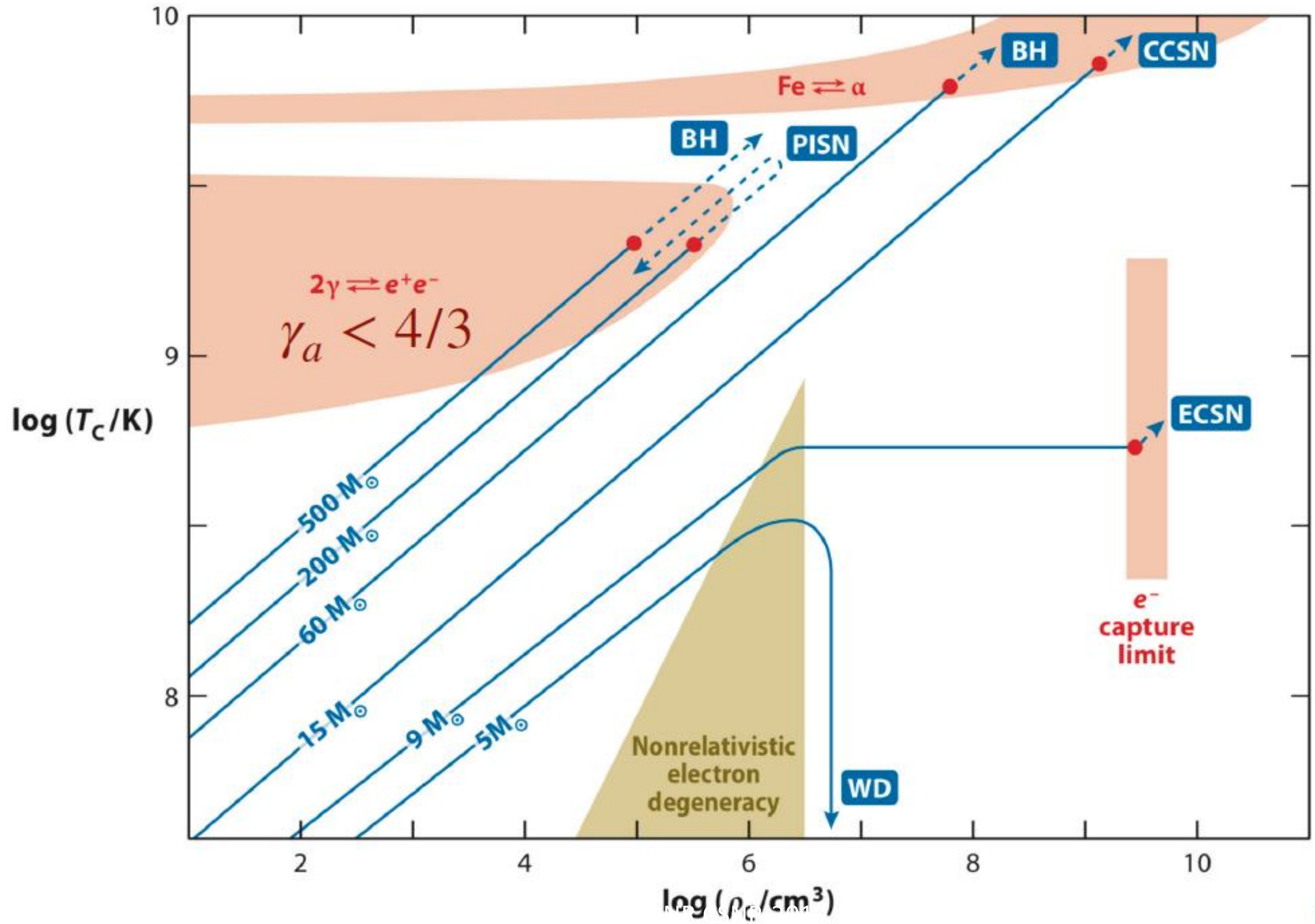

Langer (2012)

BH from massive stars

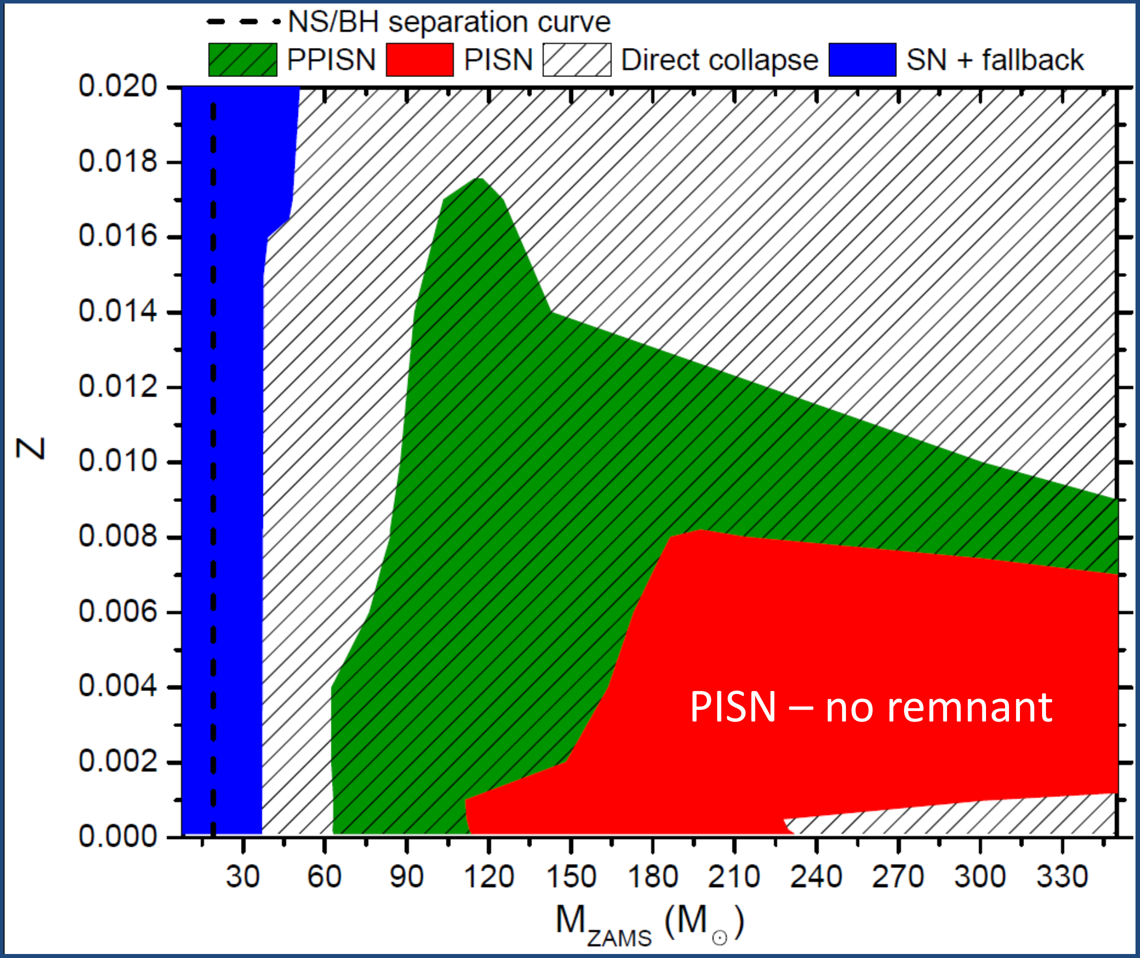

Spera,Mapelli 2017

Pair instability SNe (PISNe, Fowler & Hoyle 1964), pulsational PISNe (PPISNe) (Woosley 2017)

Dependence on the metallicity and stellar wind mass loss

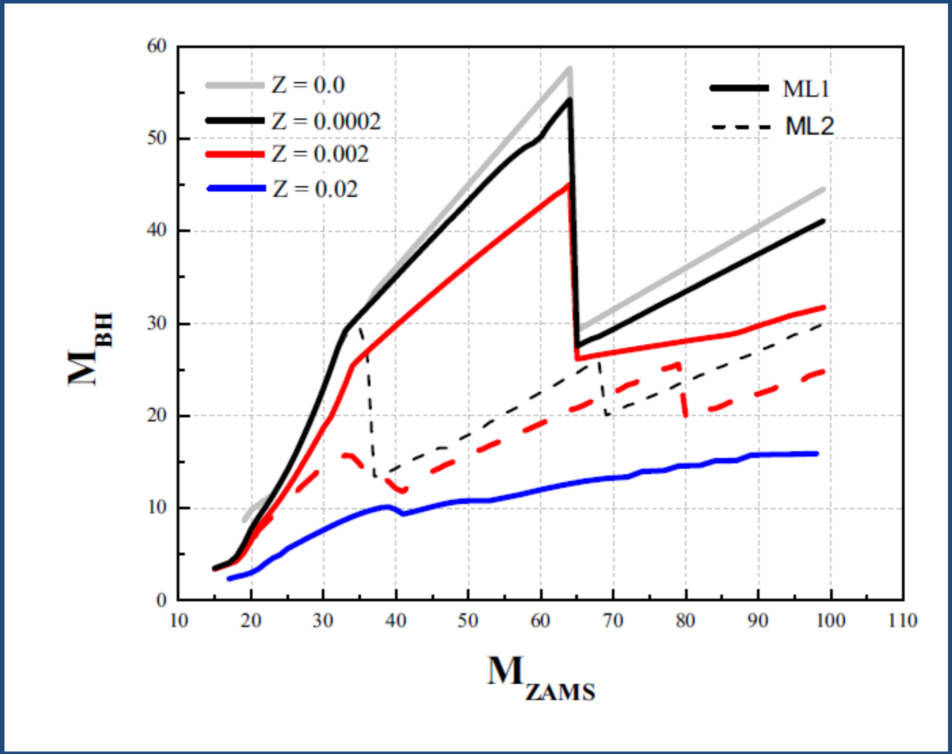

Fryer et al 2012, Giacobbo et al. 2018

Additional effects in binaries:

- Initial spin misalignment
- Tidal synchronization of the envelope
- Common envelope phase
- Star formation and metallicity history in galaxies

$$\Psi\left(z, \frac{Z}{Z_\odot}\right) = \psi(z)\Phi(Z/Z_\odot),$$

$$\Phi(Z/Z_\odot) = \frac{\hat{\Gamma}[0.84, (Z/Z_\odot)^2\, 10^{0.3z}]}{\Gamma(0.84)}$$

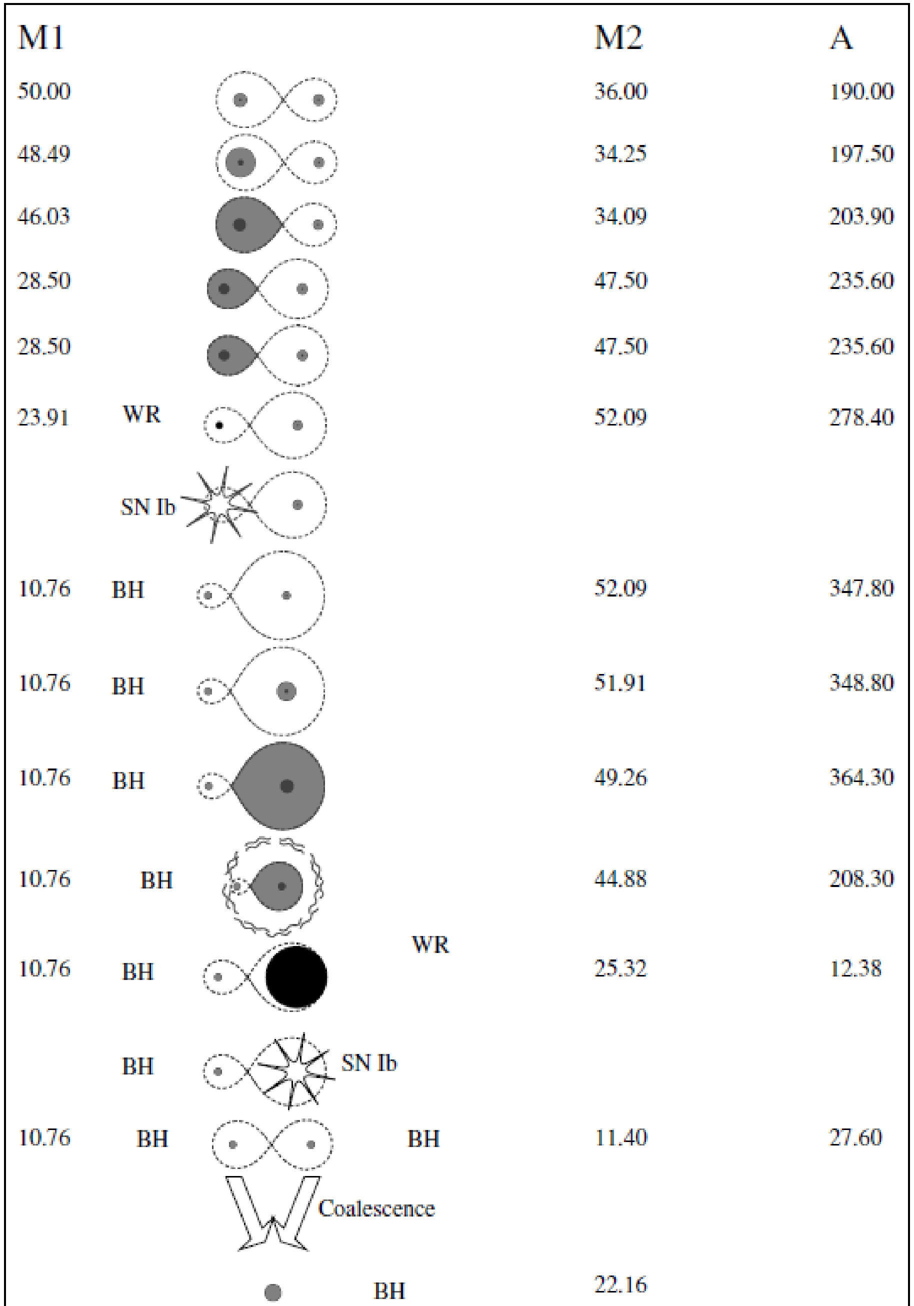

- Initial ZAMS mass
- Fraction of collapsed mass

$$k_{BH} = M_{BH}/M_*$$

- Possible kick

$$\frac{w_{BH}}{w_{NS}} = \frac{M_* - M_{BH}}{M_* - M_{OV}} = \frac{1 - k_{BH}}{1 - M_{OV}/M_*}$$

Tutukov, Yungelson 1993 MNRAS)
Lipunov, Postnov, Prokhorov 1997 MNRAS)

Mass and spin distributions before coalescence

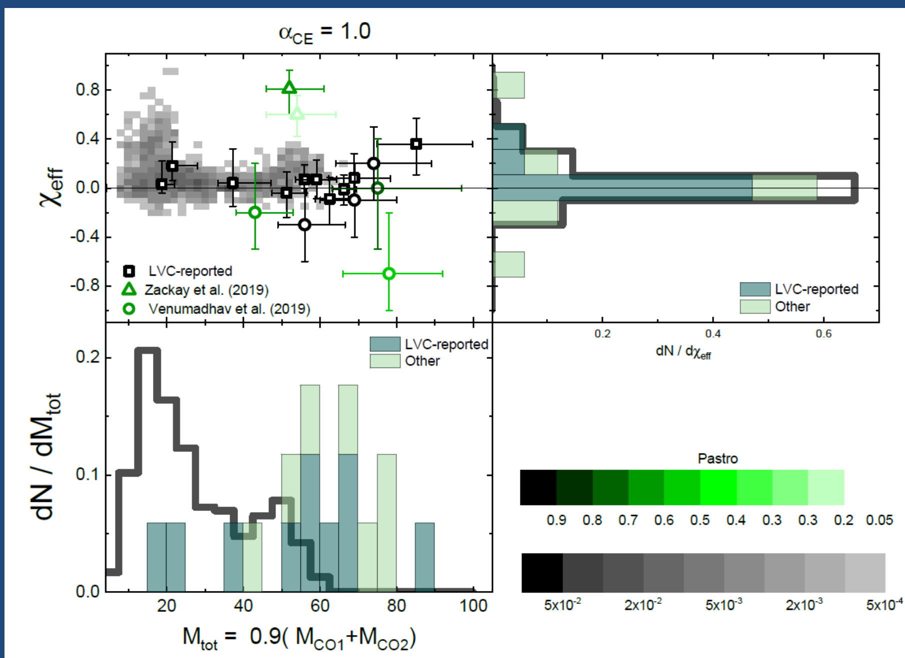

Without fallback

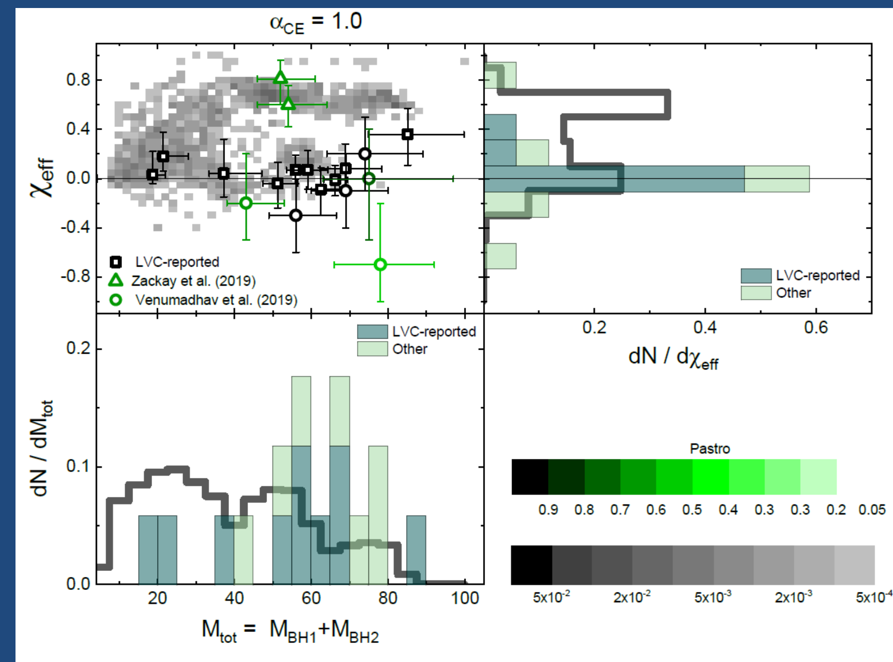

+ fallback from envelope

Postnov+ 2019, Physics-Uspekhi (in press)

MNRAS 483, 3288–3306 (2019)

BH+NS systems (not yet firmly observed)

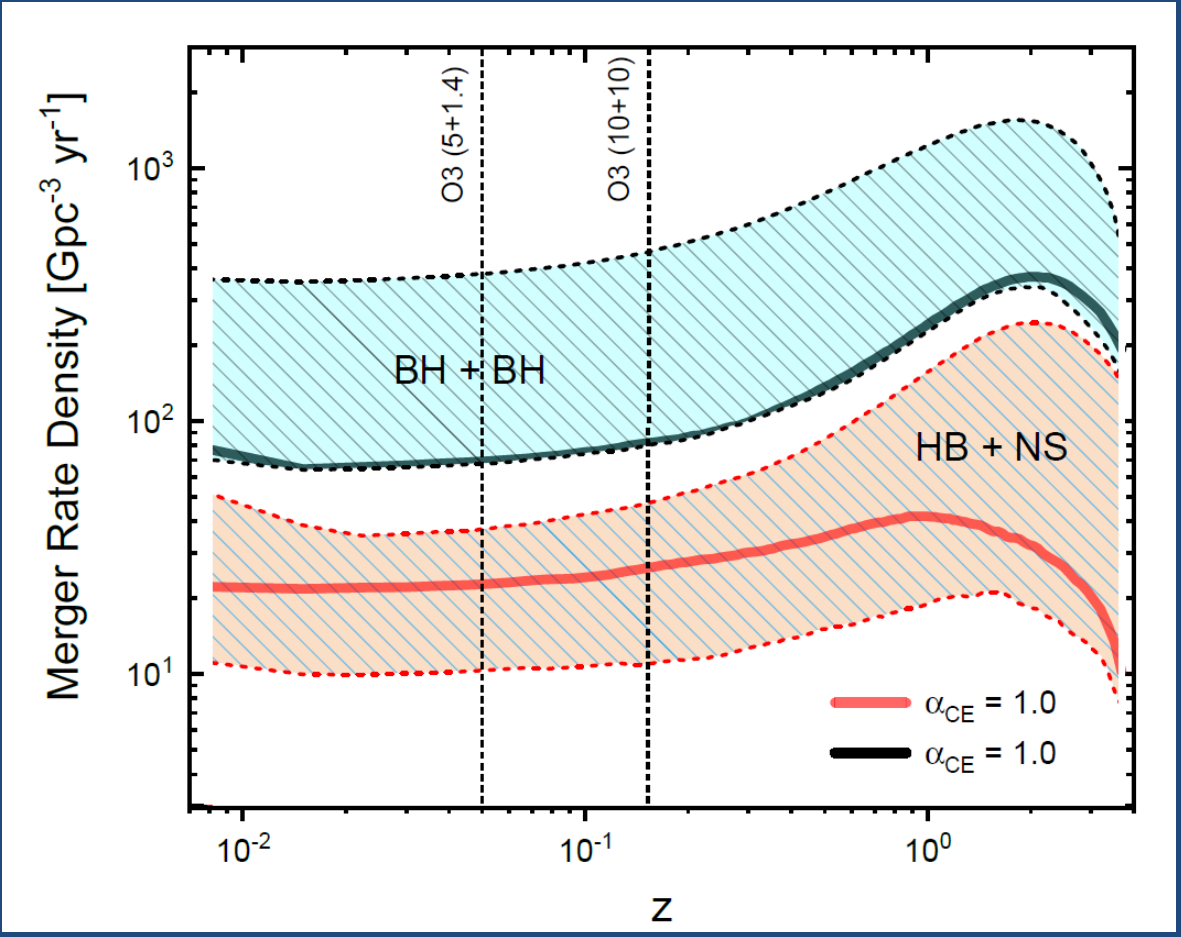

Detection rate BH+BH, BH+NS

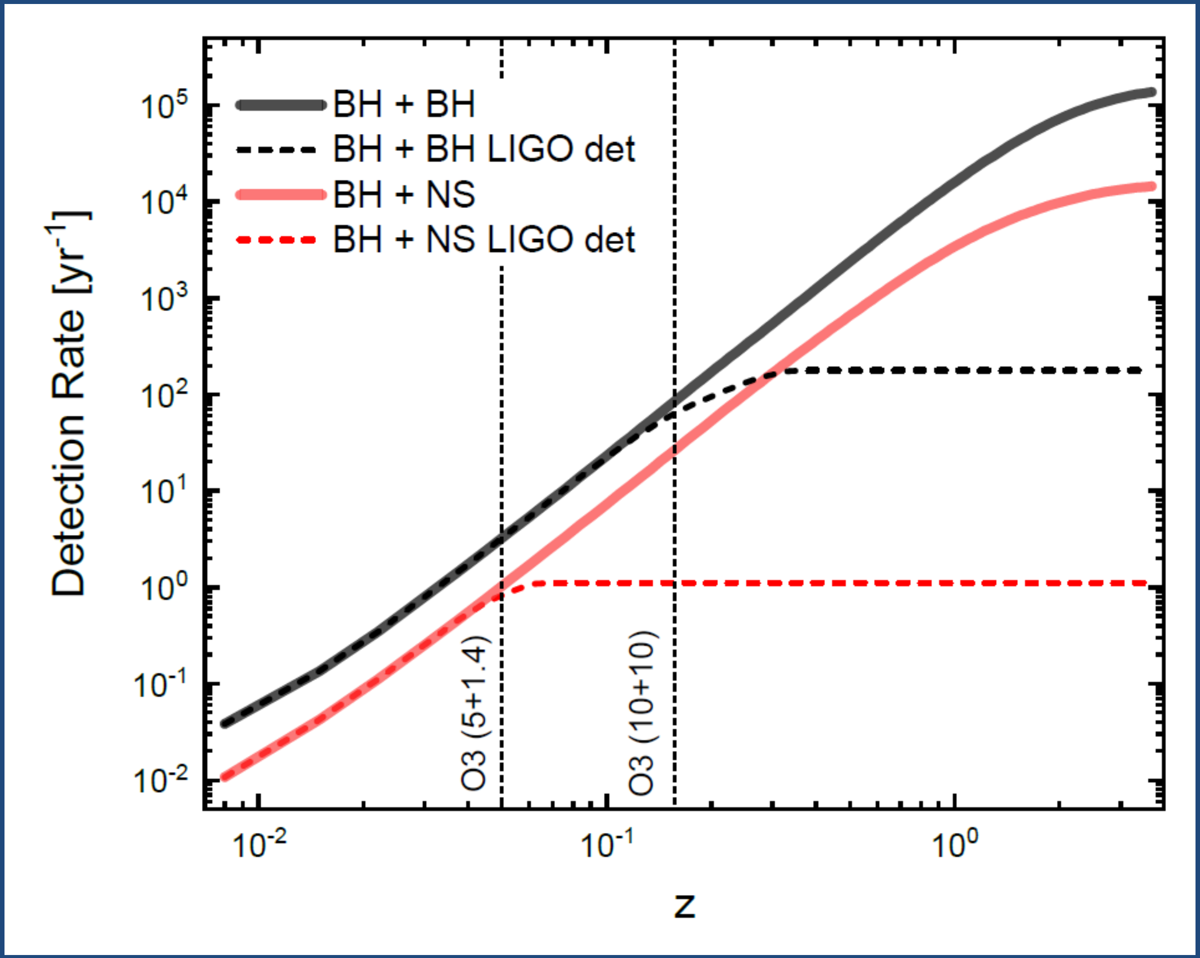

Effective spin/total mass distribution for BH+NS coalescing binaries

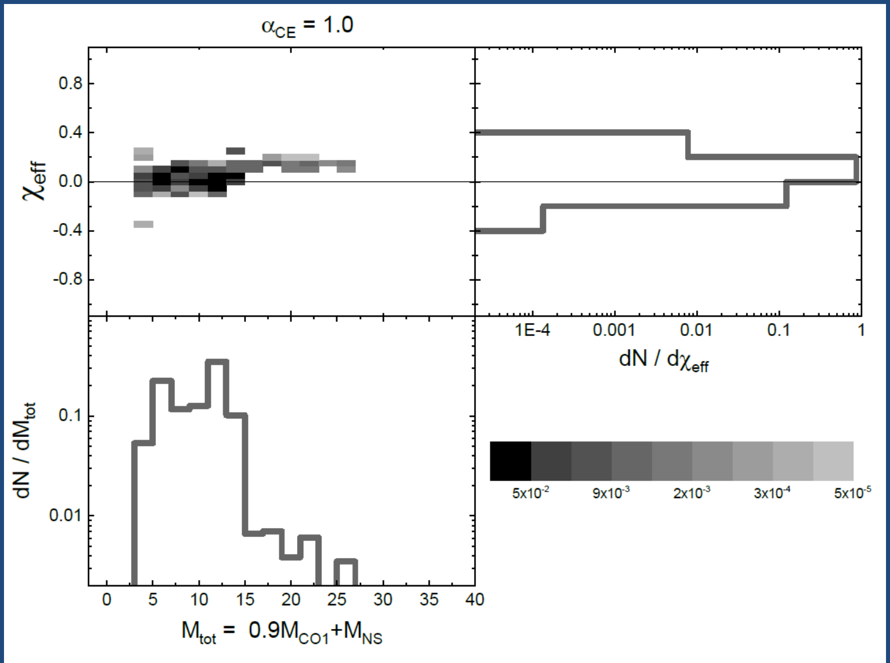

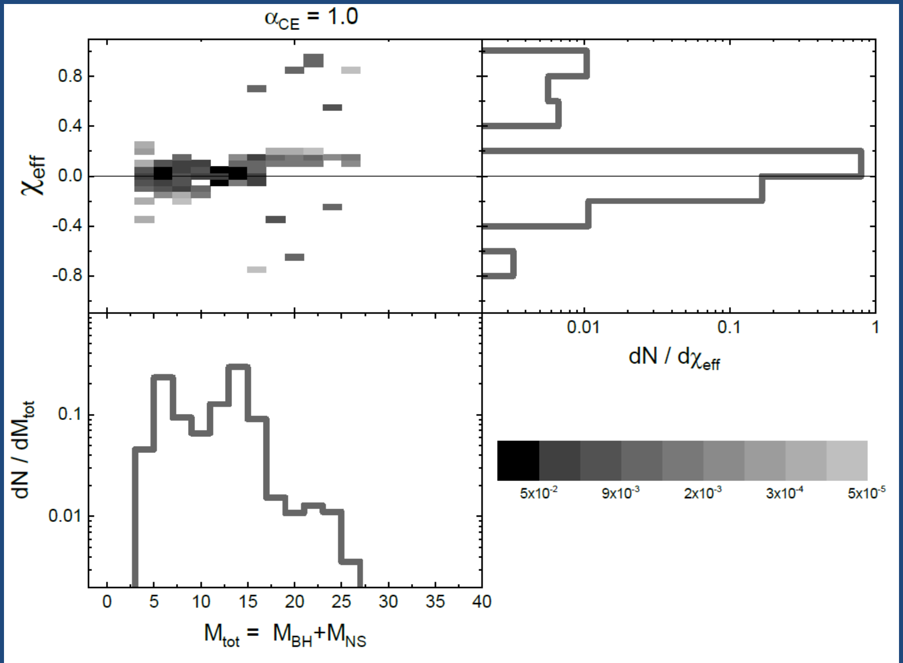

BH+BH: New physics ?

- Stellar-mass primordial black holes:
  - Can be formed in the early Universe in different models (Carr, Hawking'74)
  - Can be in binaries (Nakamura+'97)
  - Can naturally explain low spins of observed BH+BH (Bird+'16, Blinnikov+'16,…)
  - Can substantially contribute to dark matter
  - Can be seeds for growth of SMBH in galactic centers

- Present constraints on PBH abundance are very model-dependent
- Stellar evolution predicts maximum BH mass of about 50 $M_\odot$ (so far, LIGO/Virgo observations meet this constraint)
- Discovery of a low-spin BH with M_{bh}>50 $M_\odot$ by GW observations would challenge astrophysical BH+BH formation channels, leaving PBH a viable alternative

Accretion spin-up of PBHs

$$\hat{r}_{\rm isco} = \frac{r_{\rm isco}}{R_g} = 3 + Z_2 \pm [(3 - Z_1)(3 + Z_1 + 2Z_2)]^{1/2}$$

$$Z_1 \equiv 1 + (1 - a^2)^{1/3}\left[(1+a)^{1/3} + (1-a)^{1/3}\right]$$
$$Z_2 \equiv (3a^2 + Z_1^2)^{1/2}.$$

$$\mathrm{d}M_{\rm bh} = \frac{\tilde{e}_{\rm isco}}{c^2}\mathrm{d}M_0, \quad \mathrm{d}J_{\rm bh} = \tilde{l}_{\rm isco}\,\mathrm{d}M_0$$

$$\frac{\mathrm{d}a}{\mathrm{d}\ln M_{\rm bh}} = \frac{1}{M_{\rm bh}}\frac{c^3}{G}\frac{\tilde{l}_{\rm isco}}{\tilde{e}_{\rm isco}} - 2a$$

Bardeen, 1970:

$$a^f = \frac{1}{3}\hat{r}_{\rm isco}^{1/2}\frac{M_{\rm bh}}{M_{\rm bh}^f}\left[4 - \left\{3\hat{r}_{\rm isco}\left(\frac{M_{\rm bh}}{M_{\rm bh}^f}\right)^2 - 2\right\}^{1/2}\right]$$

$$M_{\rm bh}^f/M_{\rm bh} \le \hat{r}_{\rm isco}^{1/2}$$

Accreted mass

$$M_{\rm d} = \frac{M_{\rm bh}^f - M_{\rm bh}}{1 - \epsilon_r}$$

$$\epsilon_r \equiv 1 - \sqrt{1 - \frac{2}{3}\frac{1}{\hat{r}_{\rm isco}(a)}}$$

(Novikov, Thorne 1973)

For Schw. BH: $a^f \approx 9/\sqrt{6}\,\Delta M/M \approx 3.674\,\Delta M/M$

Accretion in a circular binary

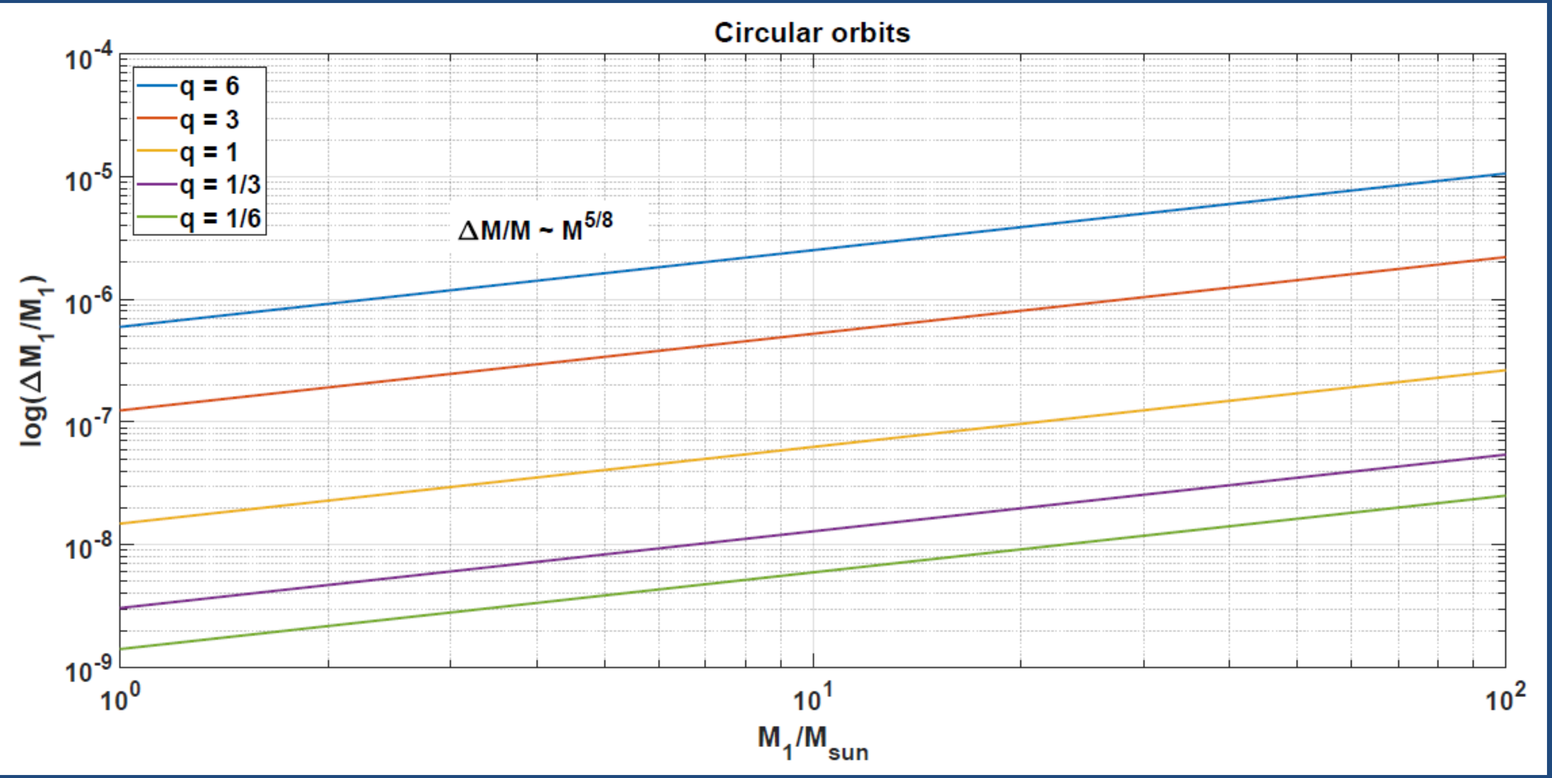

1904.00570, JCAP

ISM 10^{-24} g/cm ^{3}

Accretion in eccentric orbits

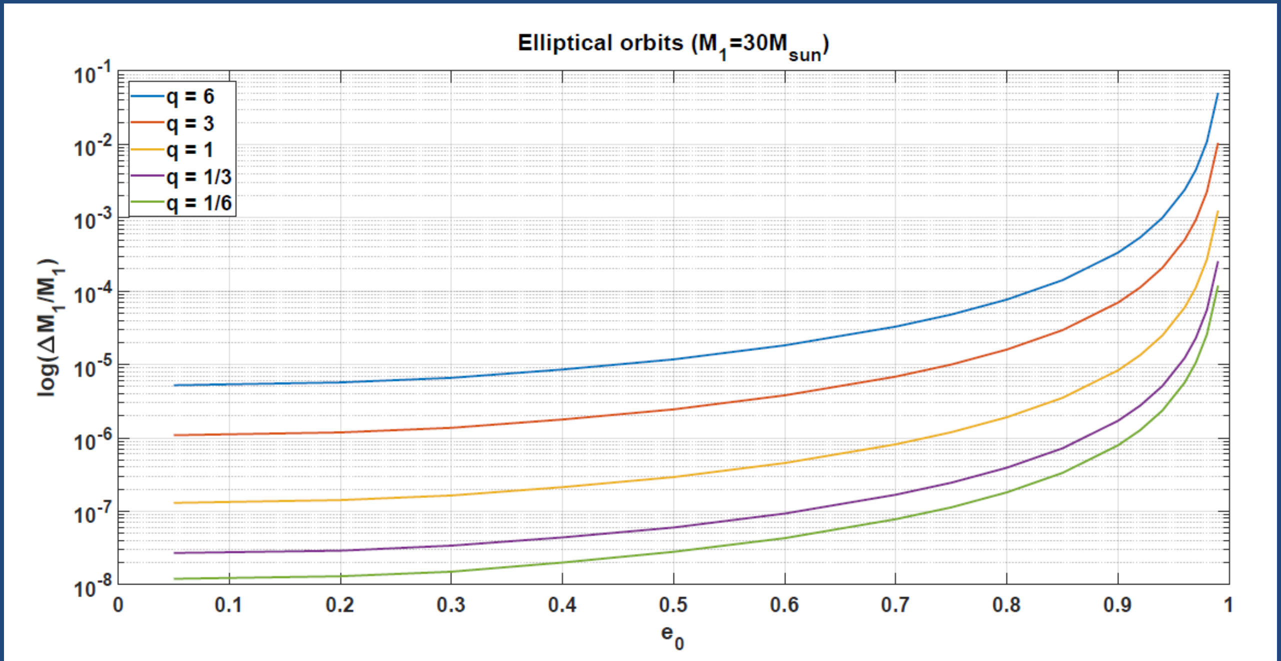

$$
\left.\frac{\Delta M_1}{M_1}\right|_e \approx 10^{-5}\left(\frac{\rho}{10^{-24}\mathrm{g\,cm^{-3}}}\right)\left(\frac{M_1}{30M_\odot}\right)^{5/8} q^{3/4}(1+q)^{15/8}\left(\frac{0.1}{1-e_0^2}\right)^{2.58}
$$

$$
\approx 10^{-5}\left(\frac{\rho}{10^{-24}\mathrm{g\,cm^{-3}}}\right)\left(\frac{\mathcal{M}}{30M_\odot}\right)^{5/8} q(1+q)^2\left(\frac{0.1}{1-e_0^2}\right)^{2.58}.
$$

1904.00570, JCAP (2019) 044

Maximum effective spin of binary PBH

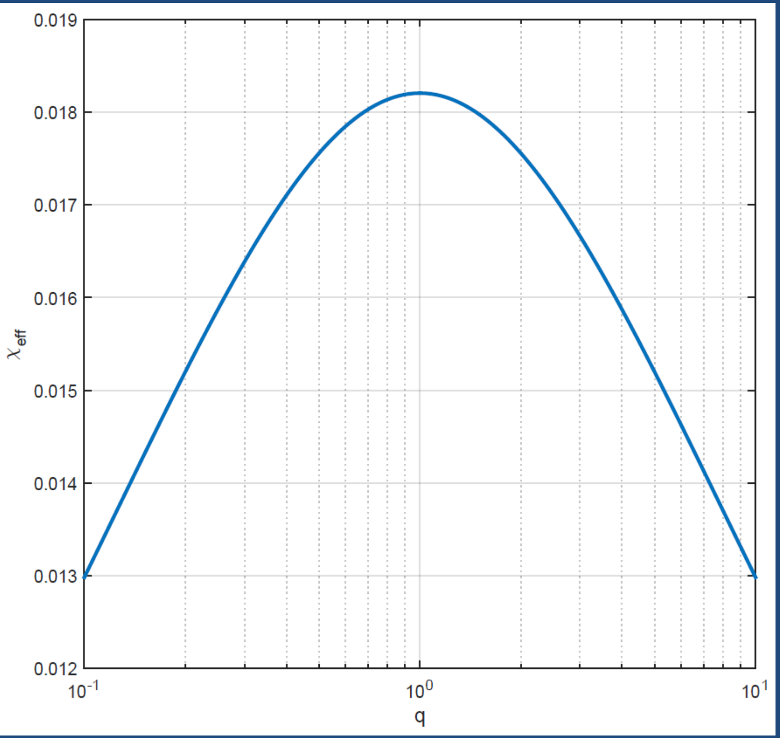

$$\chi_{eff,\max} \simeq 0.01(\rho/10^{-24}\mathrm{g\,cm^{-3}})(\mathcal{M}/30\,M_{\odot})^{0.97}(c_s/10^{-5})^{-2.75}$$

BH+BH: Conclusions

- Large masses and low effective spins of coalescing binary BHs can be explained by the standard astrophysical formation channel from evolution of massive binary stars
- Additional fallback of envelope onto newborn BH can significantly spin-up BH ➔ more heavy BH are expected to rotate faster than lighter ones
- Effective spins of BH+NS coalescences could span a wide range from -0.4 to 0.4 and even higher (if fallback is assumed)
- Primordial binary BH can be spun-up by accretion up to a few percent effective spins

Gravitational waves from binary neutron star mergings. Multi-messenger astronomy.

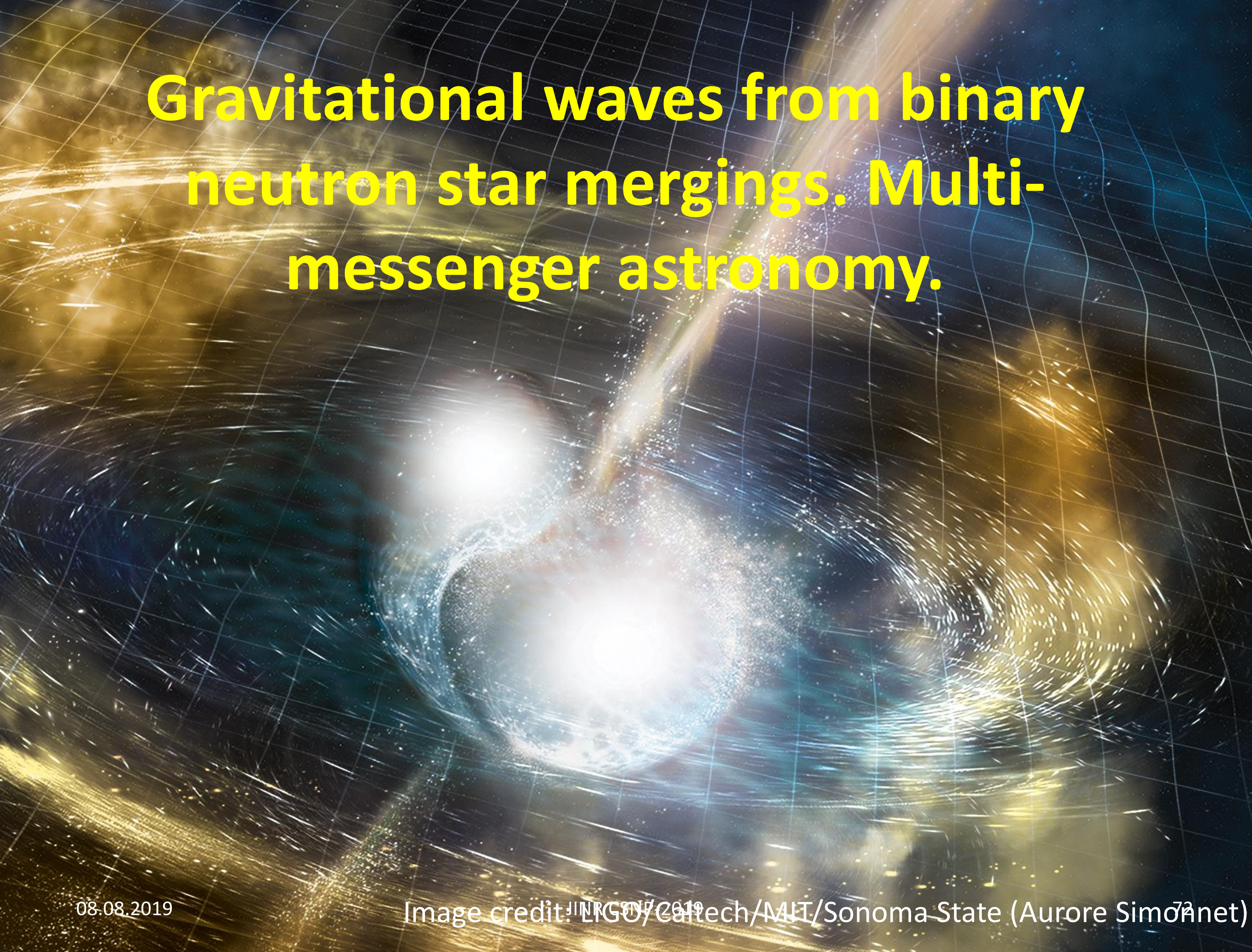

Image credit: LIGO/Caltech/MIT/Sonoma State (Aurore Simonnet)

Binary neutron stars

- Known as binary pulsars since 1975 (PSR 1913+16)
- LIGO O2 detection horizon (2017) ~80 Mpc, O3: ~125 Mpc
- GW 170817 associated with GRB 170817A
- Gamma-ray emission from binary NS first predicted by Blinnikov, Novikov, Perevodchikova (SvA 10, 422, 1984)
- Optical transient (kilonova) in NGC4993 (~40 Mpc)
- O3 candidate S190426c (~150 Mpc), no EM counterpart detected

GW170817

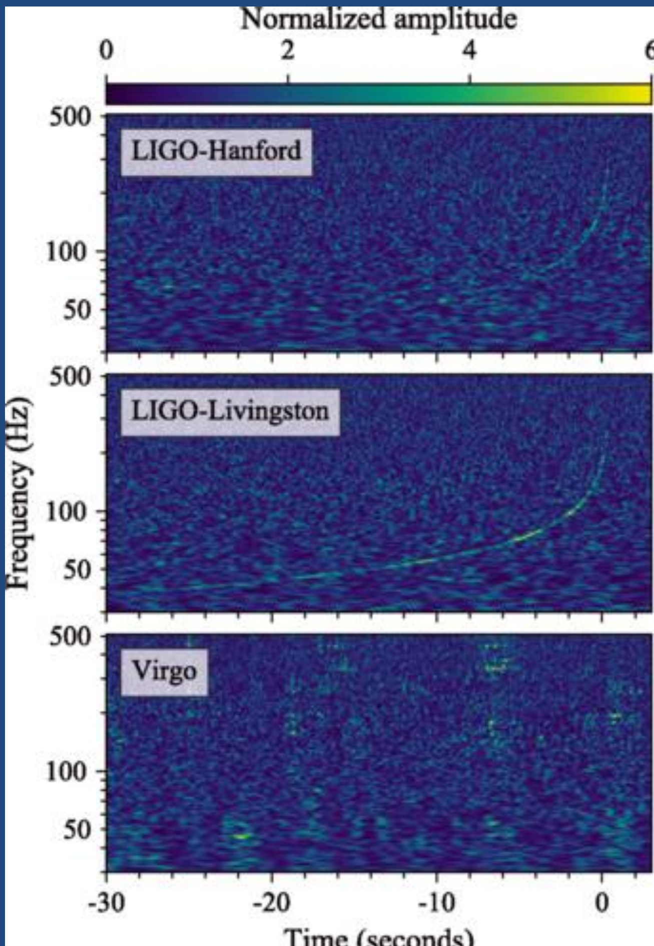

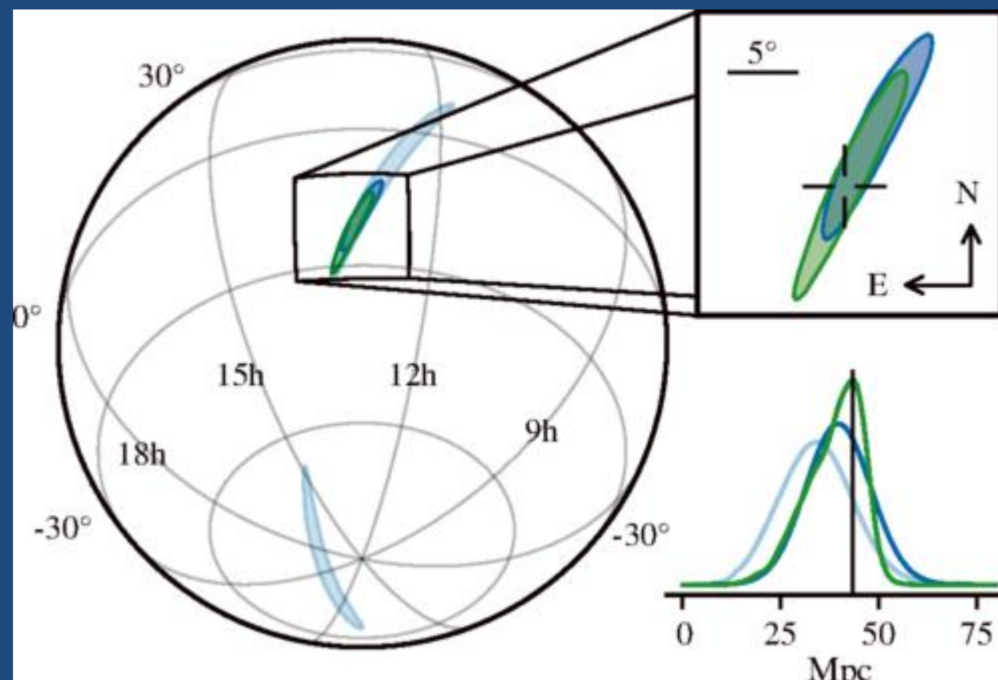

PRL 119, 161101 (2017)

2LIGO+VIRGO localization

Parameters of GW 170817 from GW data only

	Low-spin prior ($\chi \leq 0.05$)	High-spin prior ($\chi \leq 0.89$)
Binary inclination θ_{JN}	146^{+25}_{-27} deg	152^{+21}_{-27} deg
Binary inclination θ_{JN} using EM distance constraint [108]	151^{+15}_{-11} deg	153^{+15}_{-11} deg
Detector-frame chirp mass $\mathcal{M}^{\rm det}$	$1.1975^{+0.0001}_{-0.0001}$ $M_\odot$	$1.1976^{+0.0004}_{-0.0002}$ $M_\odot$
Chirp mass $\mathcal{M}$	$1.186^{+0.001}_{-0.001}$ $M_\odot$	$1.186^{+0.001}_{-0.001}$ $M_\odot$
Primary mass m_1	(1.36, 1.60) $M_\odot$	(1.36, 1.89) $M_\odot$
Secondary mass m_2	(1.16, 1.36) $M_\odot$	(1.00, 1.36) $M_\odot$
Total mass m	$2.73^{+0.04}_{-0.01}$ $M_\odot$	$2.77^{+0.22}_{-0.05}$ $M_\odot$
Mass ratio q	(0.73, 1.00)	(0.53, 1.00)
Effective spin $\chi_{\rm eff}$	$0.00^{+0.02}_{-0.01}$	$0.02^{+0.08}_{-0.02}$
Primary dimensionless spin χ_1	(0.00, 0.04)	(0.00, 0.50)
Secondary dimensionless spin χ_2	(0.00, 0.04)	(0.00, 0.61)
Tidal deformability $\tilde{\Lambda}$ with flat prior	300^{+500}_{-190}(symmetric)/300^{+420}_{-230}(HPD)	(0, 630)

$$\tilde{\Lambda} = \frac{16}{13}\frac{(m_1 + 12m_2)m_1^4\Lambda_1 + (m_2 + 12m_1)m_2^4\Lambda_2}{(m_1 + m_2)^5}$$

$$\Lambda = (2/3)k_2[(c^2/G)(R/m)]^5$$

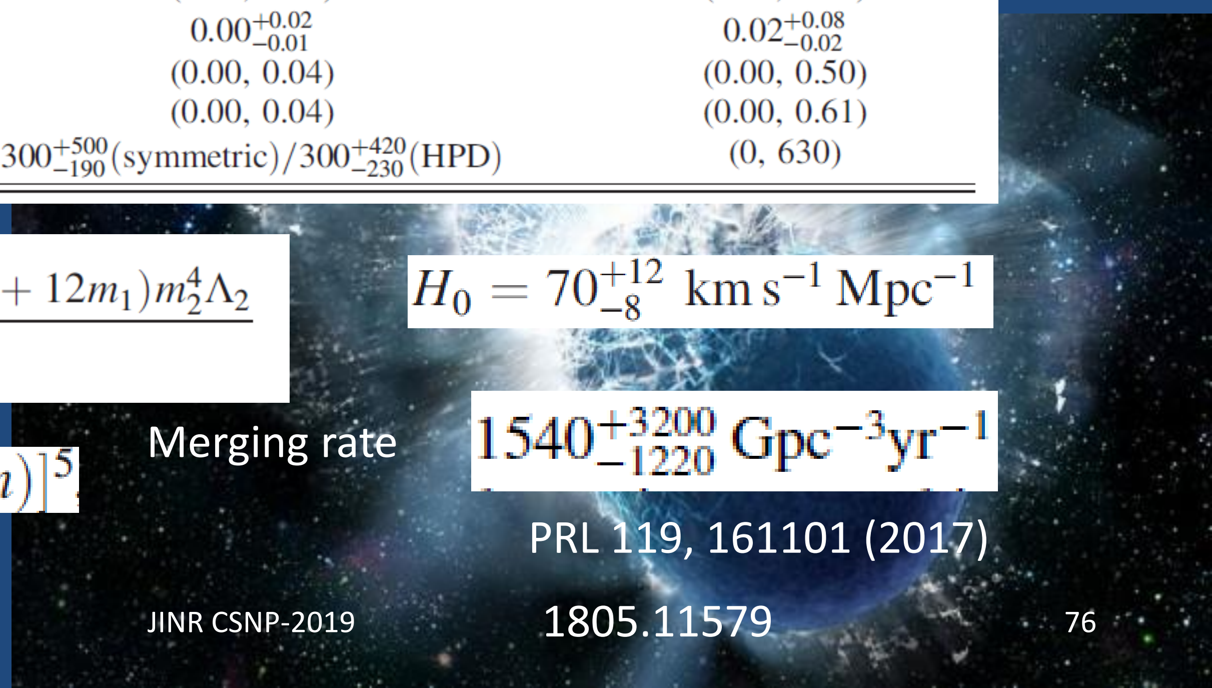

$$H_0 = 70^{+12}_{-8}\ \mathrm{km\,s^{-1}\,Mpc^{-1}}$$

Merging rate $1540^{+3200}_{-1220}\ \mathrm{Gpc^{-3}yr^{-1}}$

PRL 119, 161101 (2017)

1805.11579

NS equation of state constraints

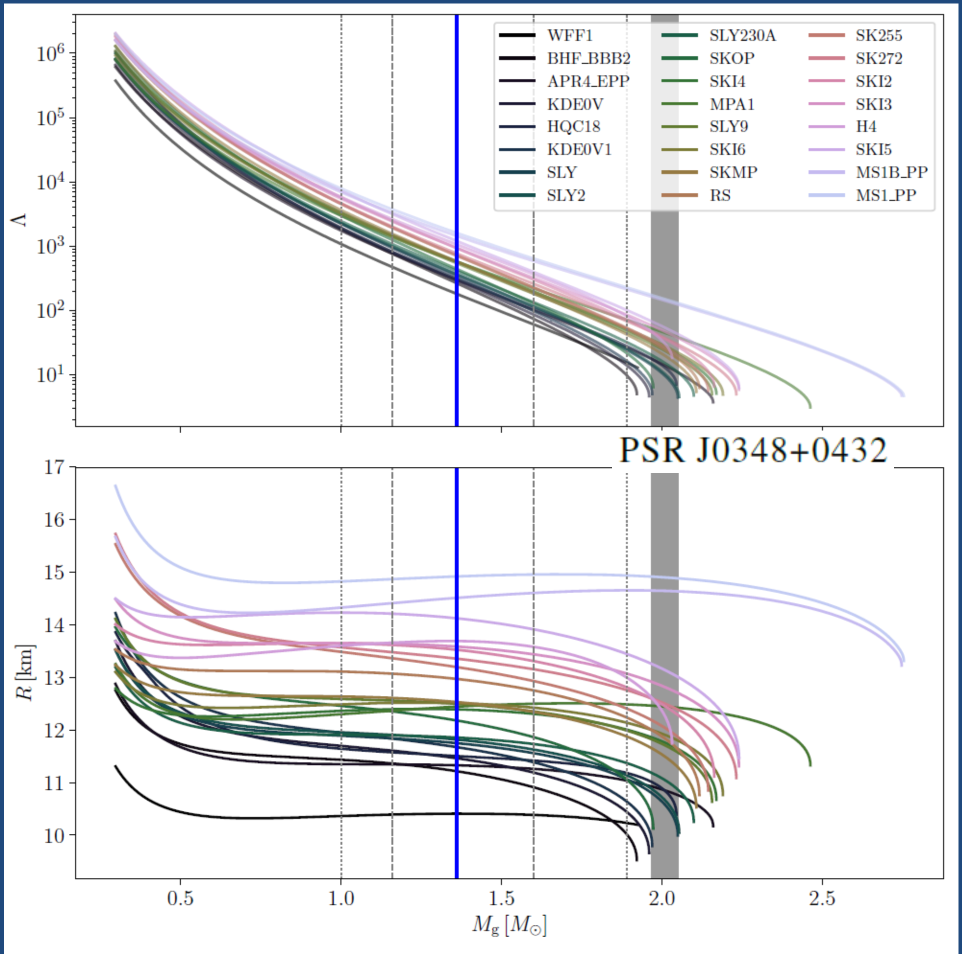

1908.01012

Tidal deformation

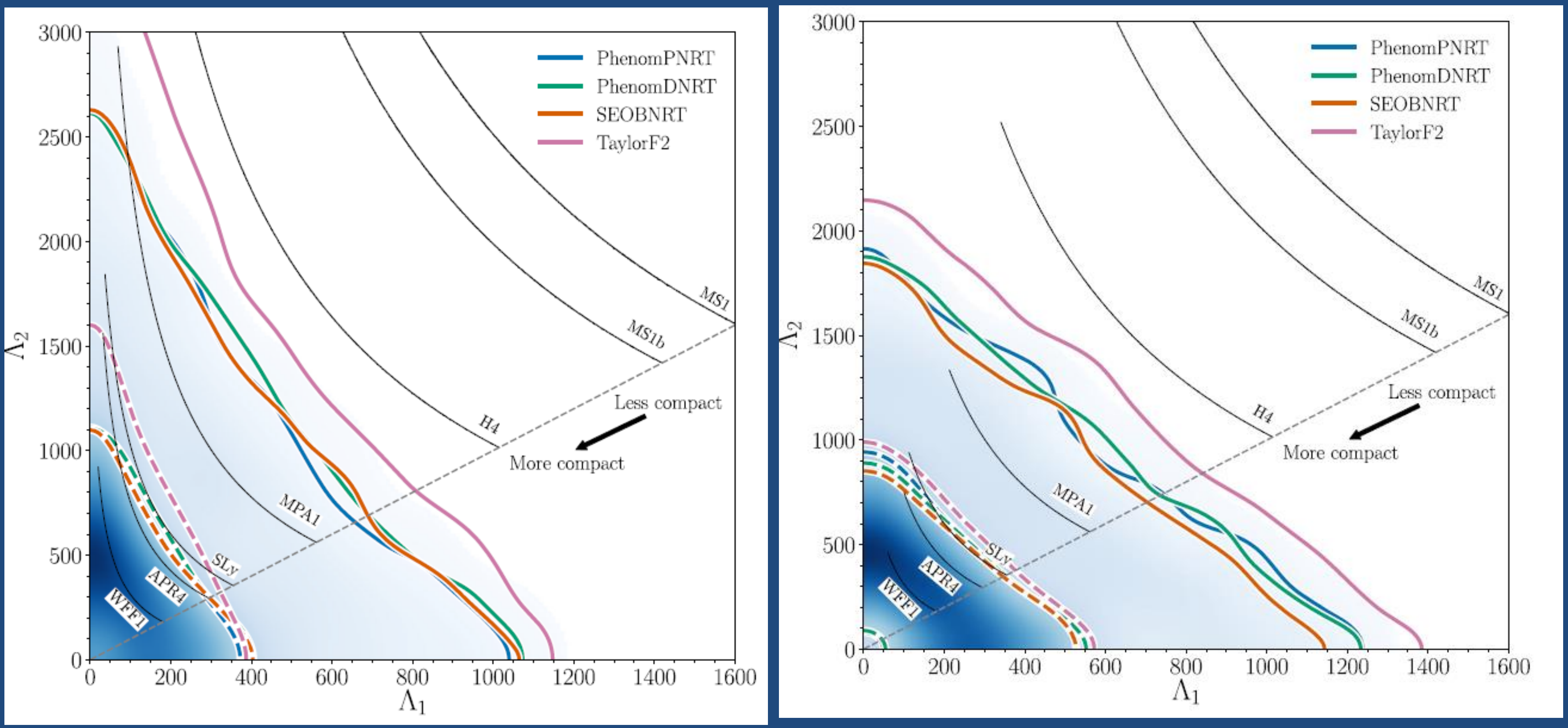

$$\Lambda = (2/3)k_2[(c^2/G)(R/m)]^5$$

1805.11579

However, BH+NS is not excluded, based on GW data Bayesian analysis!

Waveform/Method	BBH	NSBH	BHNS	BNS (common EoS)
Phenom+NRT/Nest	-	-	-	5.0
Phenom+NRT/MCMC	1.1	0.7	1.7	9.6
EOB+NRT/MCMC	1.7	1.6	4.0	5.5
TaylorF2 (7pN)/Nest	1.9	1.4	3.7	4.9
TaylorF2 (7pN)/MCMC	1.0	1.2	3.4	4.4
TaylorF2 (7.5pN)/Nest	1.6	1.3	3.2	4.4
TaylorF2 (7.5pN)/MCMC	0.9	1.0	5.5	5.0

Table 1. Bayes factors between various hypotheses on the nature of the GW170817 components obtained using different waveform approximants and two methods for computing the evidence. All Bayes factors are given in relation to the "binary neutron star with independent equations of state" hypothesis. We do not present results for Phenom+NRT/Nest when a BH is part of the binary, as the combination of precession and high spins makes this analysis computationally very expensive. We find no clear preference for any hypothesis. The table abbreviations stand for nested sampling (Nest), Markov-chain Monte-Carlo / thermodynamic integration (MCMC), binary black hole (BBH), mixed binary where the neutron star is heavier (NSBH), mixed binary where the black hole is heavier (BHNS), binary neutron star (BNS), equation of state (EoS).

1908.01012

Gamma-ray emission: GRB170817A

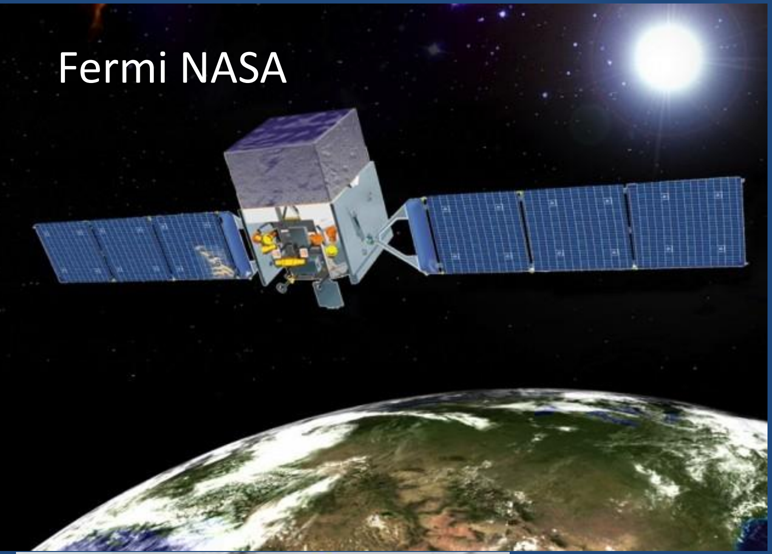

INTEGRAL ESA

Fermi GBM

INTEGRAL SPI-ACS

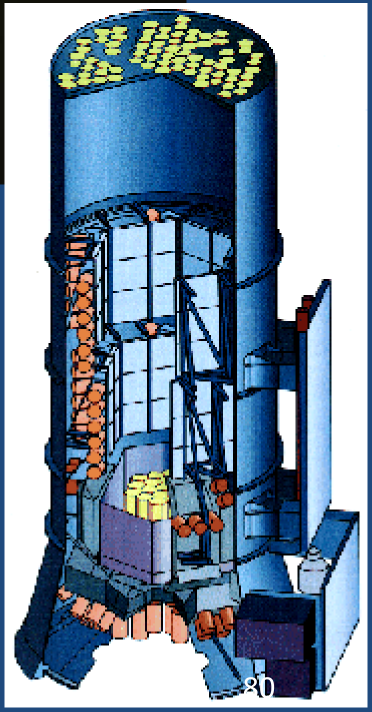

GRB170817A and GW170817

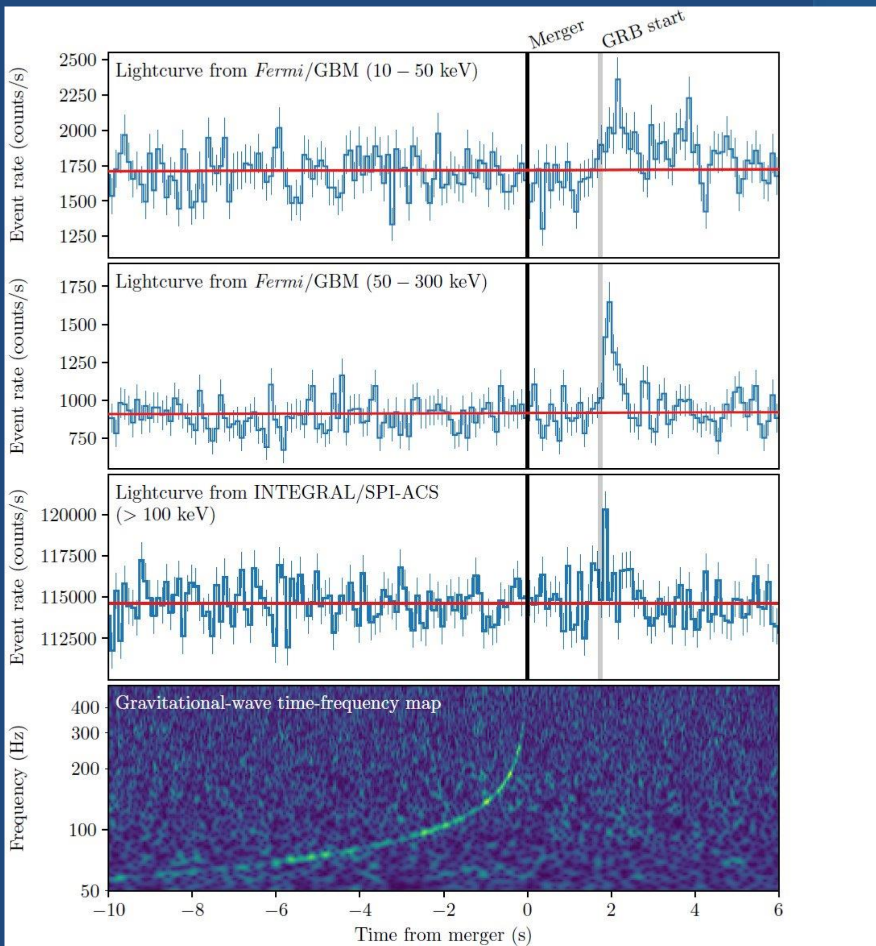

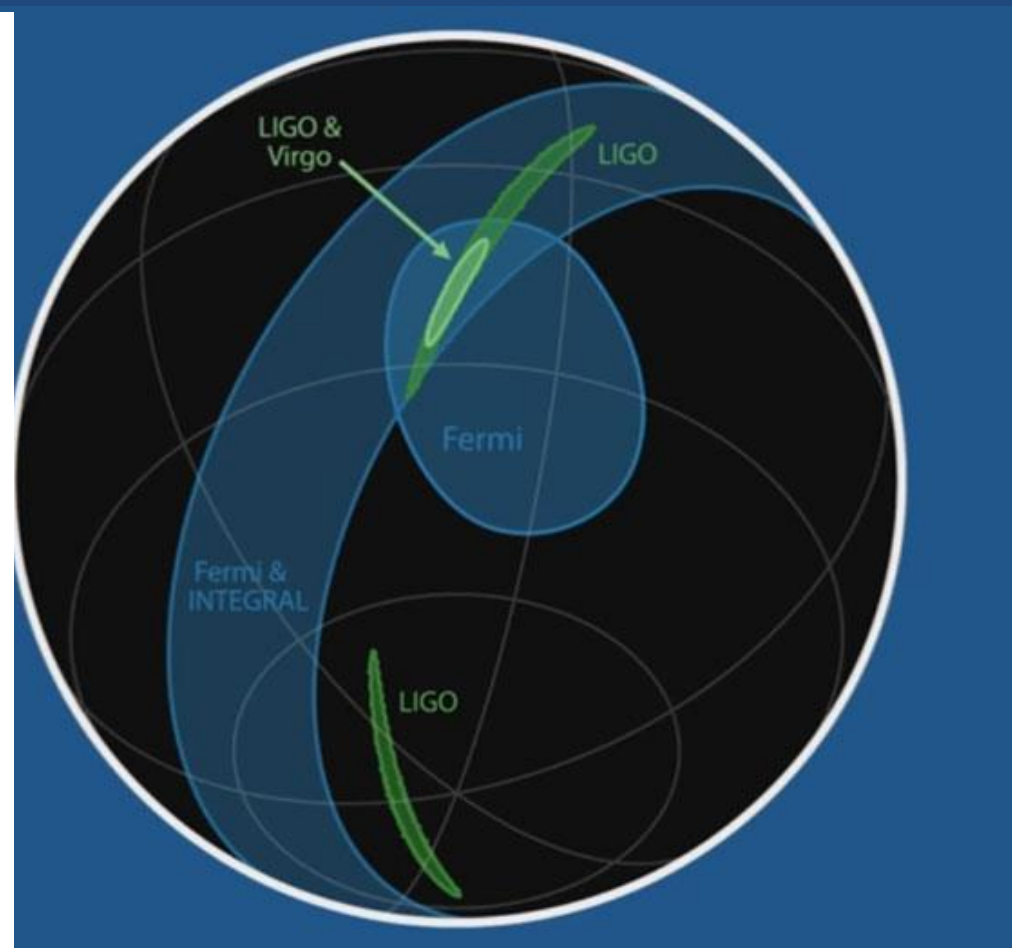

$$L_{\rm iso} = (1.6 \pm 0.6) \times 10^{47}\ {\rm erg\ s^{-1}}$$

GRB170817A

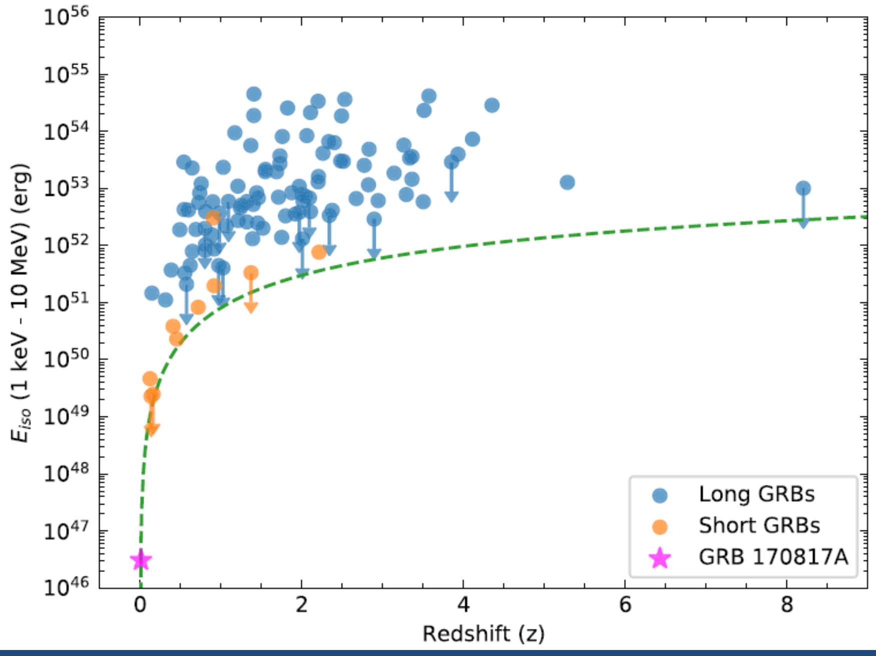

10^{56}
10^{55}
10^{54}
10^{53}
10^{52}
10^{51}
10^{50}
10^{49}
10^{48}
10^{47}
10^{46}
E_{iso} (1 keV - 10 MeV) (erg)
0
2
4
6
8
Redshift (z)
Long GRBs
Short GRBs
GRB 170817A

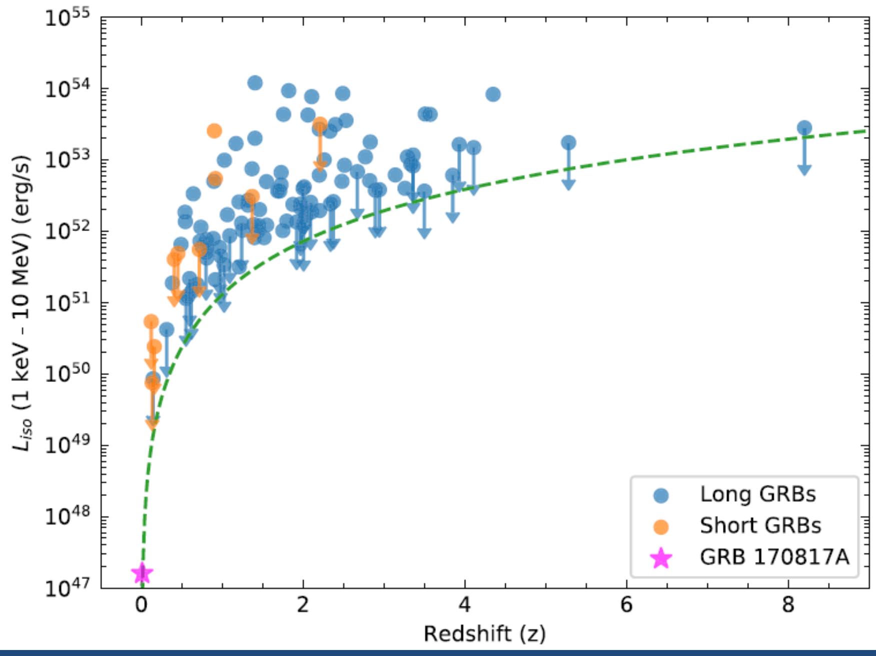

10^{55}
10^{54}
10^{53}
10^{52}
10^{51}
10^{50}
10^{49}
10^{48}
10^{47}
L_{iso} (1 keV - 10 MeV) (erg/s)
0
2
4
6
8
Redshift (z)
Long GRBs
Short GRBs
GRB 170817A

Fundamental consequences of GW/GRB observations

- 1) Velocity of GW and EM: $\Delta v / v_{\rm EM} \approx v_{\rm EM} \Delta t / D$

10 s EM delay

$$-3 \times 10^{-15} \leqslant \frac{\Delta v}{v_{\rm EM}} \leqslant +7 \times 10^{-16}$$

Simult., D>26 Mpc

- 2) Equivalence principle

Shapiro delay

$$\delta t_{\rm S} = -\frac{1+\gamma}{c^3} \int_{r_e}^{r_o} U(\boldsymbol{r}(l))\, dl$$

MW: $M=2.5\times10^{11} M_\odot$
R<100 kpc

$$-2.6 \times 10^{-7} \leqslant \gamma_{\rm GW} - \gamma_{\rm EM} \leqslant 1.2 \times 10^{-6}$$

cf. Cassini mission: $2.1 \pm 2.3 \times 10^{-5}$

ApJL, 848, L13, 2017

• 3) Number of additional dimensions

$$h \propto \frac{1}{d_L^\gamma}$$

$$\gamma = \frac{D-2}{2}$$

H_0 prior km s^{-1} Mpc^{-1}	γ	D
$H_0 = 73.24 \pm 1.74$ [22]	$1.01^{+0.04}_{-0.05}$	$4.02^{+0.07}_{-0.10}$
$H_0 = 67.74 \pm 0.46$ [21]	$0.99^{+0.03}_{-0.05}$	$3.98^{+0.07}_{-0.09}$

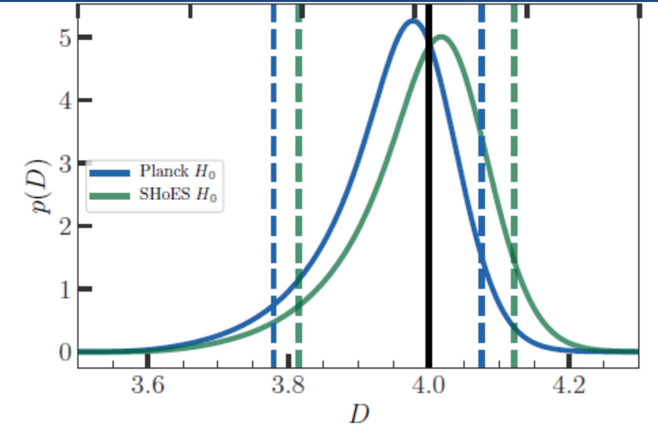

FIG. 1. Posterior probability distribution for the number of spacetime dimensions, D, using the GW distance posterior to GW170817 and the measured Hubble velocity to its host galaxy, NGC 4993, assuming the H_0 measurements from [21] (blue curve) and [22] (green curve). The dotted lines show

arXiv:1801.08160

GRB physics

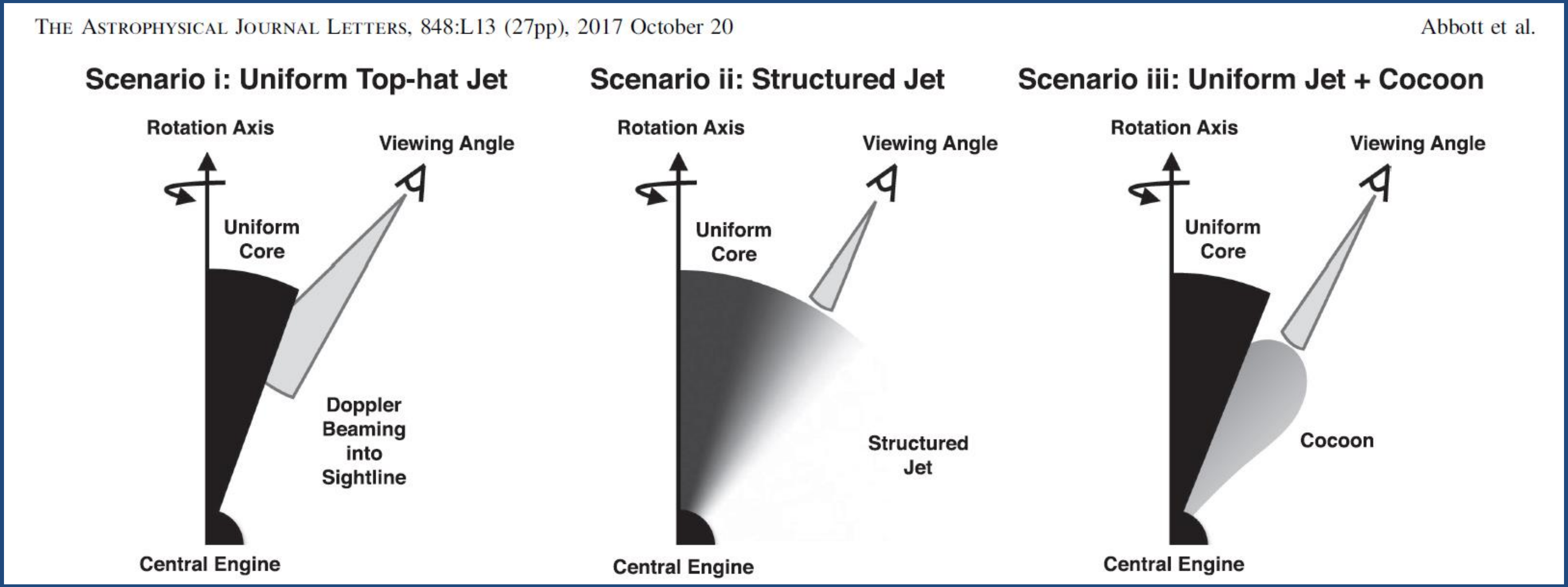
THE ASTROPHYSICAL JOURNAL LETTERS, 848:L13 (27pp), 2017 October 20
Abbott et al.
Scenario i: Uniform Top-hat Jet
Rotation Axis
Viewing Angle
Uniform Core
Doppler Beaming into Sightline
Central Engine
Scenario ii: Structured Jet
Rotation Axis
Viewing Angle
Uniform Core
Structured Jet
Central Engine
Scenario iii: Uniform Jet + Cocoon
Rotation Axis
Viewing Angle
Uniform Core
Cocoon
Central Engine

Multiwavelength followup

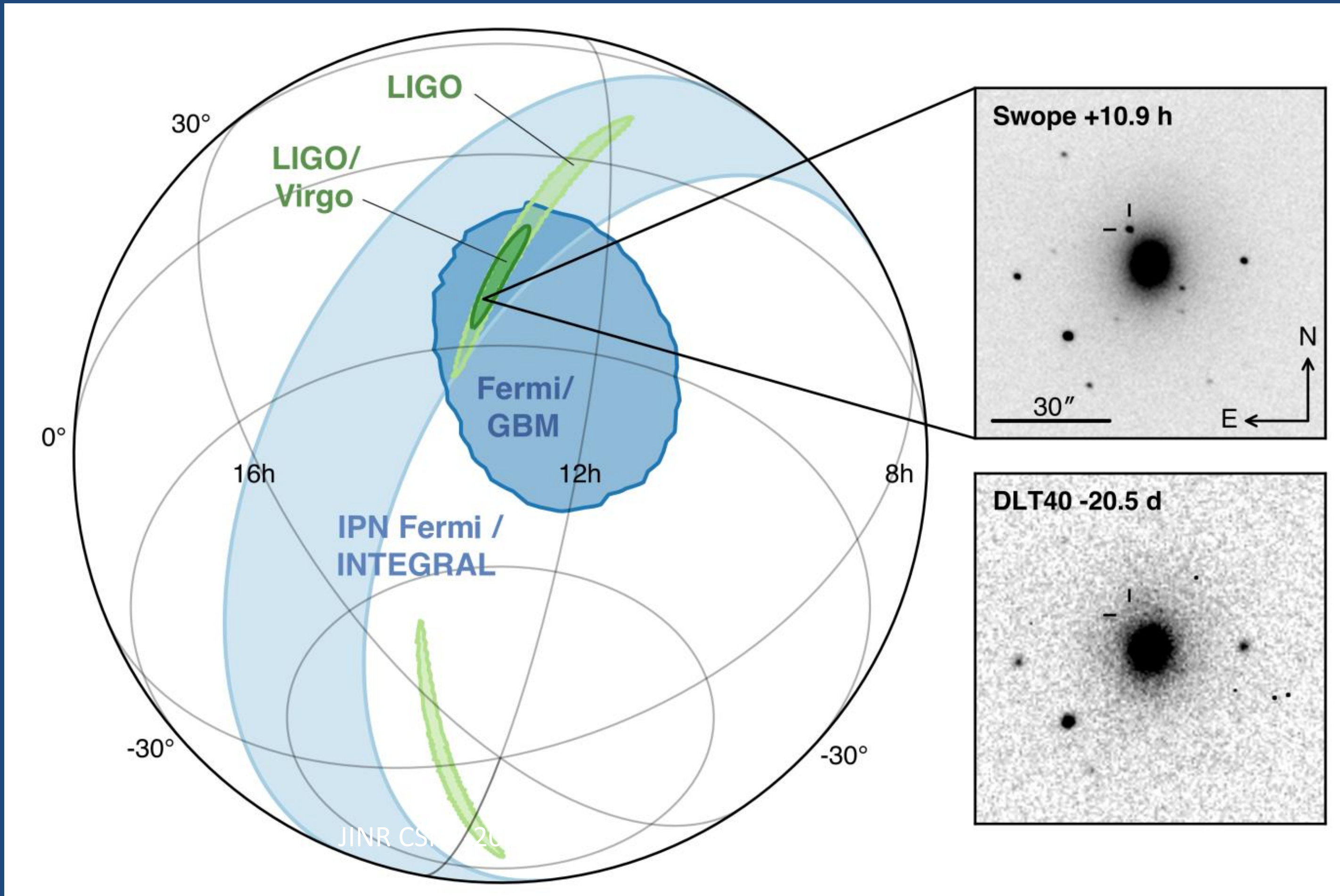

Optical, IR, X-ray, radio

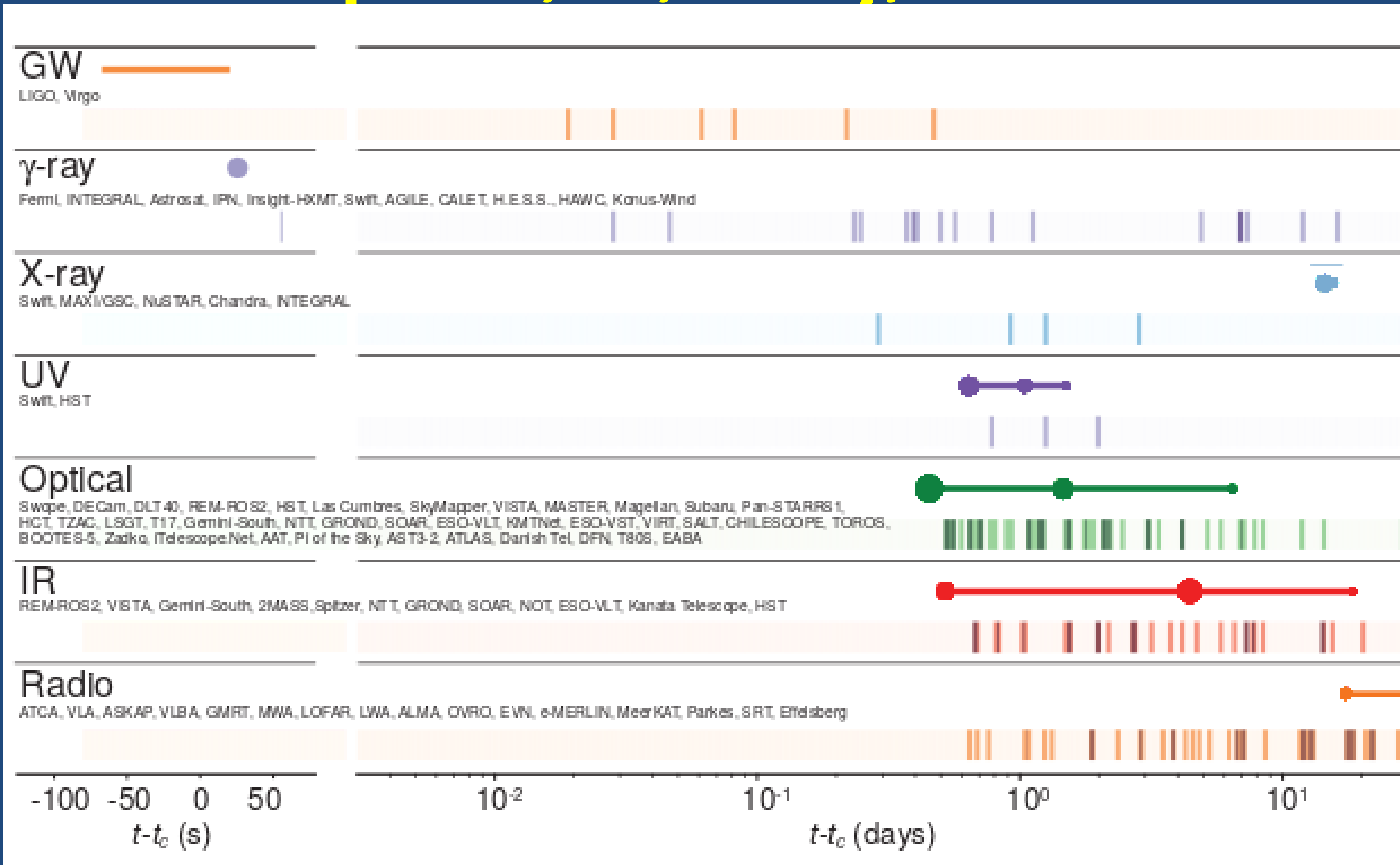

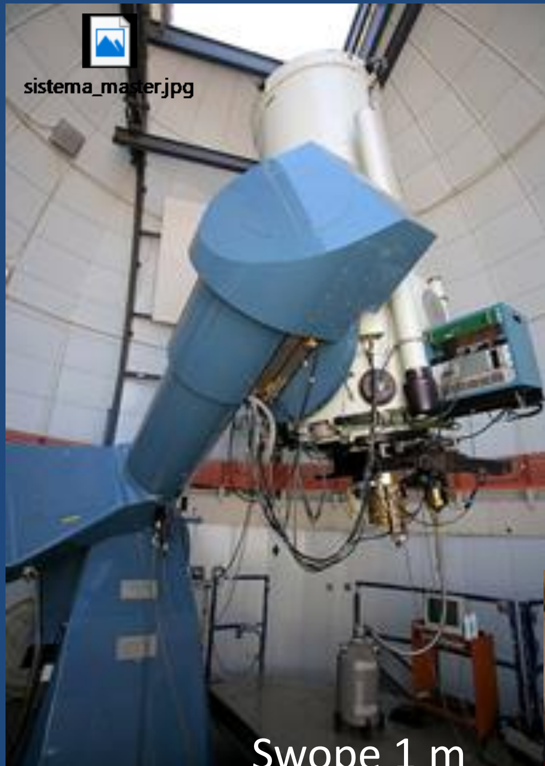

Swope 1 m


VISTA 4.1 m

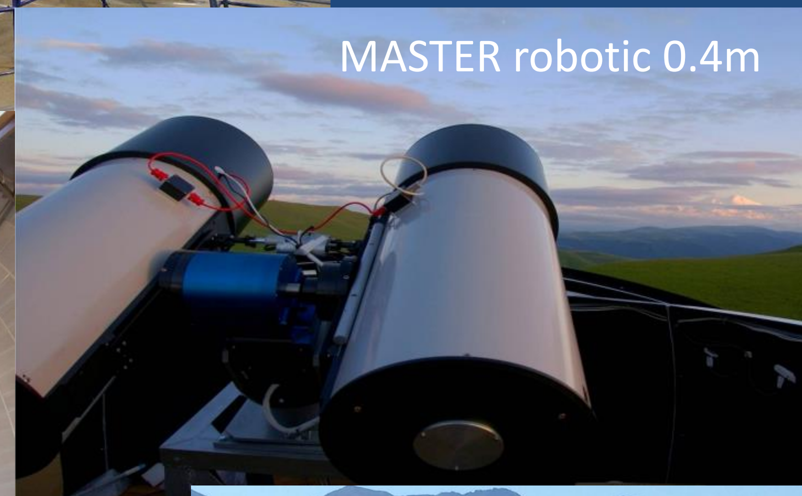
MASTER robotic 0.4m


PROMPT 0.41 m

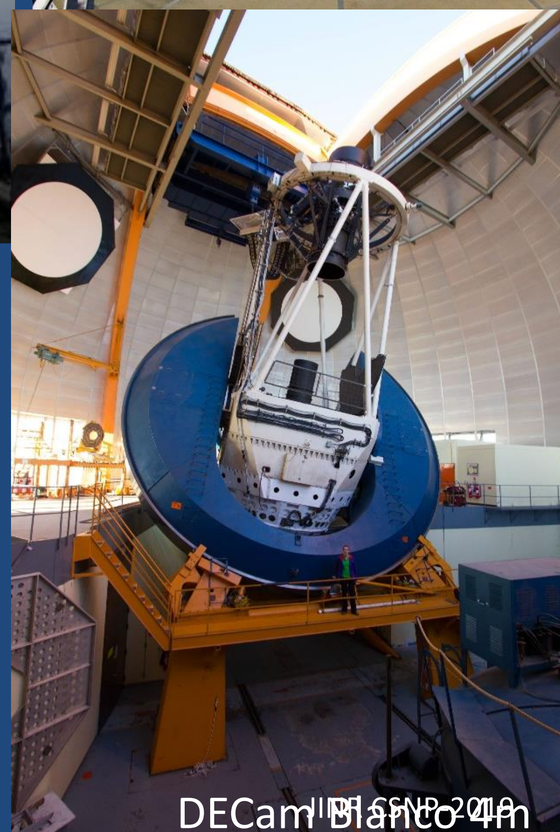
DECam Blanco 4m


Las Cumbres Chile 0.4m

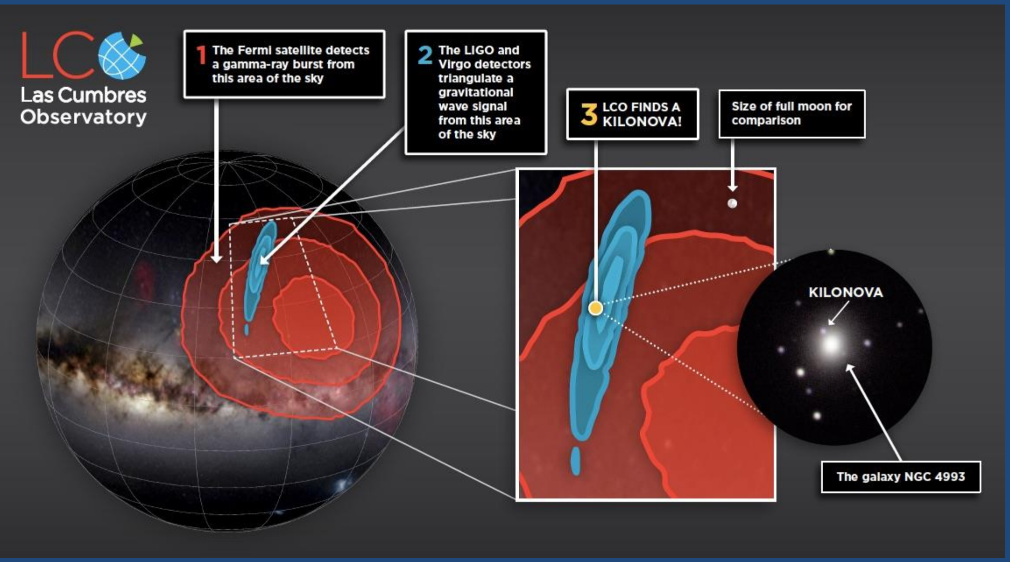
LCO
Las Cumbres Observatory
1 The Fermi satellite detects a gamma-ray burst from this area of the sky
2 The LIGO and Virgo detectors triangulate a gravitational wave signal from this area of the sky
3 LCO FINDS A KILONOVA!
Size of full moon for comparison
KILONOVA
The galaxy NGC 4993

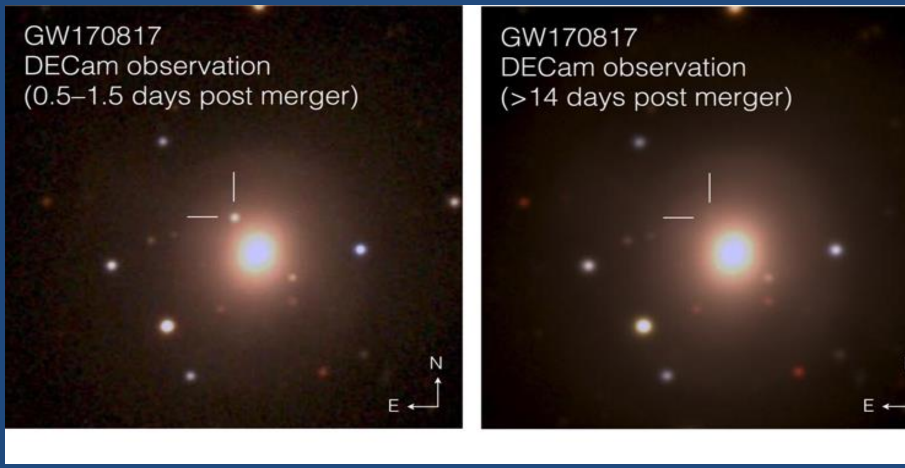
GW170817
DECam observation
(0.5–1.5 days post merger)
N
E
GW170817
DECam observation
(>14 days post merger)
E

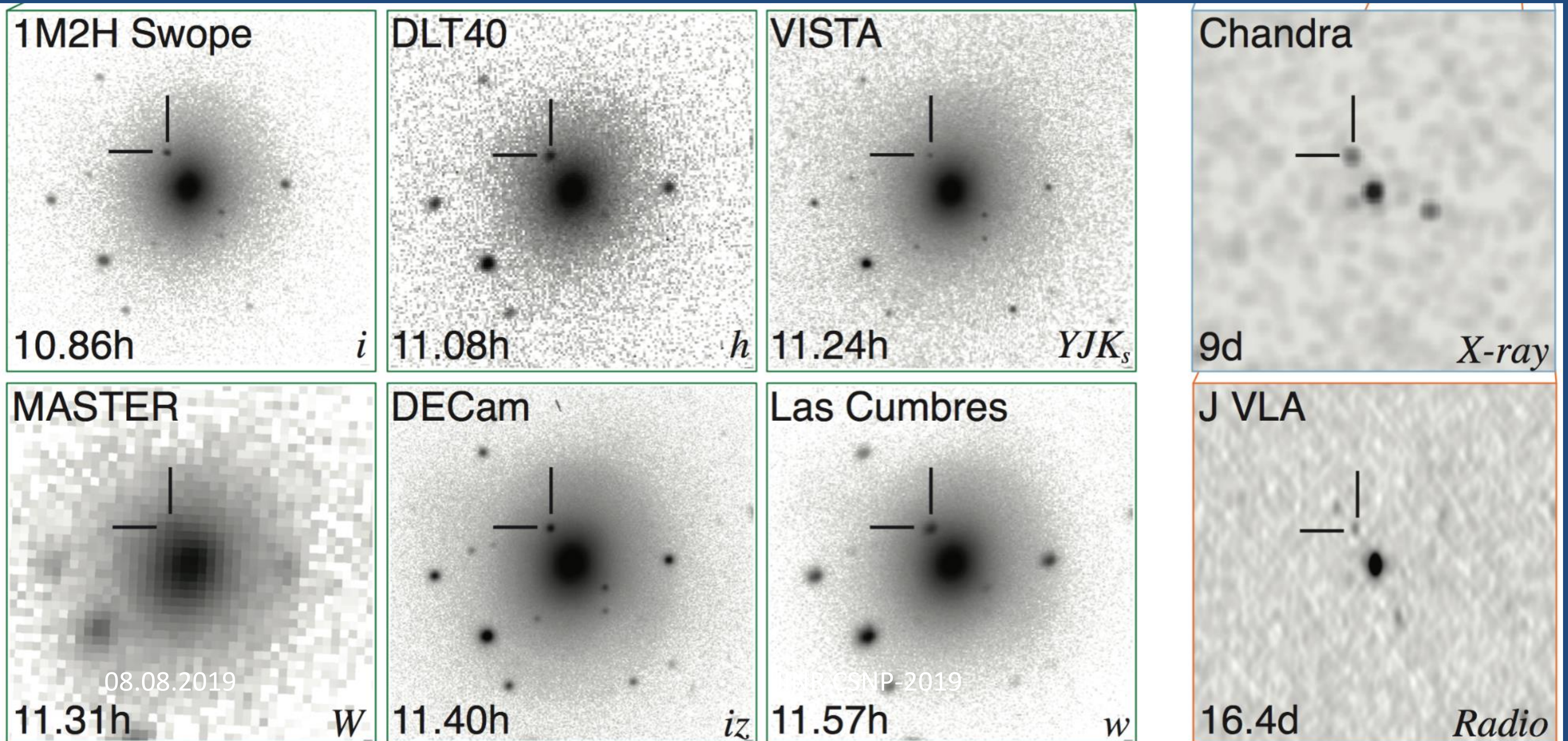
1M2H Swope
10.86h
i
DLT40
11.08h
h
VISTA
11.24h
YJKs
Chandra
9d
X-ray
MASTER
11.31h
W
DECam
11.40h
iz
Las Cumbres
11.57h
w
J VLA
16.4d
Radio

NGC 4993

NGC 4993 -- Galaxy in Group of Galaxies
(46 gal)

- 40 Mpc, E/S0

Binary BS merging

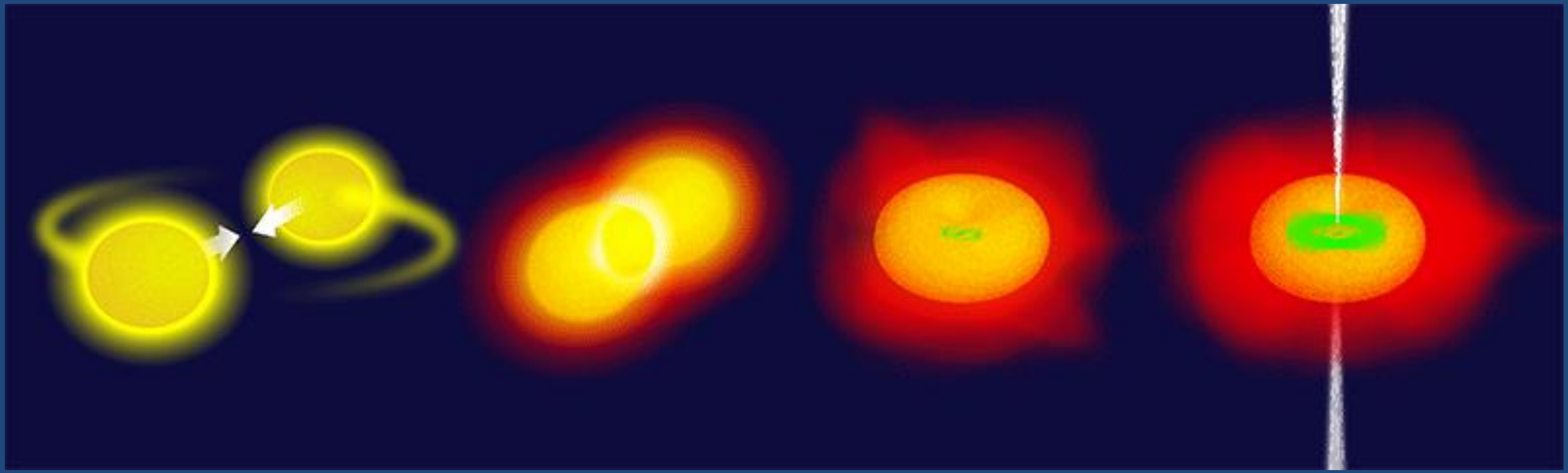

[Credit: APS/Alan Stonebraker, adapted from simulations by NASA/AEI/ZIB/M. Koppitz and L. Rezzolla]

Ejected mass ~ 0.001 solar masses

Possible outcomes

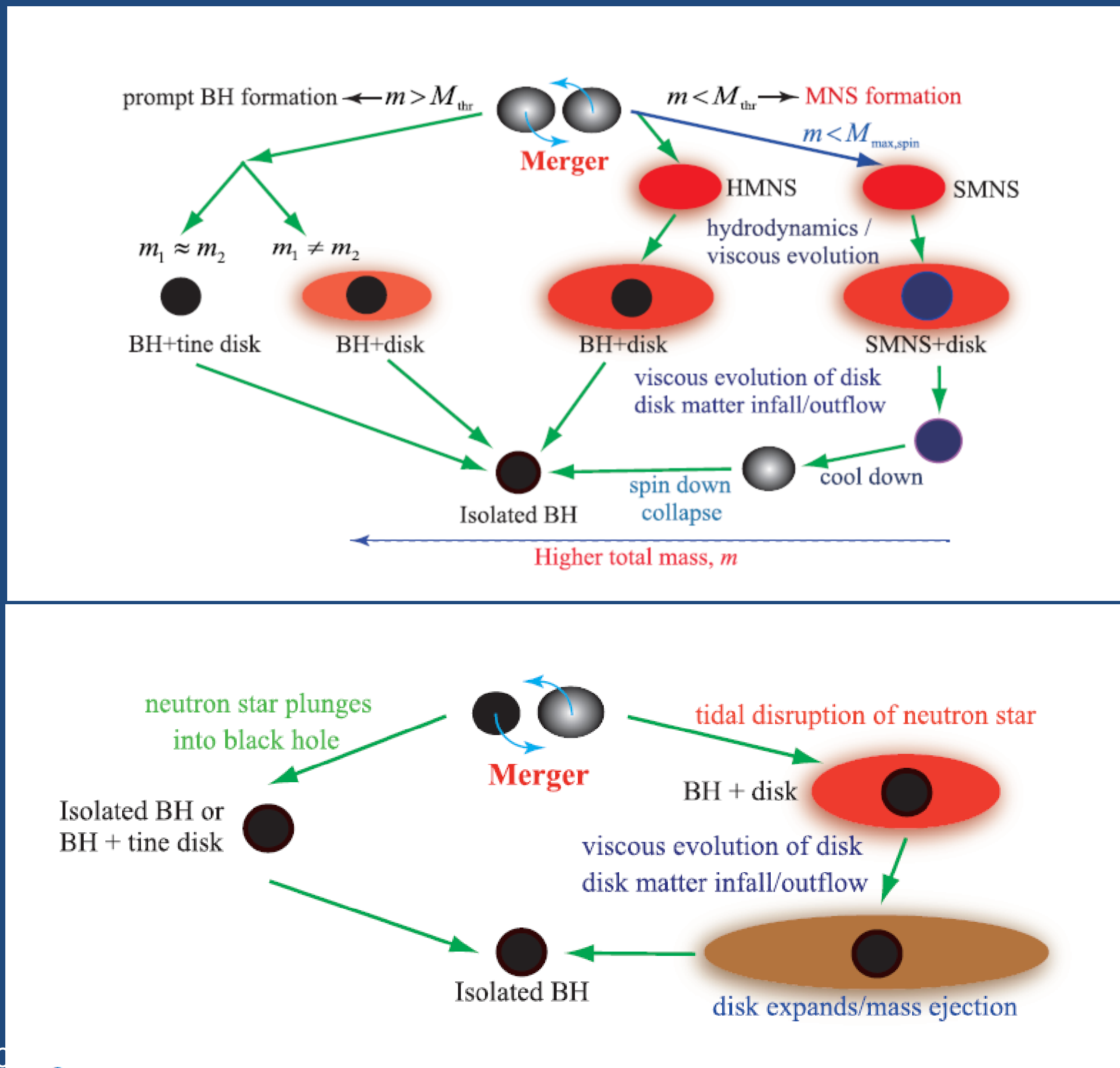

1908.02350

Mass ejection

- 'Dynamical' (merger) + 'viscous' (disc)

Type of binary	Remnant	$M_{\rm ej,dyn}$	$M_{\rm ej,vis}$	$Y_{e,\rm dyn}$	$Y_{e,\rm vis}$	$\langle v_{\rm ej} \rangle$
Low-m BNS	SMNS	$O(10^{-3})$	$O(10^{-2})$	0.05–0.5	0.3–0.5	0.15
Mid-m BNS (stiff EOS)	HMNS	$O(10^{-3})$	$O(10^{-2})$	0.05–0.5	0.2–0.5	0.15
Mid-m BNS (soft EOS)	HMNS	$\sim 10^{-2}$	$O(10^{-2})$	0.05–0.5	0.2–0.5	0.20
High-m BNS ($q \sim 1$)	BH	$< 10^{-3}$	$< 10^{-3}$	—	—	—
High-m BNS ($q \ll 1$)	BH	$O(10^{-3})$	$\lesssim 10^{-2}$	0.05–0.1	0.05–0.3	0.30
BH-NS	BH	0–0.1	0–0.1	0.05–0.1	0.05–0.3	0.30

$$Y_e = \frac{n_e}{n_p + n_n} = \frac{n_p}{n_p + n_n}$$

1908.02350

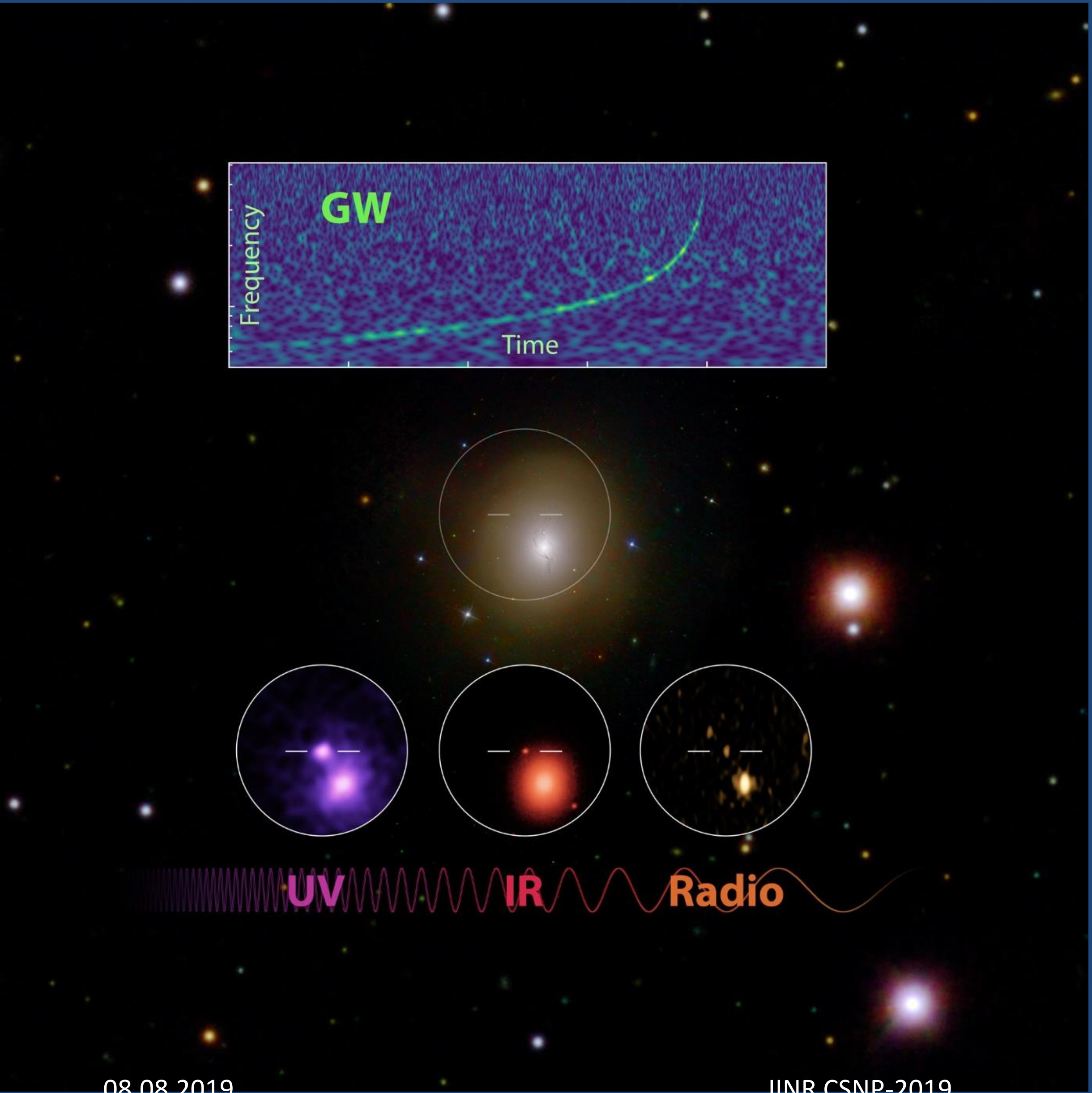
GW
Frequency
Time
UV
IR
Radio

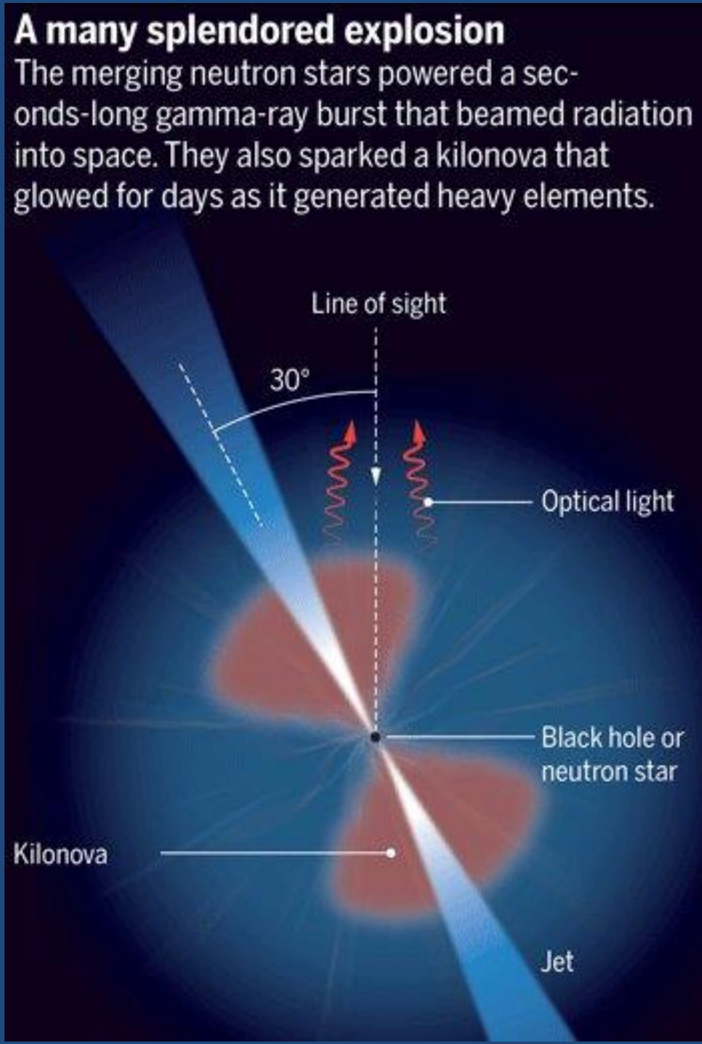
A many splendored explosion
The merging neutron stars powered a seconds-long gamma-ray burst that beamed radiation into space. They also sparked a kilonova that glowed for days as it generated heavy elements.
Line of sight
30°
Optical light
Black hole or neutron star
Kilonova
Jet

Kilonova (a x1000 Nova)

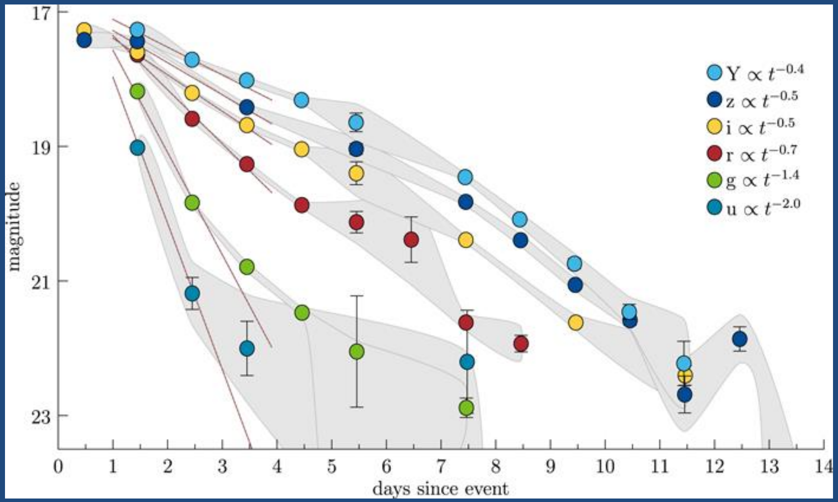

M. Soares-Santos et al. 2017

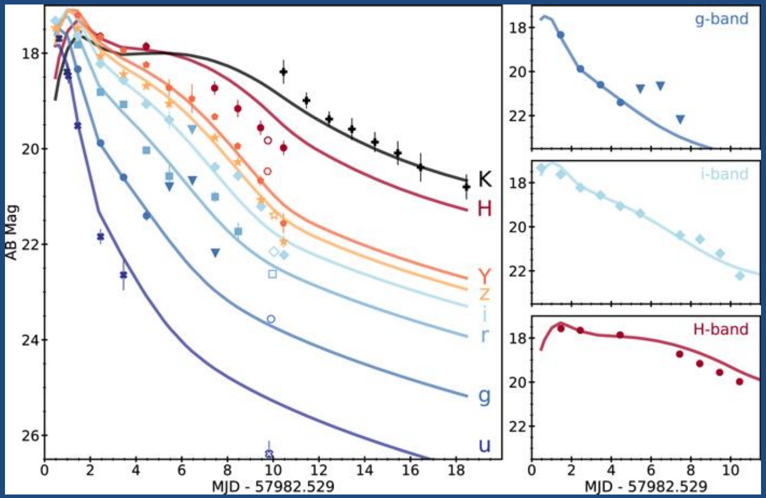

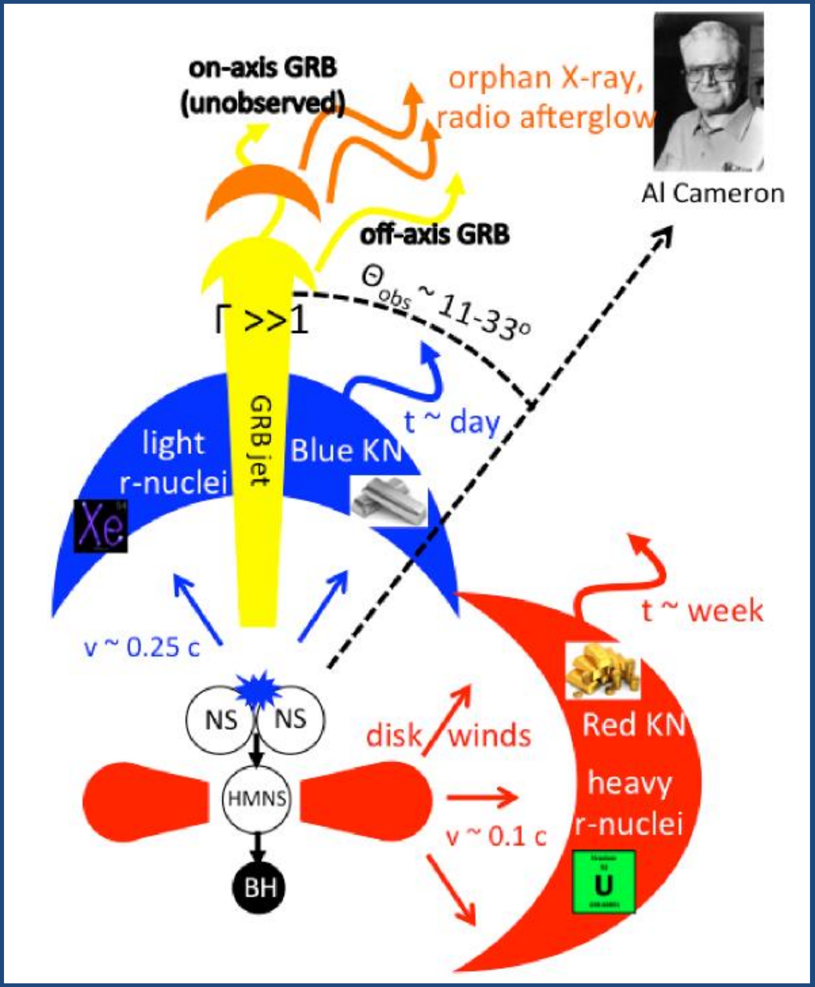

Metzger 2017

Optical and IR observations of kilonova

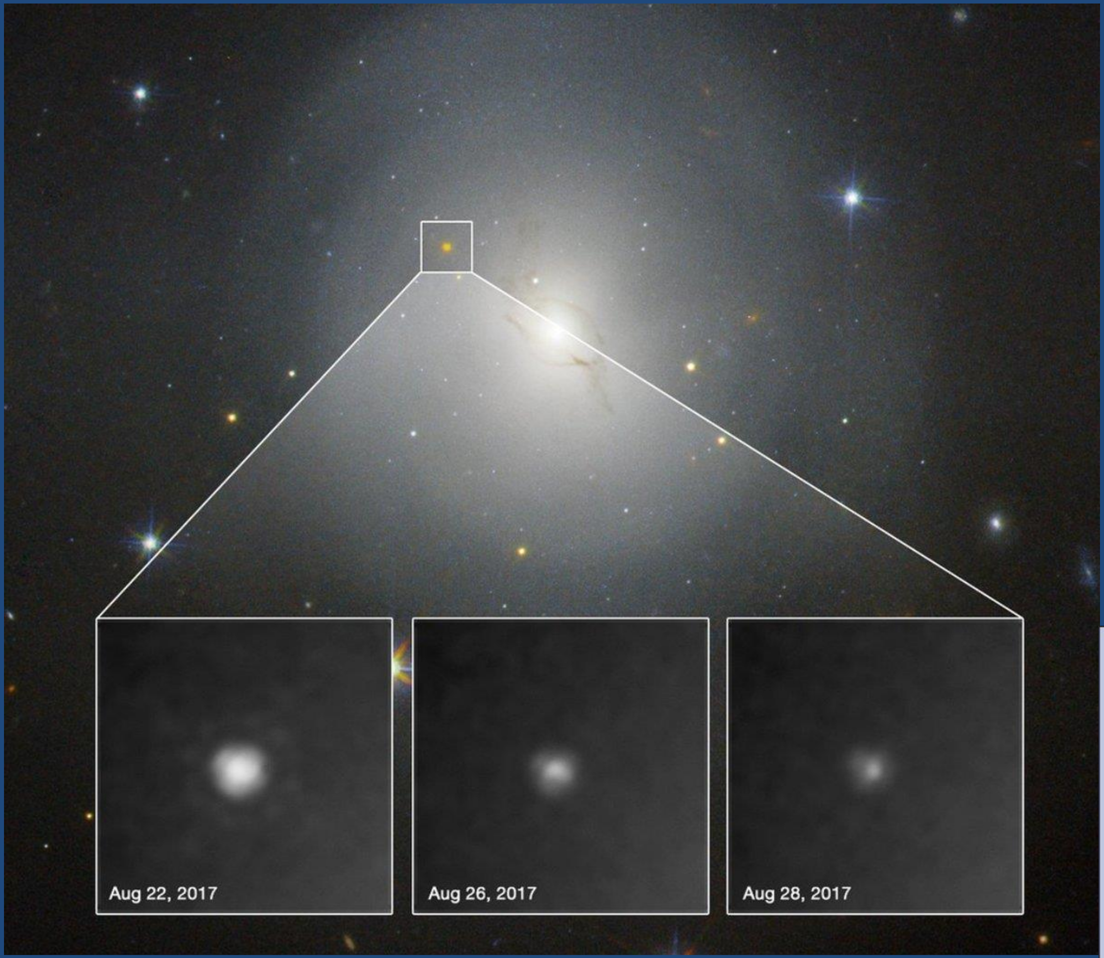

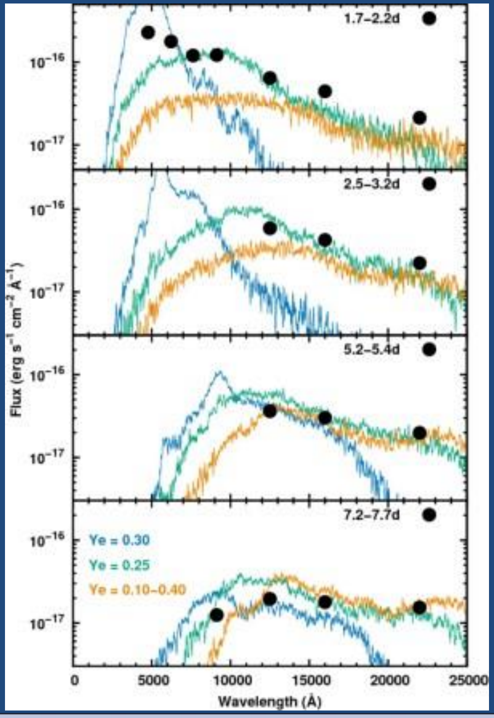

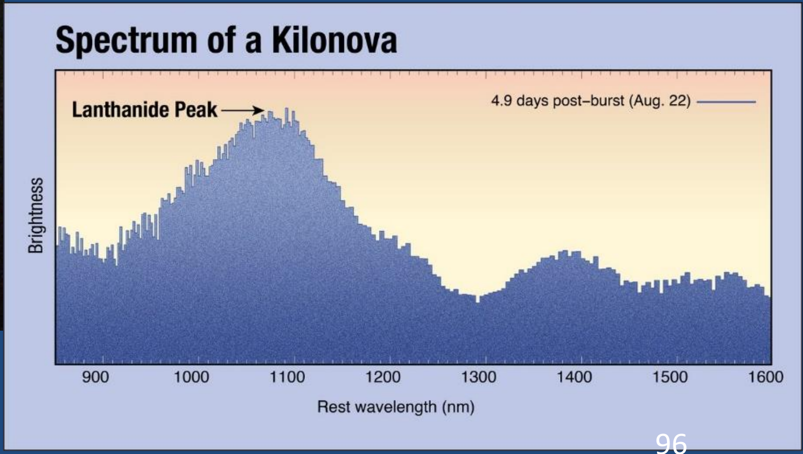

http://arxiv.org/abs/1710.05850

r-nucleosynthesis in binary NS mergings

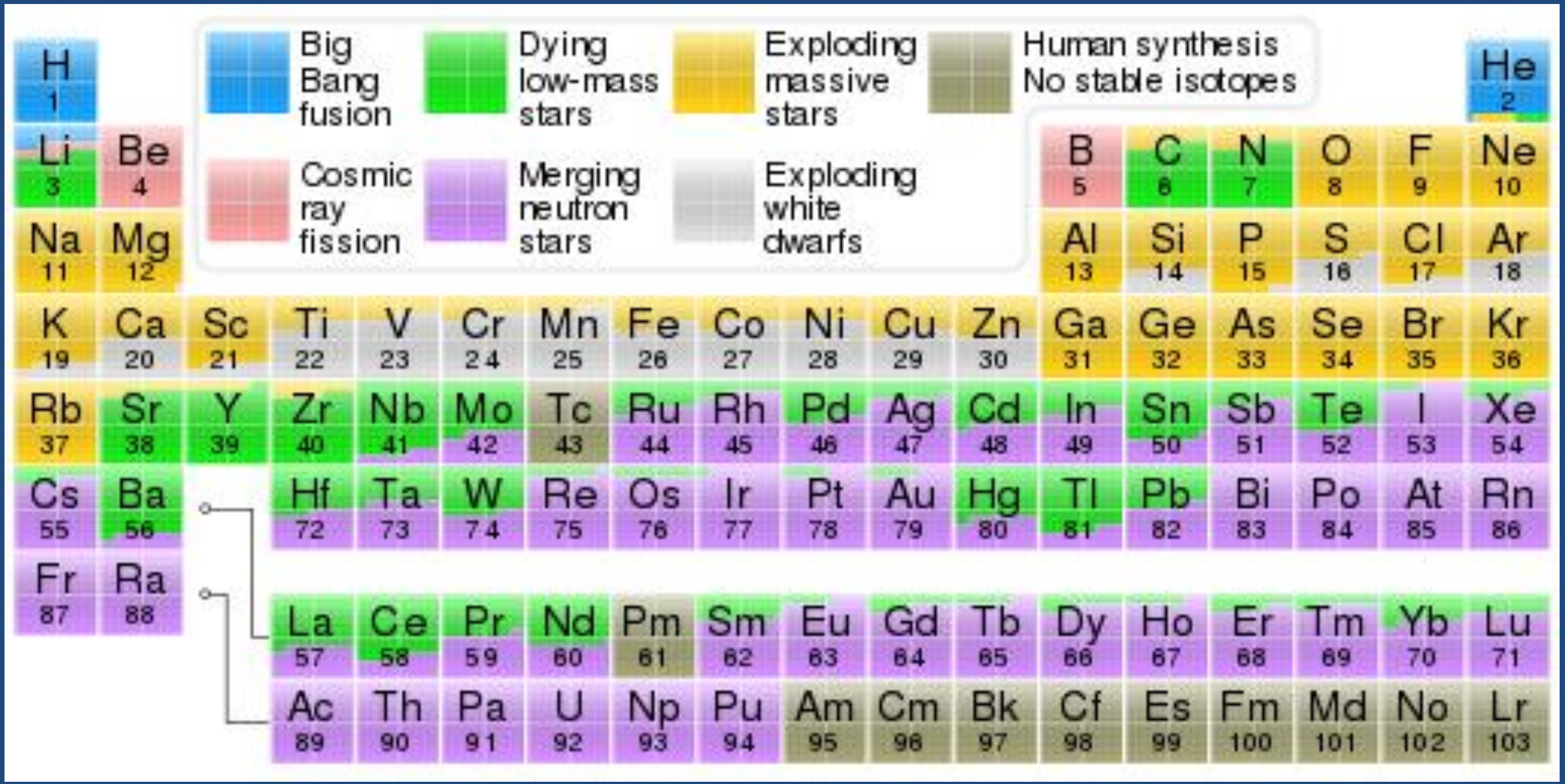

Properties of kilonova

Table 1: Key Properties of GW170817

Property	Value	Reference
Chirp mass, $\mathcal{M}$ (rest frame)	$1.188^{+0.004}_{-0.002} M_\odot$	1
First NS mass, M_1	$1.36 - 1.60 M_\odot$ (90%, low spin prior)	1
Second NS mass, M_2	$1.17 - 1.36 M_\odot$ (90%, low spin prior)	1
Total binary mass, $M_{\rm tot} = M_1 + M_2$	$\approx 2.74^{0.04}_{-0.01} M_\odot$	1
Observer angle relative to binary axis, $\theta_{\rm obs}$	$11 - 33^\circ$ (68.3%)	2
Blue KN ejecta ($A_{\rm max} \lesssim 140$)	$\approx 0.01 - 0.02 M_\odot$	e.g., 3,4,5
Red KN ejecta ($A_{\rm max} \gtrsim 140$)	$\approx 0.04 M_\odot$	e.g., 3,5,6
Light r-process yield ($A \lesssim 140$)	$\approx 0.05 - 0.06 M_\odot$	
Heavy r-process yield ($A \gtrsim 140$)	$\approx 0.01 M_\odot$	
Gold yield	$\sim 100 - 200 M_\oplus$	8
Uranium yield	$\sim 30 - 60 M_\oplus$	8
Kinetic energy of off-axis GRB jet	$10^{49} - 10^{50}$ erg	e.g., 9, 10, 11, 12
ISM density	$10^{-4} - 10^{-2}$ cm^{-3}	e.g., 9, 10, 11, 12

(1) LIGO Scientific Collaboration et al. 2017c; (2) depends on Hubble Constant, LIGO Scientific Collaboration et al. 2017d; (3) Cowperthwaite et al. 2017; (4) Nicholl et al. 2017; (5) Kasen et al. 2017; (6) Chornock et al. 2017; (8) assuming heavy r-process ($A > 140$) yields distributed as solar abundances (Arnould et al., 2007); (9)Margutti et al. 2017; (10) Troja et al. 2017; (11) Fong et al. 2017; (12) Hallinan et al. 2017

B.Metzger 1710.05931

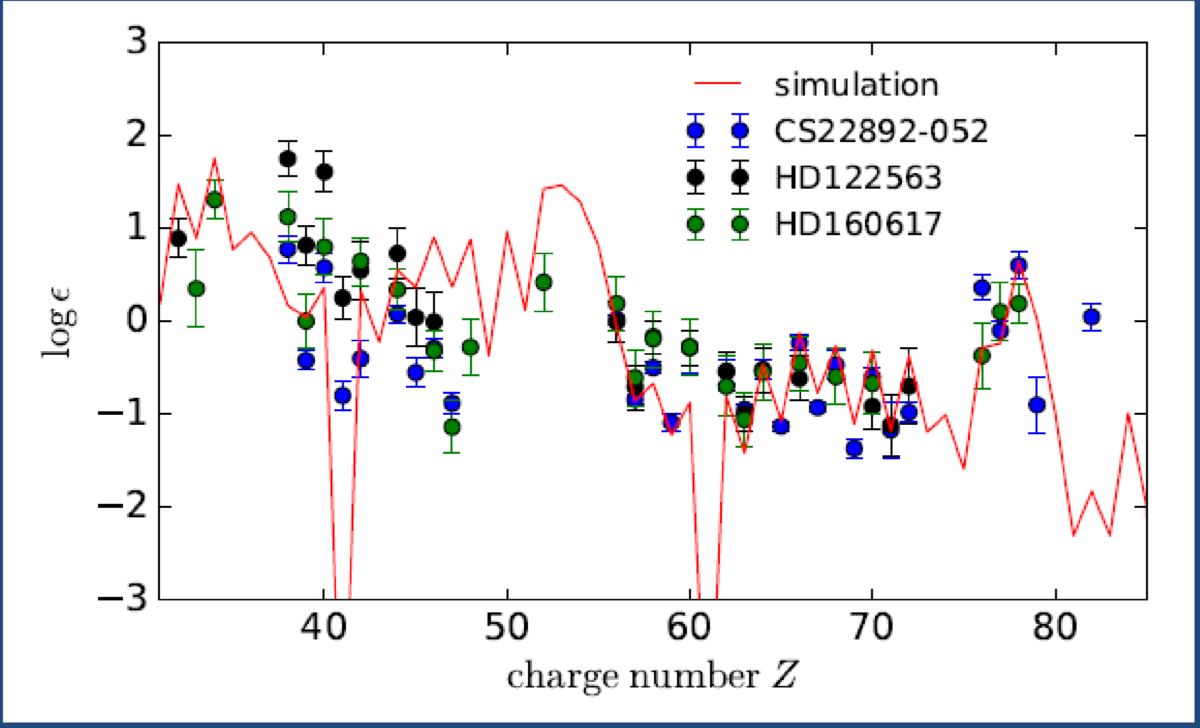

simulation
CS22892-052
HD122563
HD160617
log ϵ
charge number Z
3
2
1
0
−1
−2
−3
40
50
60
70
80

1711.00868

Prompt collapse to BH seems to be excluded

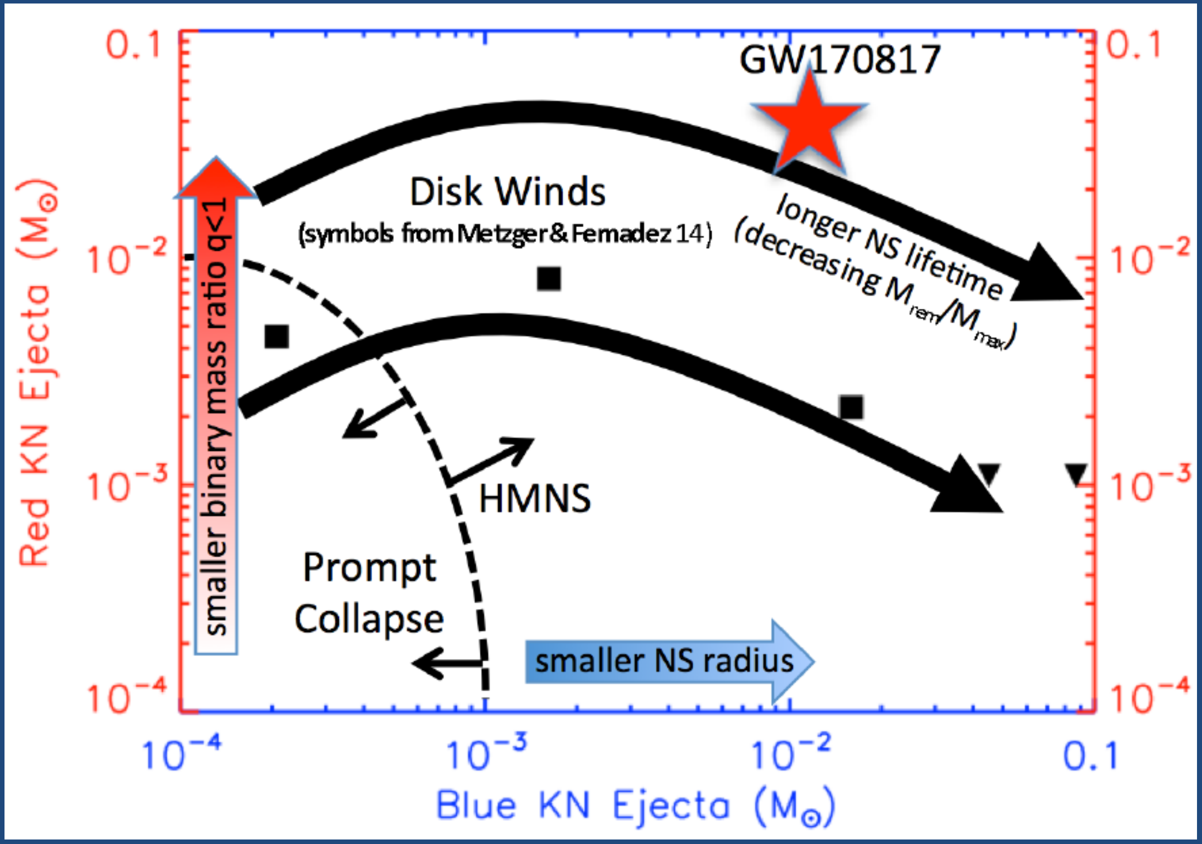

B.Metzger 1710.05931

Radio observations by JVLA

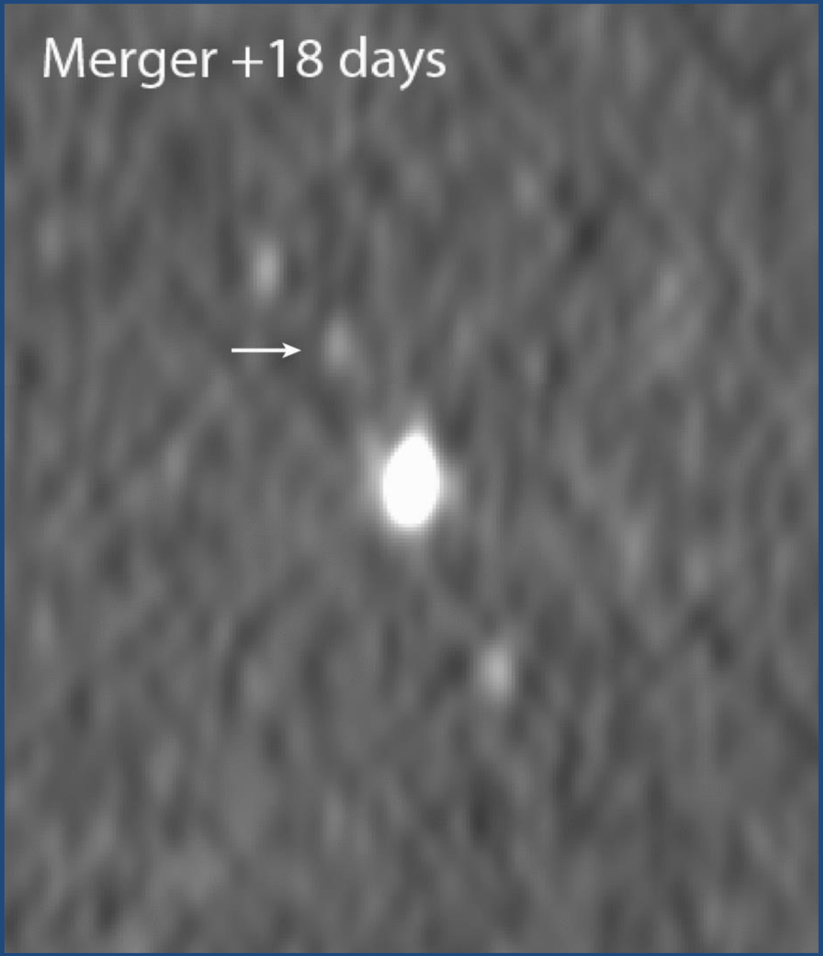

Superluminal motion of radiosource – a relativistic jet

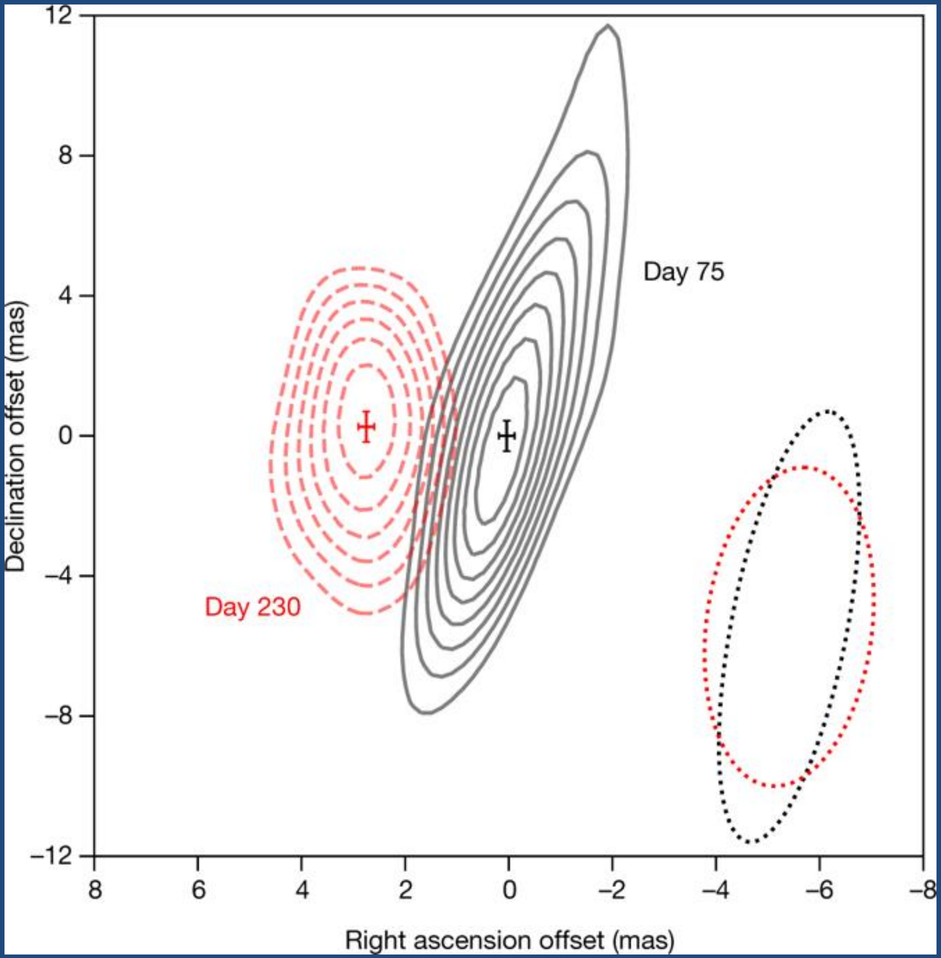

$\Gamma \approx \beta_{app} \approx 4.$

Mooley + 18, Nature 561, 355

Relativistic jet in radio

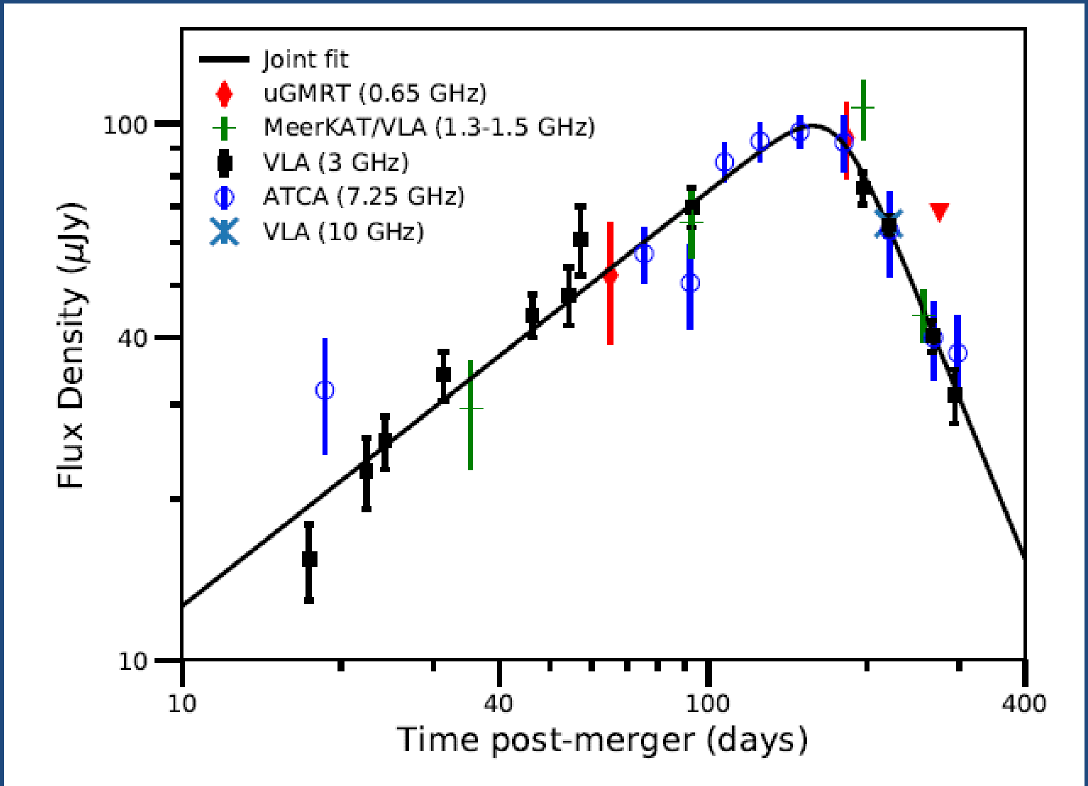

1810.12927

A structured jet model

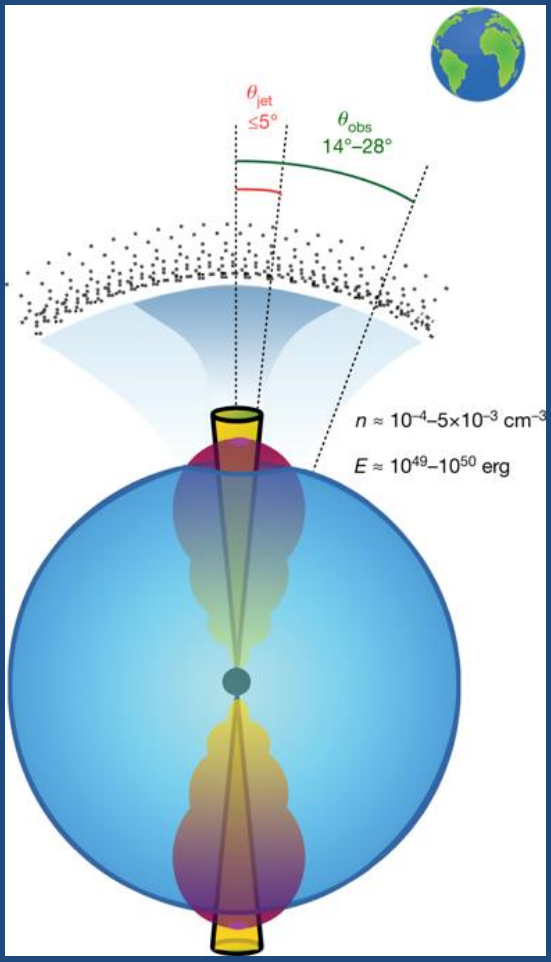

Mooley + 18, Nature 561, 355

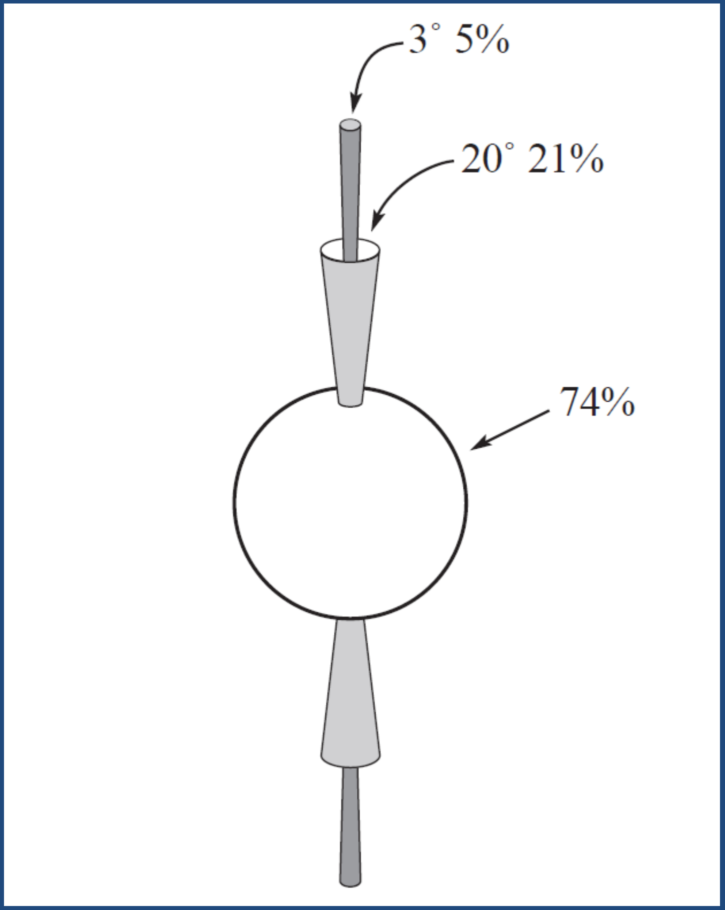

PK+ 1999, arXiv:astro-ph.9908136

GR MHD calculations

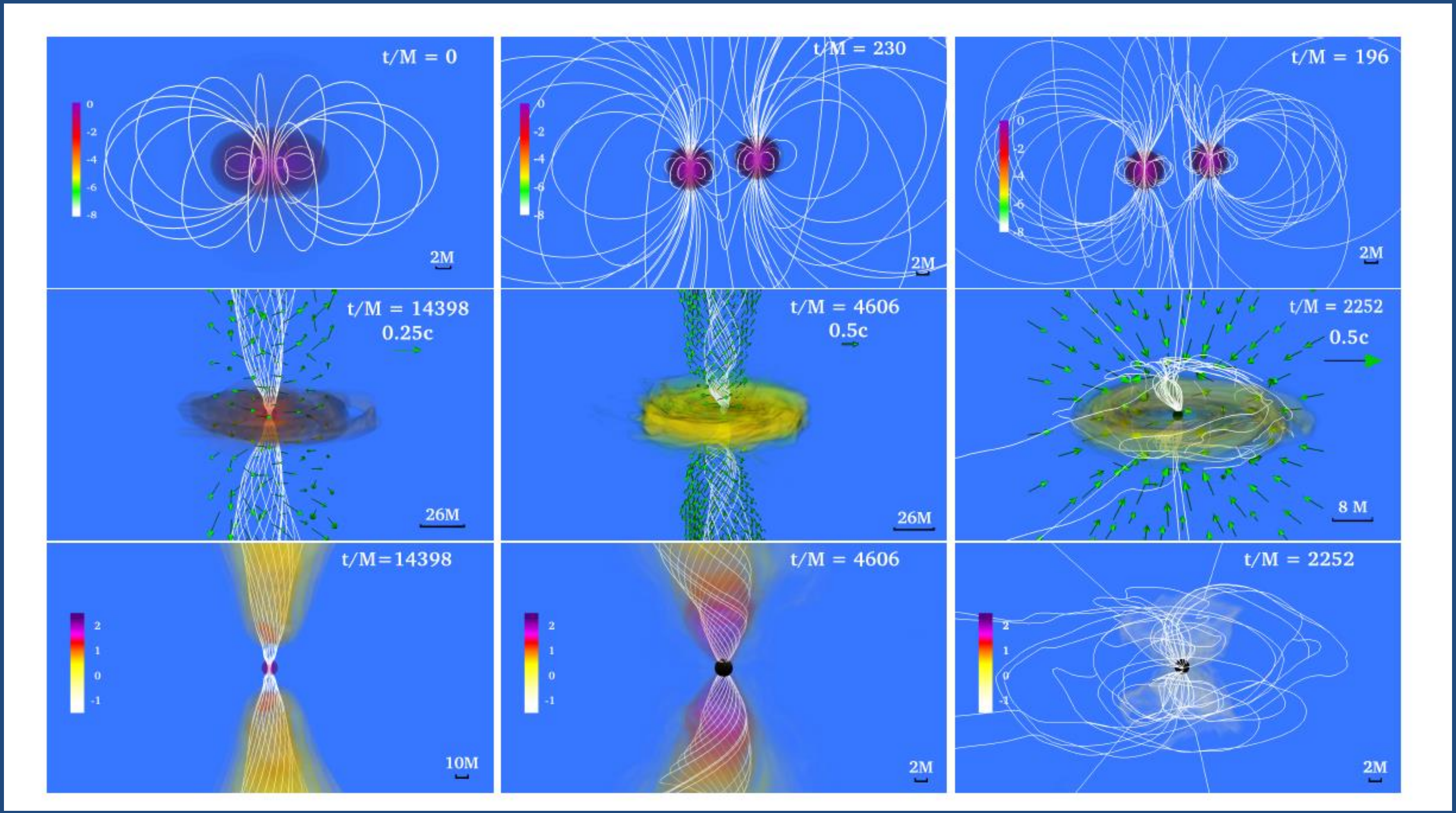

$M_{\rm max}^{\rm sph} \lesssim 2.16$

1711.00473

NS+NS: Conclusions

- GW170817 proved NS+NS and short GRB connection
- Neutron-rich mass ejection → r-process nucleosythesis → a kilonova phenomenon
- Binary NS mergings as the main production channel of r-elements in nature

Future prospects

Plans for O4 (2021)

- Install further upgrades:
    - Signal recycling mirror;
    - Input power increase to 125 W;
- Expected range for BNS in the range 100's Mpc;

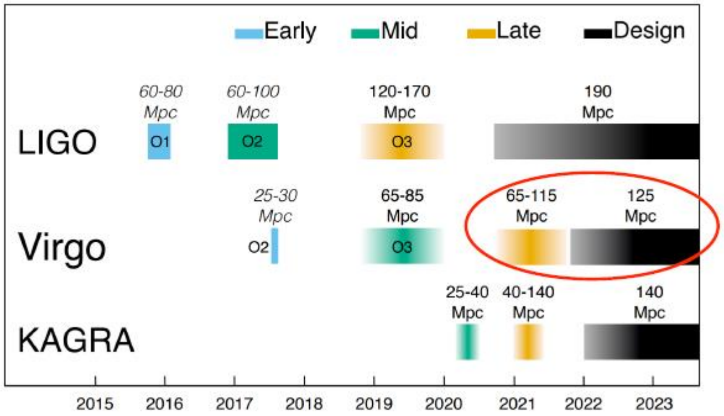

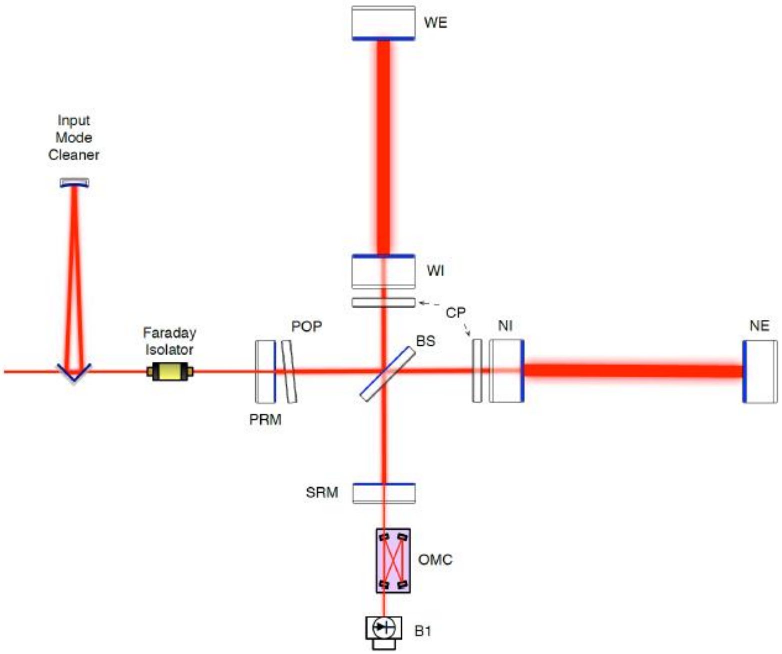

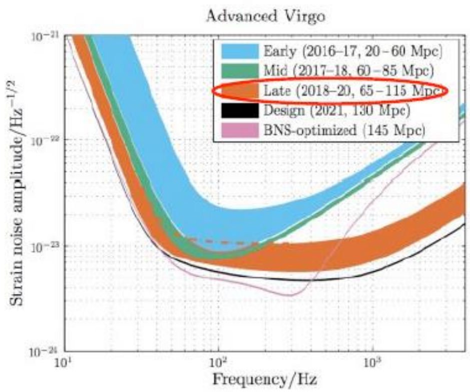

17

Localization: ~ 10 sq. degrees

Future LIGO development

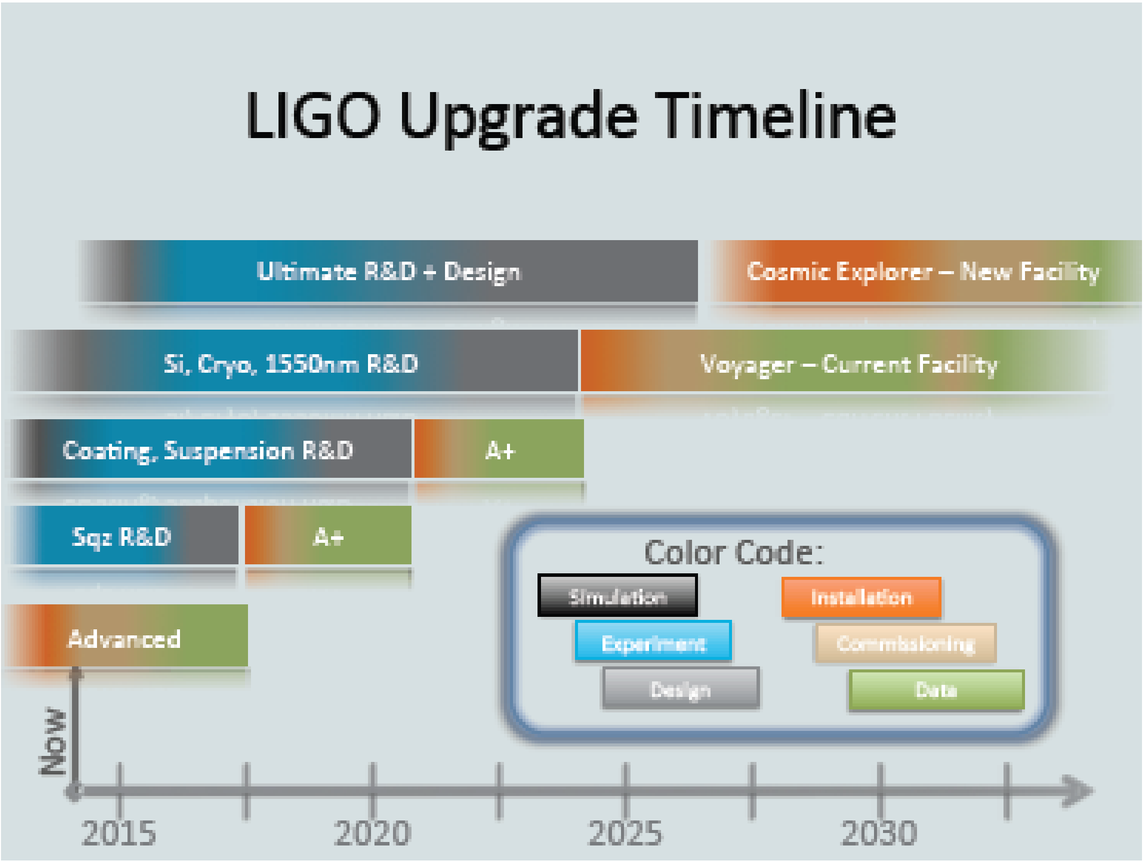

3 Projects of future LIGO detectors:

A^+
Voyager
Cosmic Explorer

https://dcc.ligo.org/LIGO-T1500290/public

40-km LIGO Cosmic Explorer (2035)

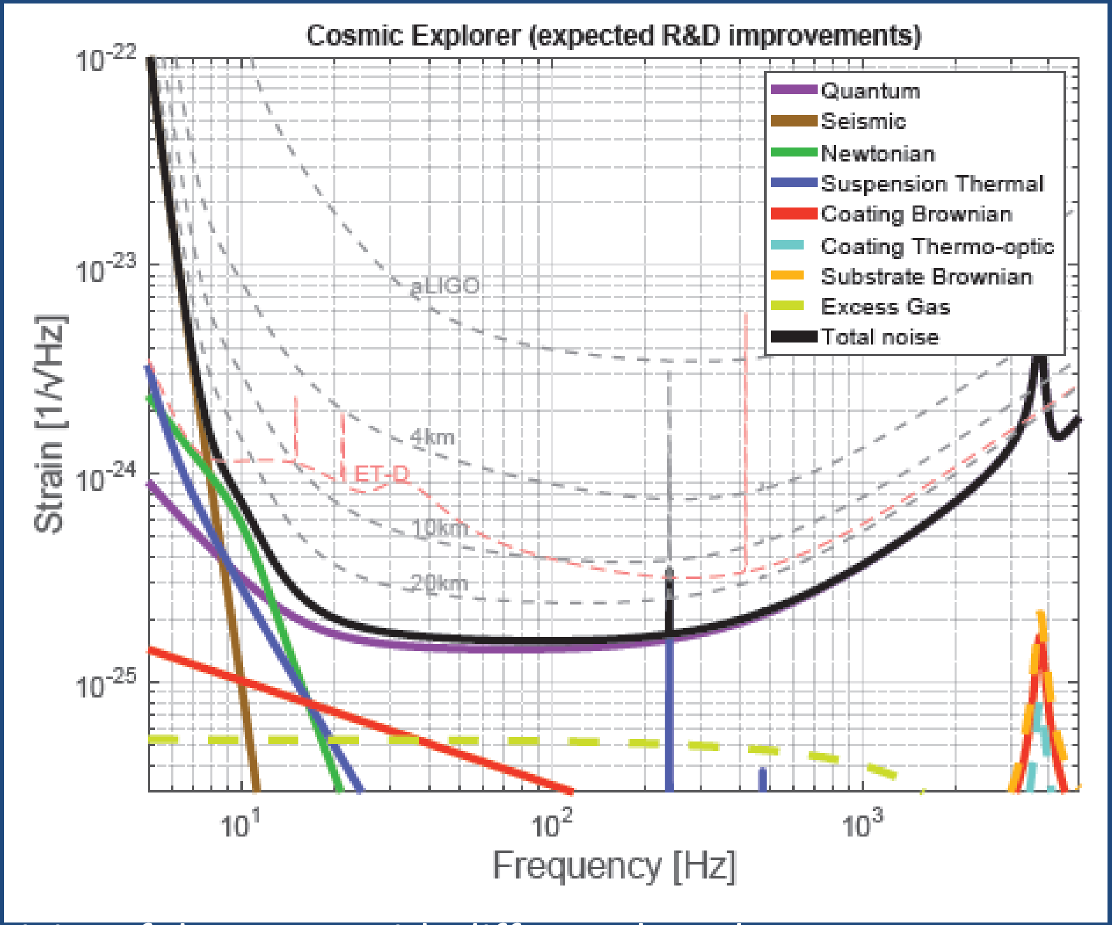

Sensitivity of detectors with different lengths.
Solid curves are for a 40km long detector

LIGO Scientific Collaboration,arXiv:1607.08697 [astro-ph.IM]

Expanded IFO network 2020+

B F Schutz

Data Innovation Institute
CARDIFF UNIVERSITY

MOSCOW NOVEMBER 2016: LEARNING FROM GW ASTRONOMY

16

Credit: B. Schutz

GW astronomy by ground-based interferometer network

- BNS ~100 /year, BBH ~ 1000 /year. BBH @ z>1.
- BNS → constraints NS EOS, GRB physics
- GR tests: BH horizon probing from ring-down tails. Deviations from GR
- Statistical measurements of M, J for NS and BH in binaries → formation mechanisms (standard, dynamical in stellar clusters, primordial BH)
- …

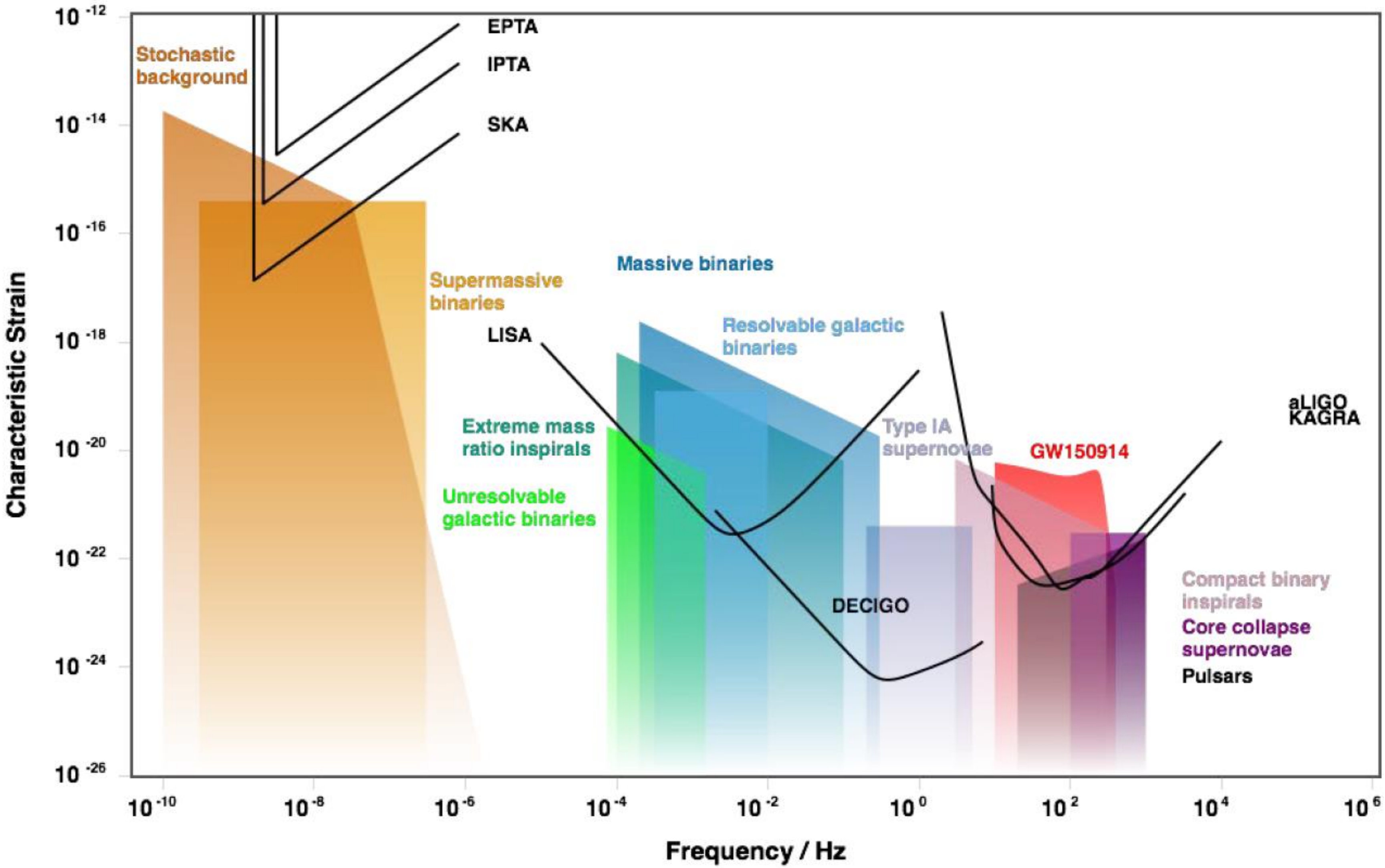

Characteristic Strain
Frequency / Hz
10^{-12}
10^{-14}
10^{-16}
10^{-18}
10^{-20}
10^{-22}
10^{-24}
10^{-26}
10^{-10}
10^{-8}
10^{-6}
10^{-4}
10^{-2}
10^{0}
10^{2}
10^{4}
10^{6}
EPTA
IPTA
SKA
Stochastic background
Supermassive binaries
Massive binaries
Resolvable galactic binaries
LISA
Extreme mass ratio inspirals
Unresolvable galactic binaries
Type IA supernovae
GW150914
aLIGO
KAGRA
DECIGO
Compact binary inspirals
Core collapse supernovae
Pulsars

Space interferometer LISA (ESA+, 2034)

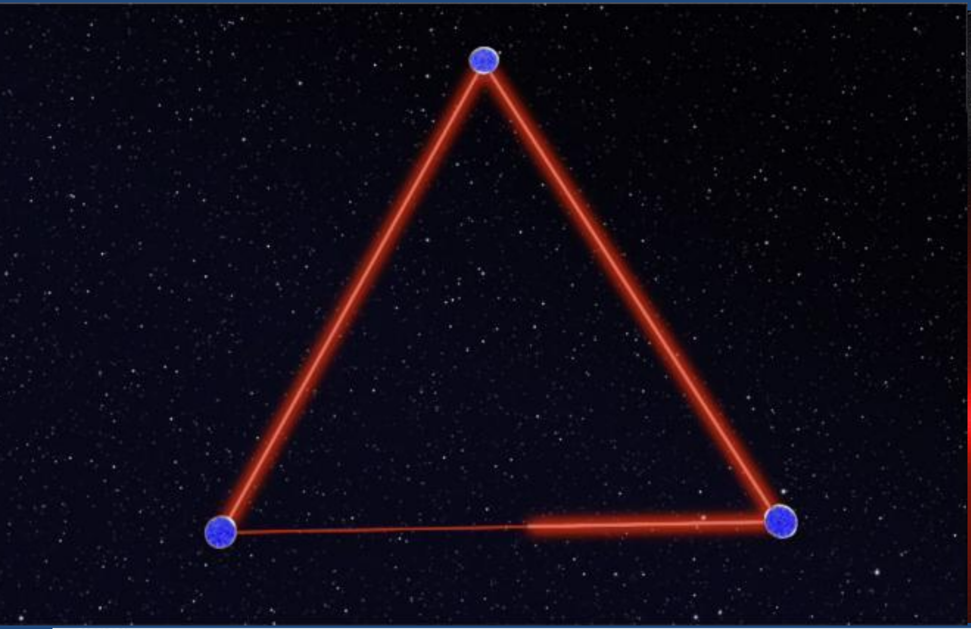

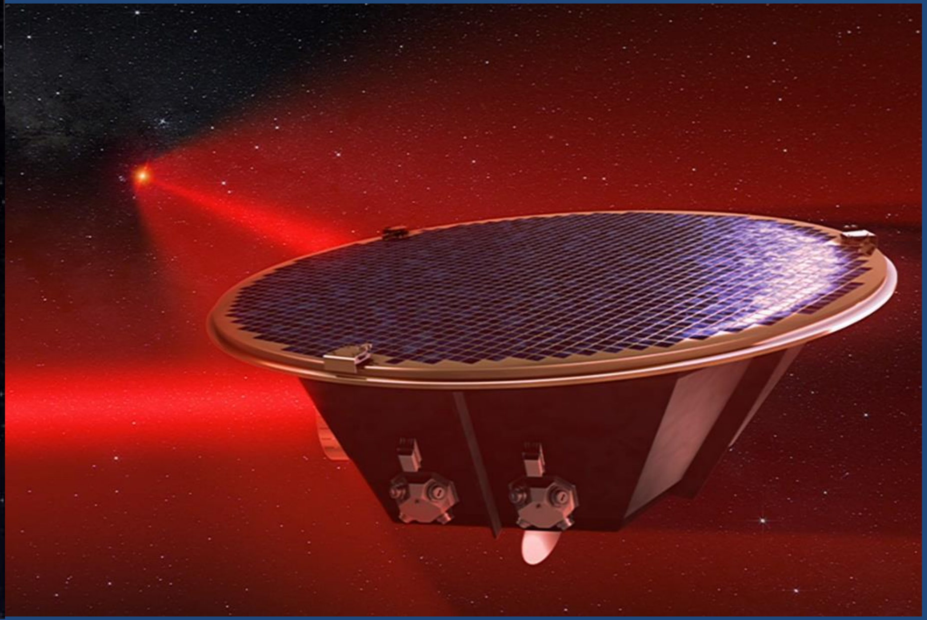

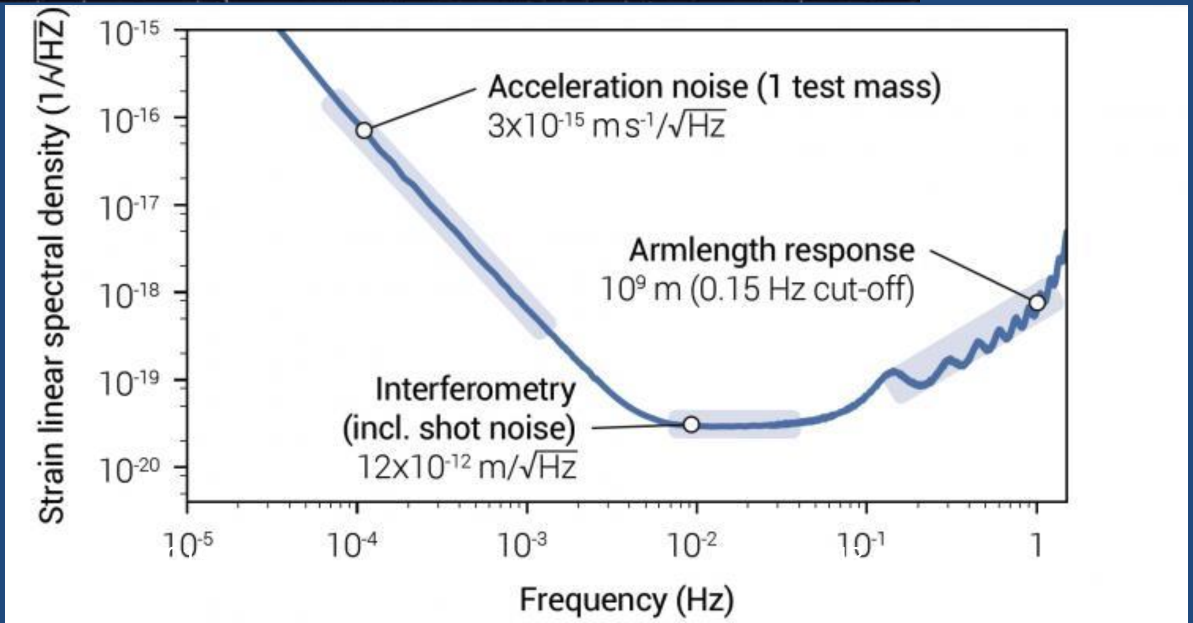

www.elisascience.org

Main LISA sources: binary SMBH in galaxies, galactic double WDs

- Central SMBH in all galaxies
- Galactic merging → formation of double SMBH
- Binary SMBH coalescence

in the Hubble time

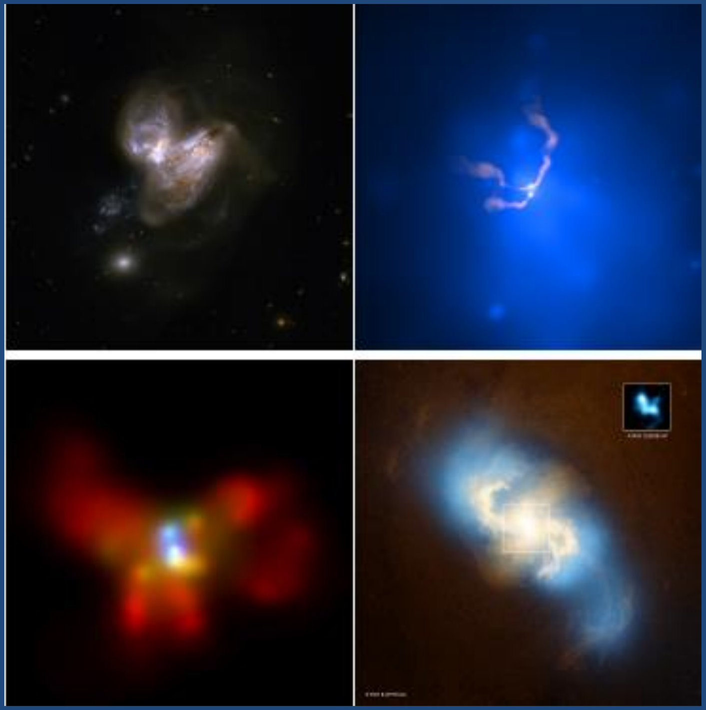

Successful LISA Pathfinder

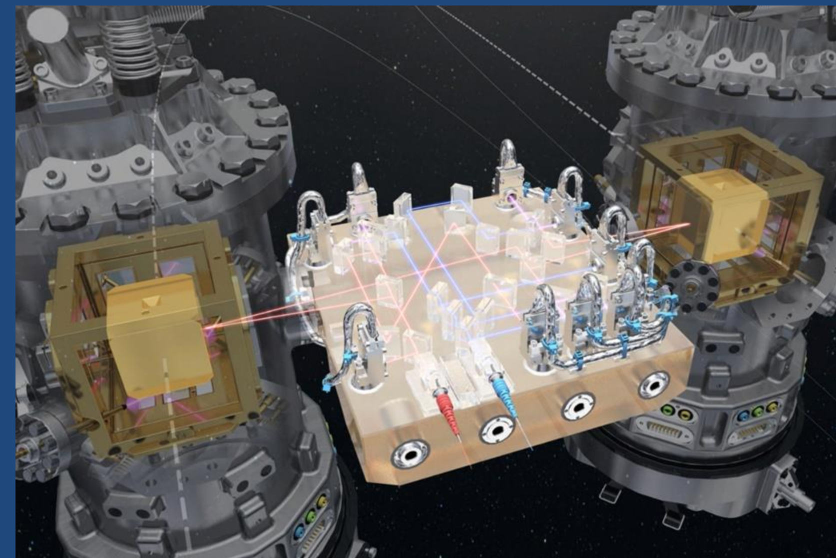

2015-2016

Two 46-mm Au-Pt 2-kg test masses

Drag-free floating mass technology

www.elisascience.org

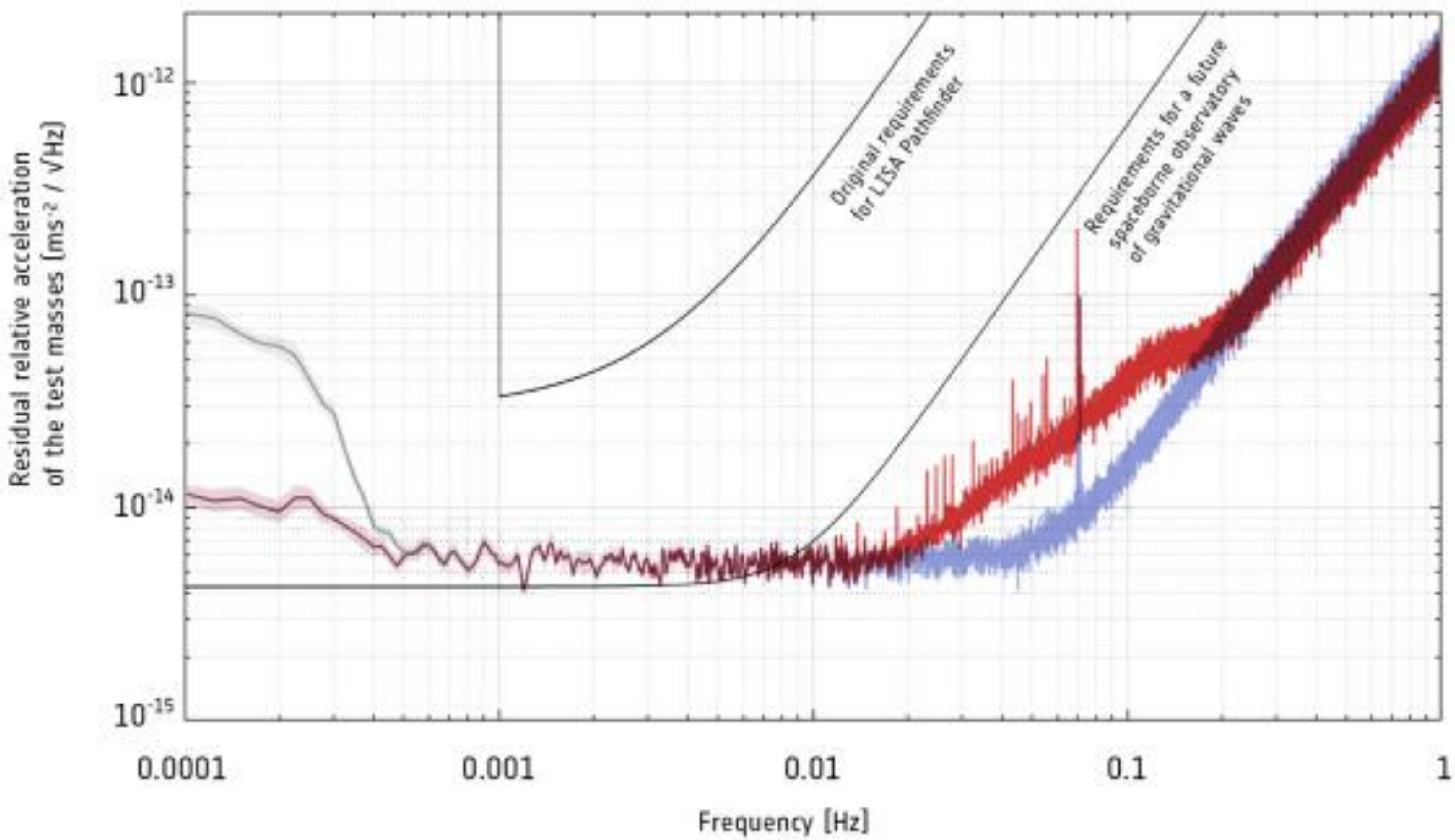
Residual relative acceleration of the test masses [ms⁻² / √Hz]
Frequency [Hz]
Original requirements for LISA Pathfinder
Requirements for a future spaceborne observatory of gravitational waves
10^{-12}
10^{-13}
10^{-14}
10^{-15}
0.0001
0.001
0.01
0.1
1

Galactic binary WDs

- ~10^7 in Galaxy; LISA verification sources; GAIA, LSST
- P_{orb} ~ a few minutes ➔ almost monochromatic GW signal

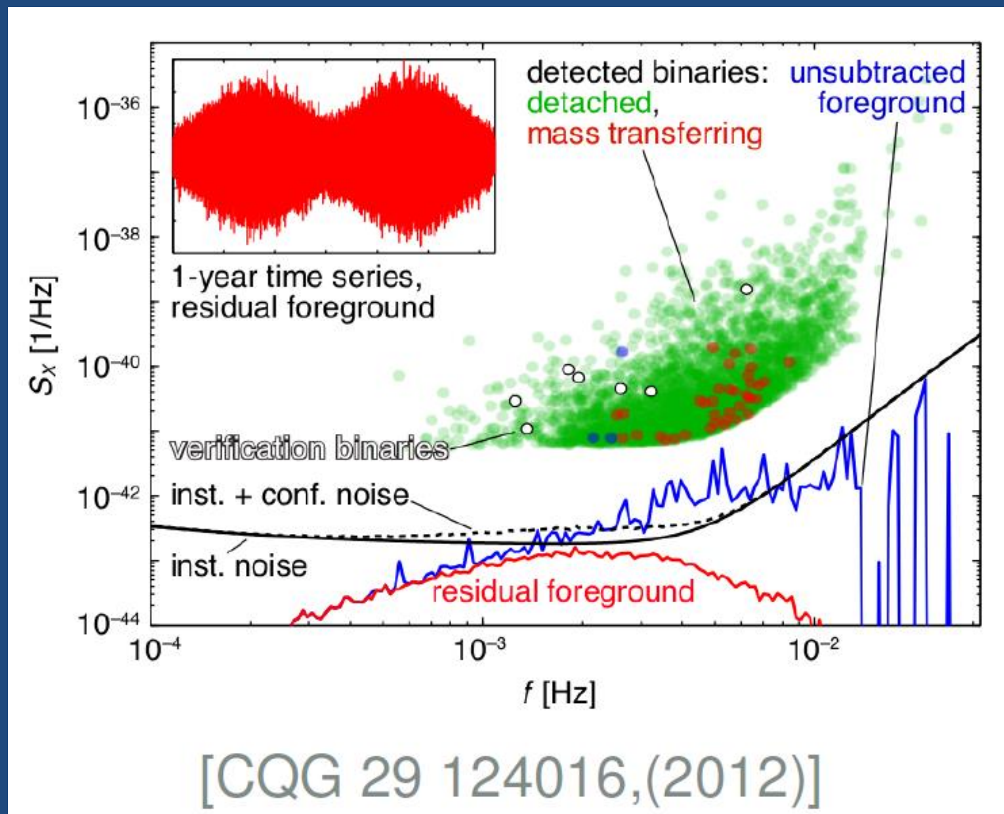

LISA data analysis

- Main difficulty: signal dominated by numerous sources

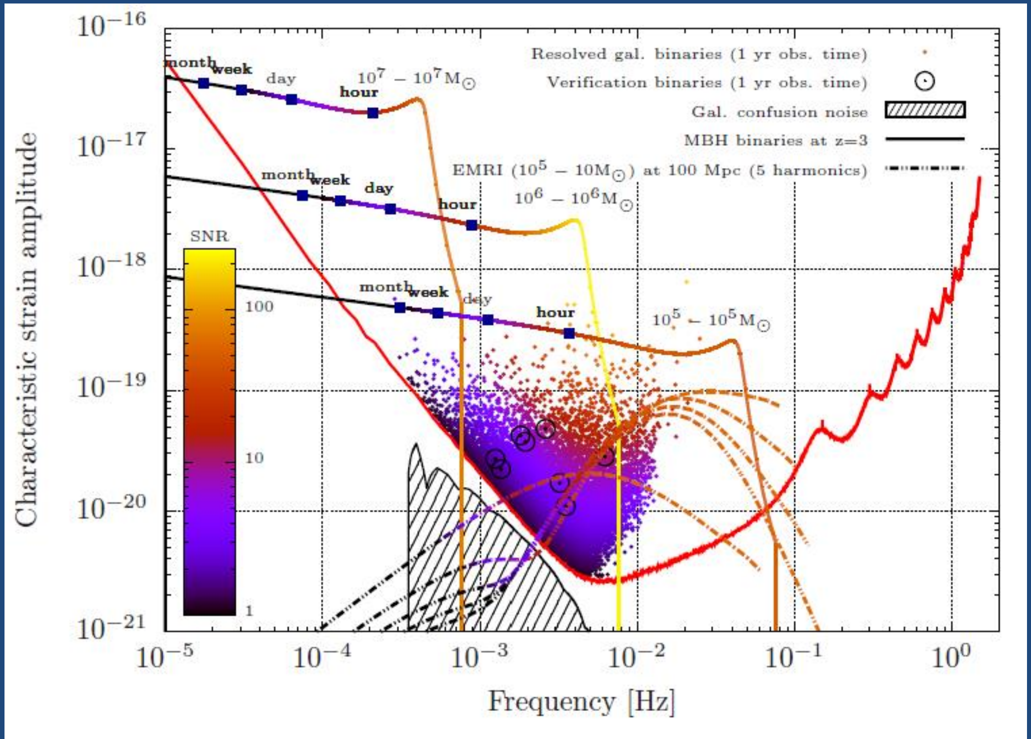

[white paper arXiv:1305.5720]